Order Number 9405581

Investigation of the role of yeast BiP in secretory pathway function and regulation

Rocco, James William, Ph.D.

City University of New York, 1993

U·M·I
300 N. Zeeb Rd.
Ann Arbor, MI 48106

INVESTIGATION OF THE ROLE OF YEAST BIP IN SECRETORY PATHWAY FUNCTION AND REGULATION

by

James W. Rocco

A dissertation submitted to the Graduate Faculty in Biomedical Sciences in partial fulfillment of the requirements for the degree of Doctor of Philosophy,

The City University of New York

1993

APPROVAL PAGE

This manuscript has been read and accepted for the Graduate Faculty in Biomedical Sciences in satisfaction of the dissertation requirement for the degree of Doctor of Philosophy

May 26, 1993
Date

Dr. Reza Green
Chair of Examining Committee

June 17, 1993
Date

Dr. Terry Krulwich
Executive Officer

Dr. Diane Applegate

Dr. Carter Bancroft

Dr. Jim Bieker

Dr. Miles Brennan

Supervisory Committee

The City University of New York

ABSTRACT

INVESTIGATION OF THE ROLE OF YEAST BIP IN SECRETORY PATHWAY FUNCTION AND REGULATION

by

James W. Rocco

Advisor: Reza Green, Ph.D.

In this study we examined the role of yeast BiP, a luminal ER heat shock protein, in the maturation of a triple glycosylation mutant of yeast prepro-α-factor (N123-ppαf). Using pulse-chase radiolabeling in combination with SDS-PAGE and HPLC, we initially observed that the mutant strain exhibited a severe defect in the secretion of αf compared to wild-type cells. Surprisingly, treatment of mutant cells with tunicamycin (TM), an inhibitor of Asn-linked glycosylation, enhanced the transport and processing of N123-ppαf, suggesting a possible *trans*-acting involvement of yeast BiP. By constructing recombinant yeast strains in which BiP expression was independent of TM treatment, and under the control of the heterologous CUP1 (metallothionein) promoter we were able to independently regulate the level of intracellular BiP. We observed that overexpression of BiP led to the retention, and subsequent degradation, of N123-pαf in a post-ER compartment. This suggested that, rather than promoting folding and transport, BiP plays a negative role in the lumen of the ER by binding mutant and malfolded proteins and promoting their degradation. Support for an interaction between BiP and N123-pαf was supported by two additional results: First, expression of N123-pαf resulted in a dose-dependent transcriptional induction of BiP mRNA. Second, co-expression of BiP and N123-pαf was inhibitory to growth in a dose-dependent manner.

Using these same recombinant strains, we also demonstrated that overexpression of BiP from the heterologous CUP1 promoter, prior to challenging the yeast cells with TM, protected the cells from the cytotoxic action of the drug, in analogy to the protective role of cytoplasmic heat shock proteins in response to thermal stress. To our knowledge, this is the first example that BiP plays a role in protecting the cell from a lethal ER stress.

Finally, the TM-mediated transcriptional induction of BiP can be suppressed by heterologous overexpression of BiP from the CUP1 promoter, suggesting that BiP is directly involved in regulating its own transcription.

ACKNOWLEDGEMENTS

First and foremost I would like to thank my advisor Dr. Reza Green for her guidance and support over the course of my training over the last four years. In addition to introducing me to an area of research that I find tremendously exciting, without her support, this thesis and my development as a scientist would not have been possible.

Second I thank the laboratory of Dr. Carter Bancroft and its members for support, supplies and companionship over the last four years. I offer special thanks to Drs. Art Jackson and Quirong Liu for early technical guidance. In addition, I offer special thanks to Wayne Pan, MD and soon to be Ph.D., for his advice and council during times of strife.

Third I thank the Department of Physiology and Biophysics and my chairman Dr. Harel Weinstein, for guidance, training and resources, as well as for generous financial support, allowing me to attend the Cold Spring Harbor Yeast Genetics Course.

I thank Drs. Phil Heiter, Mark Rose and Fred Winston from the Yeast Genetics course for their training in the methods of yeast genetics, never-ending scientific discussions, numerous reagents, and for instilling an attitude towards science that was success-oriented and exciting.

I offer special thanks to Dr. Ron Kohanski for technical guidance in the field of Biochemistry, use of his HPLC facilities, and numerous conversations in his own unique style.

I thank Dr. John Durham for listening during many hours of discussion, as well as his guidance and technical support over the duration of my Ph.D. training. Through his efforts during my moments of panic I am indebted. I thank Dr. Klaude Weiss for his patience, guidance and "worldly advice" over

the last two years, which was indispensable for the completion of my training. I also thank Dr. Bill Thornhill for his technical assistance with Western blot analysis, as well as his ability to diminish all problems into sources of humor.

I would also like to thank my peers Brian Kloss (Ph.D. to be) and Dan Fischberg (MD/Ph.D. to be) for their companionship, humor, and their not so rare insights into technical and personal matters. Without their constant presence, long hours at night and on weekends would have been unbearably lonely.

I am also indebted to my friend Karl Werner for both part-time employment and access to his computer resources, without which I would be further in debt than I already am. I also offer special thanks to my friend Mark Walsh and his wife Meg for their wisdom and emotional support, and provision of a reasonable social life when I was too busy to provide my own. I would like to thank my older brother Bill for his witty postcards, timely phone calls and other ill-conceived attempts to maintain my spirts over the last several years, all were a welcome source of distraction.

Finally I would like to thank my fiancee Caroline for her constant emotional support over these last several years. Her ability to diminish my Irish temper and Sicilian passions is unequaled, and allowed me to finish my thesis with my career relatively intact.

A special thanks goes out to the Kinsale Tavern (between 94th and 95th on Lexington Ave) where numerous meetings over pints of Liberty Ale and super burgers with unidentified participants allowed this doctoral candidate to advance to his defense.

TABLE OF CONTENTS

LIST OF TABLES

LIST OF FIGURES

I. INTRODUCTION

A. THE SECRETORY PATHWAY IN YEAST

1. *Overview*

One of the fundamental questions in cell biology is how proteins synthesized in the cytosolic compartment are targeted and transported to their final subcellular destinations. Studies of protein targeting and transport have been carried out in organisms as diverse as bacteria, yeast, plant and mammalian cells. Despite the difference in subcellular organization among these evolutionary distinct organisms, the mechanisms of protein targeting and transport seem to have been conserved. For example, translocation of prokaryotic secretory proteins across the cytoplasmic membrane of *E. coli* shares mechanistic features with the post-translational import of proteins into mitochondria and chloroplasts, as well as with the cotranslational translocation of secretory and integral membrane proteins across the membrane of the endoplasmic reticulum.

All cellular proteins, with the exception of a small number of mitochondrial and chloroplast proteins, are synthesized on either free or membrane-bound polysomes. This early segregation divides cellular protein into two distinct categories: Free polysomes, which synthesize cytosolic proteins, and proteins destined for the nucleus, peroxisome, mitochondria and chloroplast (these latter proteins are transported directly from the cytoplasm by a post-translational mechanism), and membrane-bound polysomes, which synthesize proteins that will eventually be delivered to the remaining membranes and organelles of the cell. This process is initiated by the

targeting and subsequent transfer of secretory pathway proteins into or across the membrane of the ER by a cotranslational mechanism.

In mammalian cells, signal peptide-containing secretory pathway proteins are targeted to the ER through the sequential interaction of SRP, an 11S ribonucleoprotein complex of a 7SL RNA and six proteins, which recognizes the ribosome-signal peptide complex, and the SRP receptor, an integral membrane protein of the ER, which recognizes SRP bound to the ribosome-nascent chain complex. During translation, the protein is translocated across the ER membrane. Once access to the ER lumen is obtained, these proteins are subject to a battery of posttranslational modifications including Asn-linked glycosylation, disulfide bond formation, and signal peptide cleavage, before being transported to their final destination by vesicular movement through the exocytic pathway. By this mechanism, secretory pathway proteins initially targeted to the ER can be transported to the Golgi, lysosome, secretion granules, or the plasma membrane, as well as be secreted. In addition, at each step in the pathway, in response to appropriate signals, a protein might be retained and remain associated with that particular organelle.

In the original studies of secretion in mammalian cells, metabolic labeling and cell fractionation were used to trace the intracellular pathway taken by proteins destined for export. These studies were soon followed by electron microscopic and immunocytochemical investigations to probe structures and pathways involved in intracellular transport. These methods are widely used in conjunction with molecular biological methods, which allow cloned genes to be mutagenized *in vitro* and reintroduced into cells. Investigation of the molecular mechanisms involved in directing intracellular protein traffic became possible with the development of *in vitro* protein

transport systems. The advantage of a cell-free system is that it permits biochemical fractionation, reconstitution and purification of the components of each reaction. These systems have provided further evidence for the conservation of mechanism between eukaryotic and prokaryotic protein transport, since many of the components are interchangeable. This work has paralleled the genetic analysis of protein transport, which has taken advantage of the ease of genetic approaches in bacteria and yeast. Although mammalian cells are not as easily manipulated as yeast and bacteria, a number of mammalian cell lines having defined defects in components of their secretory pathways have also been produced. The power of genetics is quite apparent when one observes the large number of secretion-related proteins identified by the complementation of bacterial and yeast mutants.

As in higher eukaryotes, the lower eukaryote, *Saccharomyces cerevisiae*, maintains the compartmentalized organization and function of its cellular organelles through the proper localization of newly synthesized lipid and protein. Yeast polyribosomes synthesizing secretory pathway proteins are directed to the ER membrane by a signal peptide, implying that, on a functional level, the underlying mechanism of ER targeting has been conserved between yeast and higher eukaryotic cells.

2. *Yeast prepro-α-factor as a model secretory pathway protein*

The work described in this thesis uses as a model secretory protein prepro-α-factor (ppαf), a peptide hormone precursor of *S. cerevisiae*. *S. cerevisiae* can exist as one of two haploid cell types; **a** cells, which secrete **a**-factor (**a**f) and express cell surface receptors for α-factor (αf); and α cells, which secrete αf and express cell surface receptors for **a**f. Mating between these haploid cells types, which results in the formation of an **a**/α diploid, is

dependent upon these secreted peptides and their corresponding cell surface receptors, the STE2 and STE3 gene products, respectively. Upon binding to its receptor, each cell's secreted peptide pheromone prepares the opposite cell type for mating by eliciting a number of well-defined responses including: (1) arrest in the G_1 phase of the cell cycle just before the initiation of DNA synthesis (genetically defined as START) [1-3]; (2) changes in the carbohydrate composition of the cell wall [4]; (3) induction of surface agglutinins that promote adhesion [5]; (4) morphological changes known as shmooing [6]; and (5) the induction of a number of other genes [7].

The protein precursors of the αf peptide are encoded within a small multigene family consisting of the MFα1 and MFα2 genes that have been cloned and sequenced [8, 9]. The 13 amino acid αf peptide is produced by the maturation of two closely related precursors of 165 and 120 amino acids encoded by the MFα1 and MFα2 genes, respectively. At least one MFα gene is required for αf production and mating, because an mfα1 mfα2 double mutant is unable to produce αf and is sterile [10]. Analysis of mfα1 and mfα2 mutants by both halo and mating assays indicate that the MFα1 gene is responsible for the majority of the αf produced by the cell [10].

The MFα1-encoded 165 amino acid precursor protein, prepro-α-factor (ppαf), contains three distinct structural regions (Figure 1): (1) a N-terminal 19 amino acid hydrophobic signal peptide that acts as a signal sequence and targets the precursor to the endoplasmic reticulum; (2) a 64 amino acid proregion that contains three Asn-linked glycosylation consensus sites; and (3) a C-terminal region containing four tandem repeats of the mature αf peptide separated from the proregion and one another by spacer peptides of 6 to 8 amino acids.

Figure 1. Secretory pathway processing of yeast ppαf.

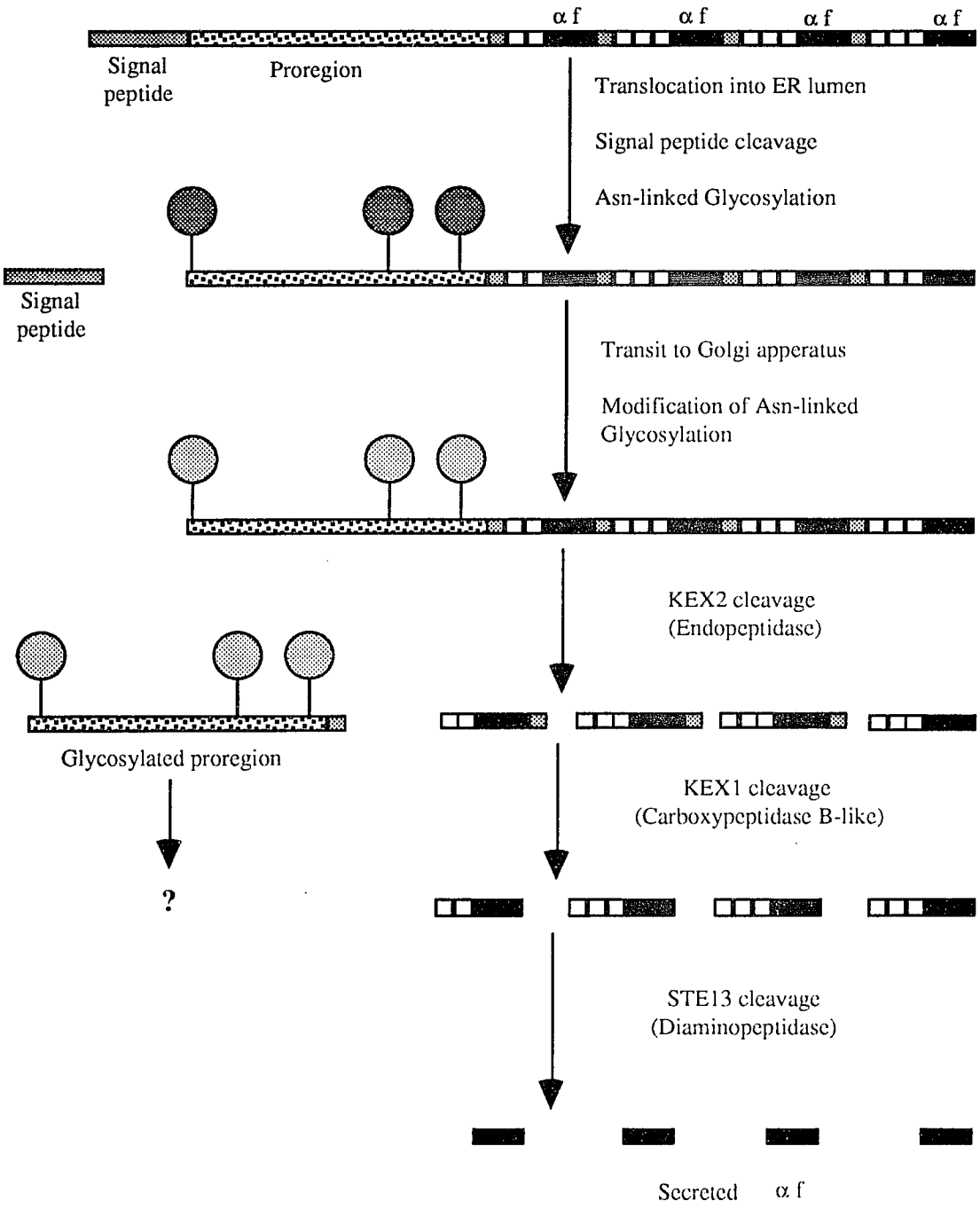

Ppαf is processed within the classical secretory pathway by a series of well-characterized steps (Figure 1) [11-15]. First, the nascent polypeptide is translocated into the ER, where the signal sequence is cleaved to produce pro-α-factor (pαf), and core oligosaccharides are added to all three acceptor asparagines within the proregion [11, 12, 16, 17]. Second, the core oligosaccharides are extended in the Golgi complex by the sequential addition of α1-6, α1-2, and α1-3 linked mannose residues, with extensive elongation of the branched α1-6 branched mannose chains resulting in the addition of 50-100 mannose residues per Asn-linked oligosaccharide [18, 19]. This is followed by the KEX2-mediated serine endopeptidase cleavage on the carboxyl side of Lys-Arg residues at the amino terminus of each αf peptide repeat [11, 20]. Third, subsequent trimming by the KEX1 membrane-associated carboxypeptidase removes the two basic amino acids from the C-terminus of each αf peptide [20]. Finally, the remaining amino acids of the spacer are removed from the amino-terminus of the αf peptides by the STE13 dipeptidyl aminopeptidase, which specifically cleaves on the C-terminus of repeating X-Ala sequences [13]. The mature αf peptide is then rapidly secreted into the extracellular medium.

Little is known about the fate of the proregion after KEX2 cleavage. Attempts to detect breakdown products that could represent the proregion using sec mutants were unsuccessful [12]. Studies in this lab using a specific proregion antibody and HPLC analysis have also been inconclusive (J. Rocco, unpublished observations), suggesting that the proregion is rapidly degraded.

The presence of easily observed, well-characterized covalent modifications that occur in discrete intracellular organelles of the secretory pathway, combined with the existence of numerous temperature sensitive

secretory pathway mutants, make ppαf ideal for studying structural maturation, processing, sorting and secretion.

3. *Genetic analysis of secretion in yeast*

To date, the genetic dissection of the mechanisms of protein sorting and intercompartmental transport within the yeast secretory pathway has been based on phenotypic methods that rely on the formation of conditional-lethal mutants. Application of these methods has led to the isolation and characterization of a large number of secretion-related genes. However, the inherent requirement for the formation of a conditional-lethal mutant may have resulted in only a fraction of the total secretory pathway genes being identified since: (1) conditional lethal mutations occur primarily in essential genes, and (2) this type of mutation occurs at a much lower frequency than a simple null mutation.

The original genetic dissection of the secretory pathway in yeast was based on the isolation of temperature sensitive (ts) mutants that become denser at the restrictive temperature. The rationale was that cells which failed to export protein at the restrictive temperature would stop growing due to the block in the secretory pathway, yet their mass should continue to increase since intracellular metabolism is not affected. The isolated mutant strains fell into two separate classes: (1) class A sec mutants accumulated invertase and acid phosphatase intracellularly and comprise 23 separate complementation groups (sec1 through 23); class B sec mutants neither secrete nor accumulate active invertase or acid phosphatase, and consist of four separate complementation groups (sec53, 55, 58 and 59). Based on thin-section electron microscopy and biochemical analysis, the original collection of SEC mutants could be classified as defective at one of four different stages of the

yeast secretory pathway: (1) failure to glycosylate and properly assemble polypeptides in the ER lumen (sec53 and 59); (2) ER to Golgi transport (sec12, 13, 16, 17, 18, 20, 21, 22, and 23); (3) intra-Golgi transport (sec7, 14); and (4) exocytosis (sec1, 2, 3, 4, 5, 6, 8, 9, 10, 15).

An example of how genetic and biochemical approaches are being used to study protein transport through the secretory pathway can be seen in the case of the sec18 mutant. When sec18 cells are metabolically labeled with ^{35}S-methionine at the restrictive temperature, glycosylated pαf accumulates within the ER. The wild-type SEC18 gene product was cloned by complementation of the growth defect [21]. At the same time, a mammalian protein, NSF, was identified by its ability to support vesicular transport in an in vitro reconstituted system [22]. After cloning of the cDNA of NSF, sequence analysis found it to be 48% identical in amino acid sequence to the yeast Sec18p. Further, Sec18p could replace NSF in the mammalian assay. Subsequent analysis of sec18 mutants demonstrated that Sec18p is required for transport between ER and Golgi, as well as for later steps in transport.

To identify genes that code for components of the translocation machinery, a direct selection for temperature sensitive translocation-defective mutants was developed [23, 24]. Mutants were selected by their inability to translocate a fusion protein consisting of the prepro region of ppαf fused to the cytosolic enzyme histidinol dehydrogenase (His4Cp). At the restrictive temperature, mutants defective in ER translocation are able to grow on histidinol, since they fail to sequester the histidinol dehydrogenase activity of the fusion protein into the ER lumen. Three genes were identified that appear to encode components of the yeast translocation machinery (SEC 61, 62, and 63). Consistent with this role, all three mutant strains accumulate the untranslocated precursors of yeast secretory pathway proteins at the

restrictive temperature [24, 25]. The specific translocation defects in the sec62 and sec63 mutant strains have been reproduced *in vitro*, using yeast microsomal membranes isolated from the mutant cells at the restrictive temperature; this supports the idea that at least two of the three proteins are ER associated. In addition, these three proteins can be purified as a multisubunit complex with two additional unknown proteins from a detergent solubilized membrane fraction treated with the thiol-reversible cross-linking agent dithio-bis-(succinimiidylpropionate) (DSP) [26]. This result is consistent with the view from mammalian studies that a multisubunit protein machine (translocon) translocates proteins across the ER membrane.

DNA sequence analysis of the SEC62 gene predicts a 32 kD protein with two potential transmembrane domains, while the SEC63 gene was predicted to encode a 73 kD protein with three potential membrane spanning domains. Further analysis of the SEC63p revealed that an internal 70 amino acid domain that is predicted to lie within the ER lumen has 43% sequence identity to the amino terminus of the *E.coli* heat shock protein DnaJ [27]. In *E. coli*, DnaJ interacts with the hsp70 homologue DnaK to promote bacteriophage replication. By analogy to the interaction between DnaJ and DnaK, this loop in SEC63p may recruit the yeast ER luminal hsp70 analog BiP to the translocation apparatus [27]. In support of this hypothesis, mutations within this loop inactivate SEC63p.

Several interesting discrepancies have emerged between yeast and mammalian systems. First, not all secretory proteins are equally affected by mutations in SEC61, 62 and 63 [24, 28]. Second, in vitro studies using yeast ER microsomes demonstrated that a number of yeast secretory pathway proteins, including ppαf, can be post-translationally translocated across the ER membrane [29, 30], suggesting that fundamentally different mechanisms may

operate in membrane translocation in yeast. Third, mutations in yeast BiP, the ER luminal hsp70 [31], as well as mutations in the cytoplasmic hsp70s [24, 28] inhibit translocation, a result with no clear counterpart in mammalian cells.

Based on these results, a yeast model is developing in which two separate translocation systems operate in parallel, with different secretory pathway proteins utilizing the separate systems to different degrees [32]. Some proteins, like ppαf, can engage the translocon in three separate ways: (1) in an SRP-dependent co-translational manner; (2) in an SRP-independent co-translational manner; and (3) in a post-translational hsp70-mediated manner. Other proteins may require strictly co-translational translocation and thus would engage the translocon only prior to the termination of protein synthesis (as observed in mammalian cells).

4. *Role of Glycosylation in Protein Sorting and Secretion*

The initial ER-localized steps of Asn-linked glycosylation in *S. cerevisiae* and higher eukaryotes are quite similar, and involve the stepwise formation of a core oligosaccharide chain on dolichol phosphate that has the composition $Glc_3Man_9GlcNac_2$. This oligosaccharide is then co-translationally transferred en bloc from the dolichol lipid carrier to the amide group of asparagine in an Asn-X-Thr(Ser) sequon within the nascent polypeptide chain [33, 34]. The three Glc residues are then rapidly removed by Glucosidases I and II. In yeast, one mannose (and in higher eukaryotes up to three mannoses) may be removed from the glycoprotein prior to transport to the Golgi [33]. Subsequent processing, however, is quite different in yeast than in higher eukaryotes. In higher eukaryotes, the core oligosaccharide is converted to a complex glycan containing only three mannose residues substituted sequentially with galactose, sialic acid, and N-acetylglucosamine, as well as

fucose [33]. In contrast, processing in yeast involves the addition of mannose residues within the Golgi leading to the formation of three distinct types of Asn-linked oligosaccharides: (1) a modified core oligosaccharide of $Man_{8-15}GlcNac$, as typified by Carboxypeptidase Y [35]; (2) an intermediate length extension of the core containing over 50 mannose residues, as typified by both invertase and acid phosphatase [36]; and (3) large extensions of the core containing 100-200 mannose residues, as typified by the cell wall mannoproteins. Synthesis of these distinct outer chains takes place in the Golgi apparatus through the stepwise addition of mannose residues catalyzed by a series of mannosyltranferases [19, 37].

The role of glycosylation in secretory pathway protein sorting and secretion is not uniform. Certainly, early studies that suggested that glycosylation is required for all protein secretion have been disproved [38], since numerous examples of non-glycosylated secreted proteins exist [39]. Two general approaches have been used to investigate the role of Asn-linked glycosylation in the cell. The first approach relies on the use of glycosylation inhibitors, while the second approach uses site-directed mutagenesis of cDNA to disrupt Asn-linked glycosylation sites. This latter approach may offer advantages over the use of drug treatments, since it makes it possible to study the effects of Asn-linked glycosylation without the secondary effects.

The drug tunicamycin (TM) competitively inhibits the transfer of GlcNac-1-P from UDP-GlcNac to Dol-P to generate Dol-PP-GlcNac, the first step in the assembly of the lipid-linked oligosaccharide [40-42]. The inhibition is thought to be due to the fact that different portions of the TM molecule resemble either dolichol or N-acetylglucosamine, the two substrates of the transferase [43]. TM is lethal to both yeast and higher eukaryotes after prolonged exposure. TM resistant strains have been identified in yeast and

include: (1) a strain overexpressing the ALG7 gene which codes for UDP-N-acetyl-glucosamine-1-P transferase; and (2) a strain bearing a recessive mutation designated tun1 [44]. The ALG7 gene was cloned based on its ability to rescue cells from TM lethality when overexpressed on a multicopy plasmid (a dominant phenotype) [44, 45]. ALG7 is an essential gene and encodes a protein with two potential membrane-spanning domains and two potential Asn-linked glycosylation sites. The product of the TUN1 gene has yet to be identified.

Studies using TM indicate that there is no universal role for Asn-linked glycosylation. Whereas some glycoproteins are unaffected by TM, others fail to reach their proper cellular destination or are degraded [39]. For example, inhibition of oligosaccharide synthesis with TM results in the irreversible accumulation of inactive invertase [46]. On the other hand, glycosylation is not required for the proper localization of alkaline phosphatase [47] and carboxypeptidase Y to the yeast vacuole [48].

Studies which employ site directed mutagenesis to disrupt the glycosylation consensus sequence have also been used to study the role of Asn-linked glycosylation in the sorting process [49-52]. These studies may be more physiological, in that they avoid the massive disruption of Asn-linked glycosylation that normally results from TM treatment, as well as other secondary effects, such as inhibition of protein synthesis and changes in the secretory apparatus [53]. Use of site directed mutagenesis to eliminate either or both Asn-linked glycosylation sites in the VSV G protein revealed that glycosylation plays a general role in transport to the cell surface, since elimination of either site alone had no effect on transport while disruption of both sites resulted in intracellular aggregation [54]. In yeast, disruption of Asn-linked glycosylation sites in ppαf by site directed mutagenesis led to a reduction in αf secretion in a dose dependent manner. That is, mutants with

all three sites disrupted exhibited a greater reduction in αf secretion than mutants with either one or two sites disrupted [55]. These studies, which provide the basis for this thesis, also suggest that there are no dominant effects of individual glycosylation sites.

Delayed ER to Golgi transport of unglycosylated glycoproteins has been observed in other systems [56], and may be mediated by their interaction with the ER luminal hsp70, BiP. As described in greater detail below, BiP is induced by treatment with drugs that inhibit Asn-linked glycosylation or by mutations that cause accumulation of secretory precursors within the ER. Disruption of Asn-linked glycosylation has been shown to result in the increased association of numerous glycoproteins with BiP and a reduction in intracellular transport and secretion in higher eukaryotes [52, 57]. In Chinese Hamster ovary (CHO) cells, tissue plasminogen activator (tPA), which has three utilized Asn-linked glycosylation sites and is efficiently secreted, exhibits a transient association with BiP. Disruption of Asn-linked glycosylation by either site-directed mutagenesis or TM treatment resulted in reduced levels of secretion and increased association with BiP, an effect enhanced by high level expression [52].

The role of Asn-linked glycosylation in the structure, function, stability and folding of glycoproteins is also protein-specific. Physiochemical analyses designed to investigate this problem have been hindered by the inherent heterogeneity of the oligosaccharide chain present after biochemical purification. A recent study [58], using the yeast glycoprotein invertase, attempted to circumvent this problem by producing and isolating the glycoprotein from a sec18 mutant strain. Since the sec18 mutant is blocked in ER to Golgi transport at the restrictive temperature, the addition of outer chains in the Golgi is blocked, and core-glycosylated invertase with a

homogenous carbohydrate chain accumulates in the ER. Comparisons between the core-glycosylated, non-glycosylated and native fully-glycosylated invertase revealed several roles for carbohydrate. First, glycosylation was found to stabilize the protein against thermal and denaturant-induced inactivation and unfolding. Second, during refolding, glycosylated forms of invertase were protected against aggregation and could refold after guanidine denaturation at high concentrations. In contrast, non-glycosylated invertase could only be recovered at extremely low protein concentrations where folding rather than aggregation becomes rate-limiting. This effect of glycosylation was similar for both core-glycosylated and high mannose forms. These results support the hypothesis that during biosynthesis, co-translocational Asn-linked glycosylation may prevent nonspecific aggregation of the folding polypeptide chain, as well as enhance its stability once it obtains its final tertiary structure.

B. ROLE OF BIP IN THE SECRETORY PATHWAY

1. *Mammalian BiP*

The 78 kD Ig heavy-chain binding (BiP), also known as glucose regulated protein (GRP78), is an abundant soluble ER protein that is a member of the hsp70 family of stress proteins found in all eukaryotes examined to date [59], for recent reviews see [60, 61]. BiP was first identified by its increased levels of expression after glucose deprivation in fibroblasts [62]. It was later independently identified by its transient association with immunoglobulin (Ig) heavy chains prior to their assembly with light chains to form the mature Ig molecule, and through its stable association with heavy chains in the absence of light chain synthesis [63]. The two proteins were later shown to be identical, a result which linked its regulation by glucose with a biochemical

function [59]. Hypotheses regarding BiP function have had to integrate the large number of cellular perturbations that result in an induction of BiP synthesis including: (1) inhibition of Asn-linked glycosylation; (2) low glucose levels [64]; (3) disruption of intracellular calcium stores [65, 66]; (4) infection by enveloped viruses [67, 68]; (5) expression of mutant ER proteins defective in folding [57]; and (6) increased expression levels of secretion competent proteins [52, 69, 70].

Even though the precise function of mammalian BiP is still obscure, a general role in the folding and assembly of proteins within the ER has been proposed [59, 71, 72]. Additional roles for BiP include: marking malfolded and mutant proteins for degradation [52, 56, 72]; solubilizing aggregated proteins during times of stress [59]; and the mobilization and regulation of Ca^{2+} sequestered in the ER [73].

Numerous studies have demonstrated that mammalian BiP binds to a large number of proteins traversing the ER [60, 61]. A major question concerning BiP's role is whether it is a component of the secretory pathway under normal growth conditions involved in the folding and assembly of functional proteins. Alternatively, does it function primarily during times of stress, by binding to malfolded proteins and either assisting in their refolding or targeting them for degradation. This issue has been addressed directly in mammalian cells in two recent studies [74, 75]. First, BiP was found to be stably associated with the intermediates of paramyxovirus hemagglutinin neuraminidase glycoprotein [74]. Second, BiP-heavy chain complexes can be dissociated in vivo by the addition of light chain leading to the secretion of immunoglobulin into the culture medium [75]. Thus, in this limited context, BiP can be considered a normal component of the secretory pathway, since it can regulate the transport and maturation of normal proteins.

2. *KAR2: The Yeast Homologue to Mammalian BIP*

In *S. cerevisiae*, BiP is encoded by the KAR2 gene located on chromosome X. The KAR2 gene was originally identified and isolated by two independent methods [76, 77]. Rose et al. isolated the KAR2 gene by complementing the defect in a kar2-1 mutant that exhibited a severe reduction in the frequency of nuclear fusion (karyogamy) during mating [78]. Normington et el. used a murine BiP cDNA as a probe to screen an *S. cerevisiae* cDNA library at a stringency that resulted in a single strongly hybridizing band.

The identification of the product of the KAR2 gene as the yeast homologue of mammalian BiP is based on the finding that the product of the KAR2 gene possesses significant structural similarities with mammalian BiP and shares several characteristic regulatory features. The sequence of the KAR2 gene predicts a protein of 682 amino acids that is closely related to the hsp70 class of proteins including rat BiP (67% identity), murine BiP (67% identity), yeast hsp70s (SSA1, 63% identity), Drosophilia hsp70 (59% identity), and *E. coli* DnaK (50% identity). Similar to other hsp70 proteins, the greatest degree of amino acid divergence in yeast BiP occurs in the carboxyl-terminal 100 amino acids. However, yeast BiP does contain several structural features that are absent among other hsp70 cognates but present in mammalian BiP. First, it contains an 18 amino acid, amino-terminal signal sequence that is cleaved upon entry into the ER. Second, it completely lacks potential sites for Asn-linked glycosylation, in contrast to the yeast hsp70 protein SSA1, which contains 8 potential sites for Asn-linked glycosylation; direct comparison of these two protein sequences reveals that at 6 out of 8 of these sites, a single amino acid change in BiP has disrupted the glycosylation consensus sequence.

Third, yeast BiP contains a C-terminal tetrapeptide His-Asp-Glu-Leu (HDEL) that has been shown to mediate ER retention in yeast [79] in a manner similar to the KDEL system in mammalian cells [80, 81]. Based on these structural criteria, one can propose that yeast BiP is an hsp70 that has evolved to function within the lumen of the ER. Simply put, N and C-terminal additions allow for ER targeting and retention respectively, while limited amino acid changes block the addition of potentially function-disrupting Asn-linked glycosylation.

Southern analysis of yeast genomic DNA under conditions of high stringency using the cloned KAR2 gene as probe indicated that the KAR2 gene was present in a single copy per genome [77]. Yeast BiP was subsequently shown to be essential for growth by disruption of the KAR2 gene [76, 77]. Proteinase K digestion of a crude yeast membrane fraction suggested that yeast BiP was localized to a membranous compartment that could be the ER. This interpretation was supported by immunofluorescent analysis using a polyclonal antibody raised against the carboxyl-terminal 316 amino acids of yeast BiP (most divergent) which revealed a perinuclear ring with occasional filaments extending into the cytoplasm [76]. This pattern of staining was consistent with yeast BiP being localized to the ER and nuclear envelope, since earlier electron microscopic studies of yeast have suggested that the nuclear envelope and ER are continuous [82]. Recent immunoelectron microscopic studies using the same carboxyl-terminal antibody have confirmed the localization of yeast BiP to the ER lumen and nuclear envelope [83], while EM studies in this lab using a yeast strain that overexpresses BiP have also localized BiP to the yeast ER (data not shown).

Based on similarities in amino acid sequence and manner of regulation between yeast BiP and its mammalian counterpart, yeast BiP was originally

assumed to have a role in the folding and assembly of newly synthesized proteins within the ER lumen [76, 77]. Surprisingly, analysis of a temperature sensitive mutation in BiP (kar2-159) identified a role for yeast BiP in ER translocation [31]. Analysis of three different secretory pathway proteins (invertase, ppαf and carboxypeptidase Y) synthesized in kar2-159 cells at the restrictive temperature revealed a severe block in secretion and the accumulation of non-glycosylated, signal peptide-containing, full-length precursors. Subsequent analysis using a protease protection assay demonstrated that the observed phenotype was the result of a block in translocation and not the result of yeast signal peptidase and glycosyl-transferase being dependent upon BiP for activity. An identical phenotype was also seen after depleting wild-type yeast of BiP, suggesting that the block in ER translocation was a direct consequence of a loss in BiP function [31, 84]. This conclusion was further supported by a recent study of the effects of mutations in the KAR2 gene on the translocation of ppαf in vitro [85]. In this study, yeast microsomes prepared from three independent temperature sensitive kar2 alleles (kar2-113, kar2-159 and kar2-203) exhibited temperature-sensitive deficiencies in translocation that paralleled the thermosensitivity of the alleles in vivo. In a complementary study, yeast BiP was efficiently cross-linked to a modified form of ppαf that was covalently coupled to the globular protein avidin and arrested in translocation; this result is also consistent with a direct role for BiP in ER translocation in yeast. Further studies using this same modified ppαf suggested that yeast BiP may also act at a later stage of translocation to advance the initial interaction of the secretory protein with Sec61p and thus form a mature translocation complex [85].

The conclusion that yeast BiP plays a role in ER translocation is provocative, since there is no documented requirement in the mammalian system for BiP or other ER luminal proteins during translocation. In vitro reconstituted mammalian systems using BiP-depleted rough microsomes are still able to translocate and process secretory proteins [86]. In addition, BiP was not detectable by Western blot analysis in an in vitro system composed of detergent solubilized ER proteins reconstituted into proteoliposomes. However, a similar system using a yeast microsomal detergent soluble fraction reconstituted into vesicles with soybean phospholipids was dependent upon both BiP and sec63p for translocation [87]. This differential dependence on BiP does raise the possibility that there may be mechanistic differences between the mammalian and *S. cerevisiae* systems. However, it is also plausible that BiP functions catalytically in protein translocation, and amounts undetectable by Western analysis support the reaction in the mammalian system. Alternatively, it is possible that BiP may be necessary to reset a component of the translocation apparatus after translocation, making that translocon available. The in vitro system, by not requiring multiple rounds of translocation, may not "uncover" this dependence.

Based on these studies a bifunctional role for yeast BiP may be postulated: (1) a role in ER translocation, either directly to facilitate the translocation of secretory pathway proteins, or indirectly to maintain the translocation machinery in a functional state; and (2) an ER luminal role in the folding and assembly of secretory pathway proteins after translocation. However, unlike its mammalian homologue, a direct interaction between yeast BiP and an ER luminal protein has yet to be demonstrated in vivo, and consequently, the hypothesis that it acts within the ER lumen in yeast is only a result of comparison to its mammalian counterpart. One of the aims of the

current work was to investigate a potential luminal role for BiP in yeast in the structural maturation of a soluble secretory protein.

C. SECRETORY PATHWAY REGULATION THROUGH THE INDUCTION OF BIP

1. *BiP Induction: Similarities to the induction of other heat shock genes:*

BiP is expressed constitutively at a basal level under normal growth conditions. A variety of stress conditions can increase BiP transcription from 5-25 fold in mammalian cells [66]. Inhibitors of Asn-linked glycosylation [66], sulfhydryl reducing agents [88], amino acid analogs, viral infection [67, 68], glucose depletion [64], low extracellular pH, depletion of ER calcium stores [66, 89, 90], oxygen depletion, expression of mutant, malfolded, incompletely folded or unassembled secretory pathway proteins [91-93], and overexpression of normal secretory proteins [70], can increase BiP transcription from 5-25 fold. The ability of these diverse stressors to induce BiP transcription has been attributed to their ability to damage the ER and interfere with its function, which in turn leads to the accumulation of malfolded proteins in the ER lumen.

The sequence of events that triggers elevated synthesis of BiP in response to ER stress is not known. It has been proposed that BiP is able to sense the secretory load in the ER and initiate a signaling pathway that ultimately regulates the nuclear transcription of BiP and other ER stress proteins [57], in a manner similar to the feedback regulation proposed for cytosolic hsp70 proteins (see below).

In *E. coli*, the induction of cytoplasmic heat shock genes in response to environmental stress is thought to be initiated through the sequestering of DnaK (*E. coli* hsp70 homologue) in a complex through its binding to aberrant

or malfolded cytoplasmic proteins. This in turn prevents DnaK from interacting with the heat shock transcription factor σ^{32}, which is then free to associate with the RNA polymerase core and confer the specificity required to transcribe heat shock genes [94, 95]. The abundant genetic evidence supporting this model has been recently substantiated by direct evidence for a physical interaction between DnaK and σ^{32} [96].

A similar mechanism of regulating heat shock genes has been proposed in eukaryotic cells, with the additional speculation that cytosolic hsp70 may be the "cellular thermometer" [97]. Again, the hypothesis is that free levels of hsp70 are sensed via their affinity for specific DNA binding proteins (heat shock factors) that activate the transcription of heatshock genes. If malfolded or other aberrant proteins accumulate within the cytoplasm, they will titrate out the available hsp70, leaving the heat shock factors (HSF) free to migrate into the nucleus and activate transcription, and the resultant increase in cytoplasmic hsp70 levels will continue until these HSFs are rebound by hsp70. Several lines of evidence support this "autoregulatory" model: (1) the heat shock transcriptional response is correlated with increased levels of denatured and malfolded proteins [98]; (2) activation of heat shock transcription can be blocked by protein synthesis inhibitors, suggesting that newly synthesized or malfolded or aggregated proteins initiate the response; (3) in yeast, function-disrupting mutations in two constitively expressed cytoplasmic hsp70s (SSA1 and SSA2) result in an increased level of expression of the other members of the hsp70 family under non-stress conditions [99]; (4) mutations which eliminate the HSF binding sites in the promoters of hsp70 genes block this increase in expression [100]; (5) overexpression of HSF in wild-type cells in the absence of heat shock increases the level of hsp70 [99]; (6) inactive HSF in cytoplasmic extracts can be converted to a DNA binding

form by exposure to heat, non-ionic detergents, or low pH; however addition of hsp70 blocks this conversion; and (7) overexpression of the hsp70 protein SSA1 from the yeast GAL promoter reduces the heat shock-mediated increase in expression from an exogenous SSA1-lacZ fusion [101].

Despite the large degree of indirect experimental evidence that has accumulated for this model, a direct demonstration of the negative regulation of HSF by hsp70 still is lacking, i.e. binding. This issue was partially addressed in a recent study that demonstrated that in extracts of heat-shocked cells human hsp70 associates with activated HSF to form a complex that can be disrupted by ATP [102]. In addition, formation of this complex correlated with the level of hsp70 in the cell. Further analysis using an in vitro activation assay demonstrated that addition of exogenous hsp70 completely inhibited the activation of HSF to a DNA-binding form and that this inhibition could be relieved by the addition of ATP. These results add an additional degree of complexity to the proposed model for heat shock gene activation in higher eukaryotes by proposing that HSF associates as a monomer with hsp70 in non-heat-shocked cells. This association prevents the activation of HSF into a DNA-binding form. Upon heat shock, the newly created pool of denatured and malfolded proteins competes for hsp70 binding, which in turn leads to the release of HSF. The released HSF can now form trimers and bind DNA.

While the potential similarities are obvious, the signal transduction pathway that allows malfolded proteins within the lumen of the ER to lead to the specific transcription of ER stress proteins within the nucleus is essentially uncharacterized. Certainly, any comparisons between a hypothetical feedback system operating between the ER and nucleus and the current general model for the transcriptional regulation of cytoplasmic heat shock genes will be complicated by the additional step of transducing the

signal across the ER membrane. One study that directly addressed this issue in mammalian cells concluded that BIP was regulated in a feedback manner, since CHO cells that stably overexpressed BIP exhibited a reduced level of BiP induction in response to two traditional inducers, TM and Ca^{2+} ionophore (A23187) treatment [103]. Further support for a feedback mechanism comes from a recent study in yeast, where the authors used a yeast strain containing a KAR2 promoter-*lac*Z reporter construct and a GAL promoter-BiP construct to demonstrate a reduced level of β-galactosidase activity after exposure to TM when cells were grown on galactose [104].

While the nature of the signaling pathway is unknown, the initial stimulus that activates this pathway is currently under intense scrutiny. Based on the results of the "feedback" studies, current hypotheses have focused on an indirect mechanism of sensing the level of malfolded or mutant proteins within the ER through their interaction with BiP, with the signal being either the depletion of free BiP or the formation of a BiP-protein complex (bound BiP).

Experimental attempts to determine between whether free BiP or bound BiP is the signal have been inconclusive. In one study, the authors claimed that the level of bound BiP was the signal, based on an in vivo analysis using COS cells transformed with immunoglobulin μ chain cDNA. The formation of a stable complex between μ chain and BiP correlated with the induction of ER stress proteins as measured by both Northern and Western analysis [93]. Unfortunately, the authors did not entertain the possibility that a *decrease* in the level of free BiP could be responsible, an alternative hypothesis supported by their data. Evidence for the level of free BiP being the signal is more substantial. The experiments in CHO cells support the hypothesis that the level

of free BiP is the initial signal, since overexpression of BiP dampens the transcriptional response.

Further support for a feedback mechanism where the level of free BiP is sensed comes from a study in yeast where the C-terminal retention signal of yeast BiP (HDEL) was deleted, resulting in the loss of intracellular BiP through secretion. The compensatory increase in the synthesis of BiP can be attributed to a feedback mechanism dependent upon the level of free BiP within the ER lumen, since the intracellular levels of BiP were found to be identical in both the wild-type and HDEL containing strains, while the level of potential substrates should be unchanged [105].

To monitor the levels of free BiP, the cell must be able to distinguish between bound and unbound, or free BiP. Insight into how this could be accomplished comes from two studies which analyzed the role of BiP post-translational modifications on binding [106, 107]. In the first study, heat shock and glucose starvation were shown to reduce the incorporation of radiolabeled ADP-ribose into BiP in avian and mammalian cells. In the second study, free BiP was shown to be post-translationally modified by phosphorylation and ADP-ribosylation, and both modified and unmodified forms of BiP coexist within the cell. Most importantly, BiP bound to Ig heavy chain was not labeled with either radioactive phosphate or adenine. Further, when BiP was induced by glucose starvation, the ratio of unmodified (bound) to modified (free) forms of BiP increased, possibly indicative of an increase in the level of bound BiP. Thus one could postulate that the cell monitors the level of free BiP through a mechanism that is dependent upon the ratio of modified to unmodified BiP.

2. *Transcriptional Regulation of KAR2 Gene Expression*

Yeast BiP appears to be regulated in a manner similar to mammalian BiP, since drug treatments and mutations that lead to the accumulation of secretory proteins within the ER lumen result in an increase in KAR2 mRNA levels [76, 77]. However, in contrast to mammalian cells, transcription of KAR2 is also stimulated by heat shock [76, 77]

Recently, two detailed analyses of the KAR2 promoter were performed by generating a set of 5' unidirectional deletion mutants lacking progressively larger segments of upstream sequences [104, 108]. Based on these analyses, a 236 bp XhoI-SalI fragment was shown to contain all the information necessary to transcriptionally regulate the KAR2 gene. In addition, construction of a series of 5' deletions within this 236 bp fragment resulted in the identification of three *cis*-acting separate transcriptional control elements: (1) a 22 bp sequence located between -131 to -110 that conferred responsiveness to the presence of malfolded proteins within the lumen of the ER referred to as the unfolded protein response element (UPR); (2) a GC-rich region located between -148 to -133 that is similar in sequence to the consensus element for binding of the mammalian transcription factor Sp1, and is responsible for the high level of constitutive expression of the KAR2 gene; and (3) a 20 bp region between -168 to -149 containing the consensus sequence for the heat shock element (HSE) that responds to elevated temperatures. By constructing a series of 10 bp deletion mutants within each of the three identified elements it was determined that these elements work independently of each other. Further analysis of the UPR element demonstrated that it was capable of conferring transcriptional induction to the accumulation of malfolded proteins within the ER lumen to a heterologous CYC1 promoter. Using DNA gel shift analysis, a trans-acting factor that binds specifically to the UPR element was also

identified (UPRF-1). Similar to the results reported for the heat shock transcription factor HSF, UPRF-1 is present in equal concentrations in both stressed and unstressed cell extracts, suggesting that the transcriptional activation that occurs in response to the accumulation of unfolded proteins within the ER lumen may involve the modification of a pre-existing pool of UPRF-1.

D. MT EXPRESSION IN YEAST AND ITS REGULATION BY COPPER

The ability an organism to survive in an environment that contains either toxic or excessive concentrations of essential metal ions is a well conserved stress response. The detoxification of metal ions can occur either by regulating their uptake, a mechanism more common in prokaryotes [109, 110] or by intracellular sequestration, a mechanism preferred by eukaryotes [111]. While *S. cerevisiae* requires copper (Cu^{2+}) at low concentrations for proper growth [112], Cu^{2+} is a potent fungicide at higher concentrations. In yeast, resistance to the toxic effects of excessive Cu^{2+} is mediated through the induction of metallothionein (MT), a low molecular weight (6.5 kD) cysteine-rich, Cu^{2+} binding protein encoded by the CUP1 locus [113, 114]. The CUP1 promoter satisfies many of the criteria for an efficient and regulated yeast promoter [113]. Most importantly for this work, addition of Cu^{2+} to the media results in a 25-fold increase in the transcriptional induction of the CUP1 gene.

Since MT represses its own gene transcription, the induction ratio of a plasmid-borne MT gene fusion is directly proportional to the number of MT genes present on the yeast chromosomes [115, 116]. When a cup1-disrupted strain is used as a host, transcription is partially constitutively active, while if a chromosomally amplified $CUP1^r$ strain is used, a complete repression to basal levels is observed. Thus, by choosing an appropriately yeast strain a range of

basal and inducible transcription levels of CUP1 gene expression can be selected. In this work, we use the CUP1 promoter to provide an exogenous means of regulating BiP expression.

E. BRIEF HISTORY OF THIS PROJECT

The work described in the thesis grew out of a collaboration between our lab and that of Dr. Janet Kurjan. Dr. Shari Caplan, as a Ph.D. student in the Kurjan lab, constructed a large number of mutant MFα1 genes and substituted then individually for the wild-type chromosomal MFα1 gene. She then tested their functionality using two bioassays that detect secreted αf: Formation of halos using MATa cells (induction of G_1 arrest), and mating between α and a cells. These assays, however, are limited in their accuracy and sensitivity by technical and theoretical factors.

I entered the project at this point, having developed a quantitative biochemical assay for transport and processing of pαf. As described in the Results, the combination of pulse-chase labeling, SDS-PAGE, and HPLC allowed us to determine the functional effects of mutations in ppαf. I analyzed a large number of mutants, and the results have been published [55]. The work described here focused on the triple glycosylation mutant N123-ppαf, since it exhibited the most severe defect in transport and processing.

II. EXPERIMENTAL PROCEDURES

A. MICROBIAL TECHNIQUES

1. *Yeast*

a. Yeast Media:

The yeast media used in this project were as described [117]: Complete dextrose media (YPD) contained 1% (w/v) yeast extract (Difco), 2% (w/v) Bacto-Peptone (Difco) and 2% (w/v) glucose (Sigma); Synthetic minimal media (SD) contained 0.67% (w/v) yeast nitrogen base without amino acids (Difco), 2% (w/v) glucose, supplemented with adenine (50 μg/ml), histidine (25 μg/ml), leucine (30 μg/ml), lysine (30 μg/ml), uracil (25 μg/ml) and tryptophan (30 μg/ml) as needed (all from Sigma). For plates 2% (w/v) select agar (Sigma) was included. Media were sterilized by autoclaving at 121° C for 15 min. All supplements were added from concentrated stocks prior to autoclaving.

b. Yeast Transformations:

Yeast cells were transformed with centromeric, episomal and integrative plasmids by the lithium acetate method essentially as described [118]. Briefly, cells were incubated in TE containing 100 mM lithium acetate (TELA buffer) at 30° C for 60 min before adding sheared salmon sperm DNA (as carrier) and transforming DNA (1 μg DNA/10 OD_{600} cells). After a 30 min incubation at 30° C, cells were treated with PEG 4000 (Gibco-BRL) and heat-shocked as described. Finally, samples were spread on selective media plates and incubated at 30° C until colonies appeared. In general, colonies were clearly visible in two days and ready for picking in three days.

The temperature sensitive sec18 strain was transformed in essentially the same manner except that all the incubations were done at room

temperature and were doubled in length. In most cases yeast colonies were clearly visible in three to four days and ready for picking in four to five days.

c. Yeast DNA Quick Prep:

Total yeast DNA for PCR amplification and Southern analysis was obtained using the "Ten-minute DNA Prep for Yeast" as described without modification [119].

d. Growth curves and viability:

The growth of all yeast strains was monitored by direct counting of cell number using a Bright-Line Hemacytometer (Reichert) with phase-contrast microscopy (Zeiss) at 400X magnification.

The percent viability was defined as the absolute number of viable organisms present, divided by the total number of organisms present, dead or alive. In this study, the yeast cell was considered viable if it was capable of forming a colony on selective solid media after a defined period of growth on selective plates. The % viability was calculated by spreading equal numbers of control and TM treated cells and counting the number of colonies present after five days of growth.

e. Starting yeast strains:

The initial strains from which all strains were constructed are shown in Table 1. Strains 2C, N123 and $\alpha_1\alpha_2$ are isogenic to the parent strain W3031-B at all loci except in strain N123, where mfα1-N123 has been integrated into the MFα1 locus, and in strain $\alpha_1\alpha_2$, where LEU2 has been integrated into both the MFα1 and MFα2 loci. A summary of all the constructed strains is shown in Table 5 (see Experimental Procedures, Strain Construction).

Table 1. Starting Yeast Strains

Strain	Genotype	Source
W303-1B	MATα. ade2-1; can1-100; leu2-3,112; his3-11,15; trp1-1; ura3-1.	J. Kurjan
2C	MATα. **MFα1**, mfα2::LEU2C. ade2-1; can1-100; leu2-3,112; his3-11,15; trp1-1; ura3-1.	J. Kurjan
N123	MATα. **mfα1-N123**, mfα2::LEU2C. ade2-1; can1-100; leu2-3,112; his3-11,15; trp1-1; ura3-1.	J. Kurjan
α1α2	MATα. **mfα1::LEU2C, mfα2::LEU2C**. ade2-1; can1-100; leu2-3,112; his3-11,15; trp1-1; ura3-1.	J. Kurjan
sec18	MATα. **sec18-1**; trp1-289; leu2-3,112; ura3-52.	P. Bohni
Y262	MATα. ura3-52; **rpb1-1**.	R. Young

2. *Bacteria*

a. Bacterial Media:

The bacterial medium used in this project was Terrific Broth [120]. Media were sterilized by autoclaving at 121° C for 15'. Ampicillin was added after autoclaving to a final concentration of 50 μg/ml.

b. Bacterial Strains:

The *Escherichia coli* strains MC1000 or HB101 were used in all the molecular manipulations of this project as specified.

c. Bacterial Transformations and DNA isolation:

Transformation competent *E. coli* cells were prepared according to the original $CaCl_2$ method of Mandel and Higa [121] without modification. Transformations with plasmid DNA were as described [122]. Small (mini-preps) and large scale (maxi-preps) preparations of bacterial plasmid DNA were performed using the alkaline-lysis method as described without modification [120]. Plasmid DNA from large scale preparations was purified by precipitation with polyethylene glycol as described without modification [120].

B. PLASMID CONSTRUCTION

1. *Starting plasmids*

The plasmids used as vectors or as sources of DNA inserts for the construction of new plasmids are shown in Table 2. The oligonucleotides used for KAR2 cloning, KAR2 sequencing and the synthesis of chromosomal KAR2 probes are shown in Table 3. The resulting new constructs (described below) are shown in Table 4.

Table 2. Starting Plasmids

Name	Description	Source
Vectors:		
pGEM-1	In vitro transcription vector with the multiple cloning site flanked by **T7** and **SP6** RNA polymerase transcription initiation sites; (2865 bp); Amp selection.	Promega
pRS314	Yeast **centromeric** plasmid (TRP1 marker) with the multiple cloning site flanked by T7 and T3 RNA polymerase transcription initiation sites; (4785 bp); Amp selection.	P. Heiter
pRS316	Yeast **centromeric** plasmid (URA3 marker) with the multiple cloning site flanked by T7 and T3 RNA polymerase transcription initiation sites; (4895 bp); Amp selection.	P. Heiter
pYEP353	Yeast **episomal** plasmid (URA3 marker); (8000 bp); Amp selection.	G. Small
pYSK136	Yeast **episomal** plasmid with the TRP1 marker and with the multiple cloning site flanked by the **CUP1** promoter and **CYC1** transcription terminator (6258 bp); Amp selection.	J. Kurjan
Inserts:		
pHK2	pBR322 with the 1.7 kb **MFα1 gene** cloned into the EcoR I site; (6061 bp); Amp selection.	J. Kurjan
M13-N123	M13mp10 with the 1.7 kb **mfα1-N123** gene cloned into the EcoR I site; (8950 bp); Amp selection.	S. Caplan
pCMP171	Yeast centromeric plasmid containing a tandem repeat of the 1.76 BamH I fragment of the yeast **HIS3** gene.	M. Brennan
pGACT	pGEM-4 with the 700 bp EcoR I - Hind III yeast **Actin** gene inserted into the multiple cloning site; (3571 bp); Amp selection.	A. Tzagoloff

Table 3. Oligonucleotides

Oligo	Location	Sequence	Use
K2-3	279-296	5' - GGGGGGTCGACCATACCATGTTTTTCAAC - 3'	Cloning
K2-4	2319-2336	5' - CCCCCGTCGACTATCTACAATTCGTCGTG - 3'	Cloning
K2S1	CUP1 *	5' - GTCTTGTATCAATTGCAT - 3'	KAR2 Seq.
K2S2	401-418	5' - AGTTAGAGGTGCCGATGA - 3'	KAR2 Seq.
K2S3	641-658	5' - GATCGGTTTGAAATATAA - 3'	KAR2 Seq.
K2S4	881-898	5' - GCAAAGACAAGCCACCAA - 3'	KAR2 Seq.
K2S5	1121-1138	5' - CTATAAGATCGTTCGTCA - 3'	KAR2 Seq.
K2S6	1361-1378	5' - GAAGCCTGTCGAGAAGGT - 3'	KAR2 Seq.
K2S7	1601-1618	5' - CAACGCTTTGACTCTTGG - 3'	KAR2 Seq.
K2S8	1841-1858	5' - CACATTTGCACTTGACGC - 3'	KAR2 Seq.
K2S9	2081-2098	5' - CCTAGGTGAAAAATTGGA - 3'	KAR2 Seq.
K2-10	3-20	5' - CGAGCAAAGTGTAGATCC - 3'	Probe
K2-11	2763-2780	5' - CTCGAGCCTTTCAACTCT - 3'	Probe
K2G-1	249-271	5' - CGCTTTTTCCCTTGAGACTACTC - 3'	Probe
K2G-2	2355-2372	5' - GCTGCTGGAAGCTTCAAG - 3'	Probe

* Oligonucleotide K2S1 is homologous to a sequence in the CUP1 promoter, and sequences across the transcription start into the KAR2 coding region.

Table 4. Constructed Plasmids

Plasmid	Description
pGK2	pGEM-1 with the 2.0 kb Sal I fragment containing the **KAR2 coding region** cloned into the unique Sal I site of the multiple cloning site (4865 bp).
pGK2-HIS3	pGK2 with the 1765 bp BamH I fragment containing the yeast **HIS3** gene cloned into the unique Stu I site within the **KAR2 coding region** (6625 bp).
pHCK2	pYSK136 with the 2.0 kb Sal I fragment containing the **KAR2 coding region** cloned into the unique Xho I site between the **CUP1** promoter and **CYC1** terminator (8258 bp).
pLCK2-T	pRS314 with the 2.8 kb BamH I-Cla I fragment containing the **CUP1-KAR2-CYC1** cloned into the multiple cloning site (7585 bp).
pLCK2-U	pRS316 with the 2.8 kb BamH I-Cla I fragment containing the **CUP1-KAR2-CYC1** cloned into the multiple cloning site (7695 bp).
pLCαF-T	pRS314 with the 1.7 kb Eco R I fragment containing the **MFα1** gene cloned into the unique EcoR I site of the multiple cloning site (6485 bp).
pLCαF-U	pRS316 with the 1.7 kb Eco R I fragment containing the **MFα1** gene cloned into the unique EcoR I site of the multiple cloning site (6595 bp).
pLCN123-T	pRS314 with the 1.7 kb Eco R I fragment containing the **mfα1-N123** gene cloned into the unique EcoR I site of the multiple cloning site (6485 bp).
pLCN123-U	pRS316 with the 1.7 kb Eco R I fragment containing the **mfα1-N123** gene cloned into the unique EcoR I site of the multiple cloning site (6595 bp).
pHCαF	pYEP353 with the 1.7 kb Eco R I fragment containing the **MFα1** gene cloned into the unique EcoR I site of the multiple cloning site (9700 bp).
pHCN123	pYEP353 with the 1.7 kb Eco R I fragment containing the **mfα1-N123** gene cloned into the unique Eco R I site of the multiple cloning site (9700 bp).

2. *Construction of CUP1-KAR2 containing plasmids*

a. PCR Isolation of the KAR2 coding region and sequencing:

The coding region of the KAR2 gene was isolated from yeast genomic DNA (strain 2C) by PCR amplification using the oligonucleotide KAR2 cloning primers K2-3 and K2-4 (see Table 3). Primer K2-3 contains 18 nucleotides complementary to the 5' end of the KAR2 coding region (including the initiator codon), as well as an 11 nucleotide extension containing the Sal I restriction enzyme consensus sequence. Primer K2-4 contains 18 nucleotides complementary to the 3' end of the KAR2 coding region (including the stop codon), as well as an 11 nucleotide extension containing the Sal I restriction enzyme consensus sequence. The 100 µl PCR reaction was carried out in 25 mM KCl, 2.5 mM $MgCl_2$, 20 mM Tris-HCl (pH 8.3), 0.2 mM of each dNTP, 1.0 mM of each primer, 25 U/ml of Taq DNA Polymerase (Promega) and 1 µg of yeast genomic DNA from strain 2C as the source of the target KAR2 gene. Thirty cycles of 90 seconds at 94° C, 150 seconds at 53° C, and 150 seconds at 72° C in a Perkin Elmer Cetus DNA Thermal Cycler were used to amplify the KAR2 coding region. The reaction was than extracted with phenol/chloroform and ethanol precipitated. The PCR amplified insert was digested with Sal I to completion and the resulting 2.0 kb insert was purified on a 1.0% TBE agarose gel and ligated into the Sal I site of the plasmid pGEM-1, generating the new plasmid pGK2 (See Figure 2).

The 2.0 kb insert was shown to be identical to the published sequence for the coding region of the KAR2 gene by DNA sequencing using a series of nested oligonucleotide primers K2S1 to K2S9 (Table 3). Automated DNA sequencing was performed at the Mount Sinai DNA Core facility on an Applied Biosystems Model 373A Sequencer using Taq polymerase and dye-labeled-dideoxynucleotides.

Figure 2. Cloning of the KAR2 coding region and construction of the plasmid pGK2.

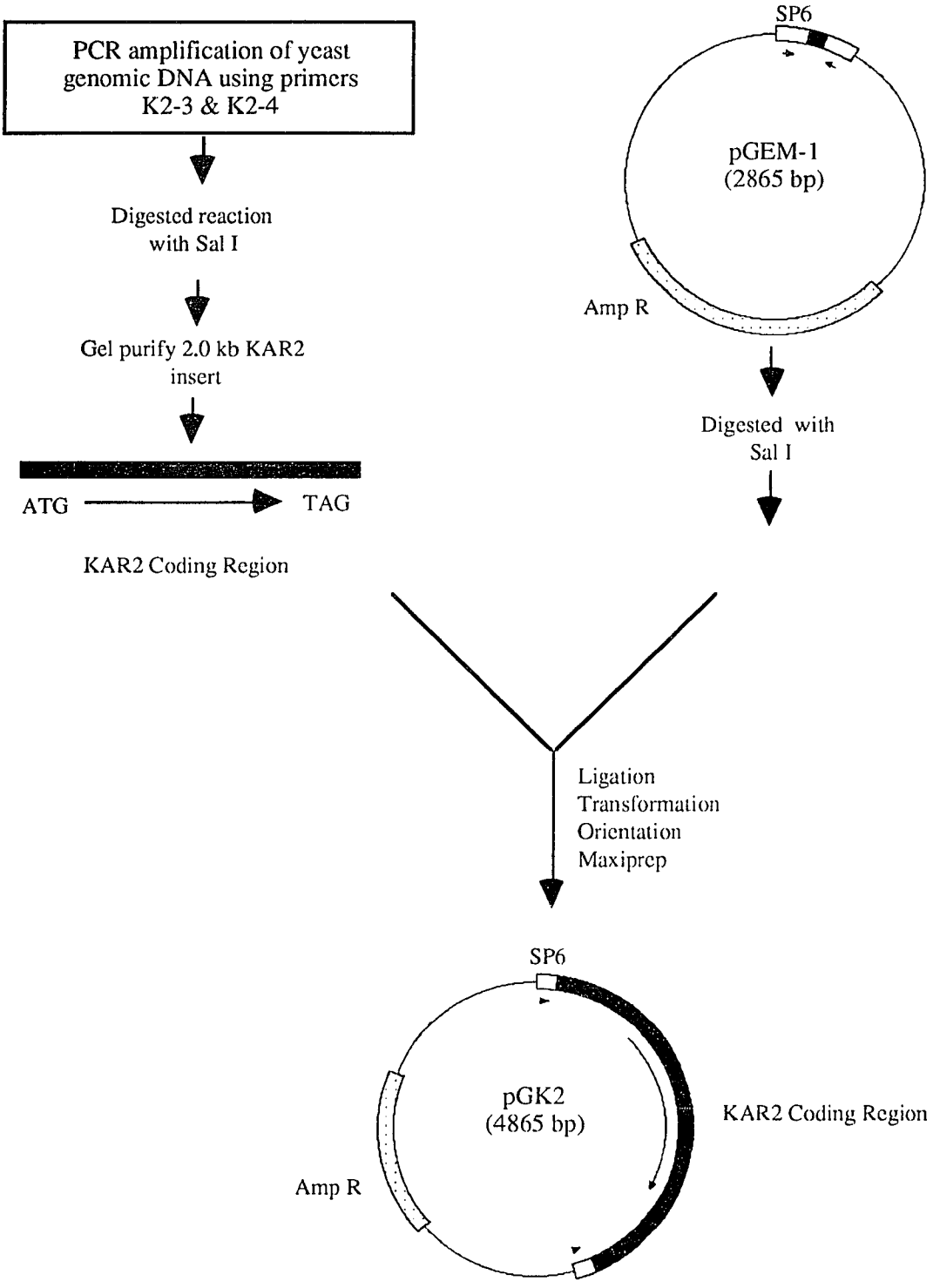

b. High-copy Cup1-KAR2 plasmid (pHCK2):

A yeast episomal plasmid with the KAR2 coding region under the control of the CUP1 copper responsive promoter was constructed as follows (Figure 3). DNA from plasmid pGK2 was digested with Sal I to regenerate the 2.0 kb insert containing the KAR2 coding region and subcloned into the unique Xho I site of the polylinker of the CUP1-containing episomal plasmid, pYSK136. This placed the coding region of the KAR2 gene between the copper-responsive CUP1 promoter and the CYC1 transcription terminator of plasmid pYSK136, generating the new episomal plasmid pHCK2.

c. Low-copy Cup1-KAR2 plasmids (pLCK2-T & pLCK2-U):

Yeast centromeric plasmids containing the CUP1-KAR2 construct were constructed as follows (Figure 4). DNA from the new plasmid pHCK2 was double digested with BamH I and Cla I, generating a 2.8 kb CUP1-KAR2-CYC1 containing insert. The insert was than gel purified and directionally subcloned into the multiple cloning sites of the yeast centromeric plasmids pRS314 and pRS316, generating the new yeast centromeric plasmids, pLCK2-T and pLCK2-U, respectively.

d. Construction of plasmid pGK2-HIS3:

As a first step in the disruption of the chromosomal KAR2 gene the HIS3 gene was inserted into the KAR2 coding region of plasmid pGK2 as follows (Figure 5). First, plasmid pCMP171 was digested with BamH I to produce a 1.76 kb DNA fragment that contained the HIS3 gene. The 5' and 3' termini were filled in with the Klenow fragment of DNA polymerase I to generate a blunt-ended fragment, which was then purified on a 1.0 % TBE agarose gel. The 1.76 kb fragment was then ligated into the unique Stu I restriction site within the KAR2 gene of plasmid pGK2 to generate the new plasmid pGK2-HIS3.

Figure 3. Construction of plasmid pHCK2.

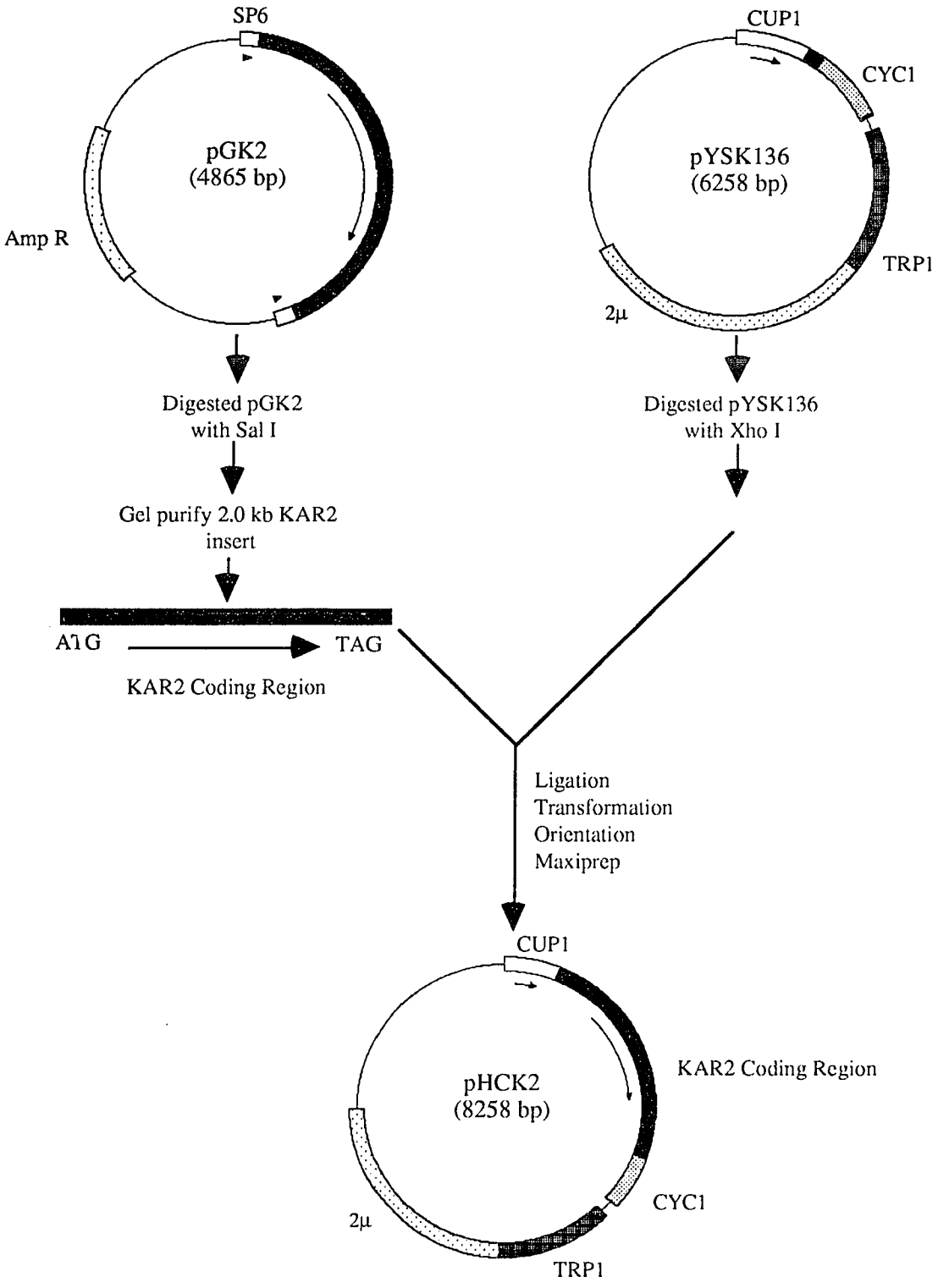

Figure 4. Construction of plasmids pLCK2-T and pLCK2-U.

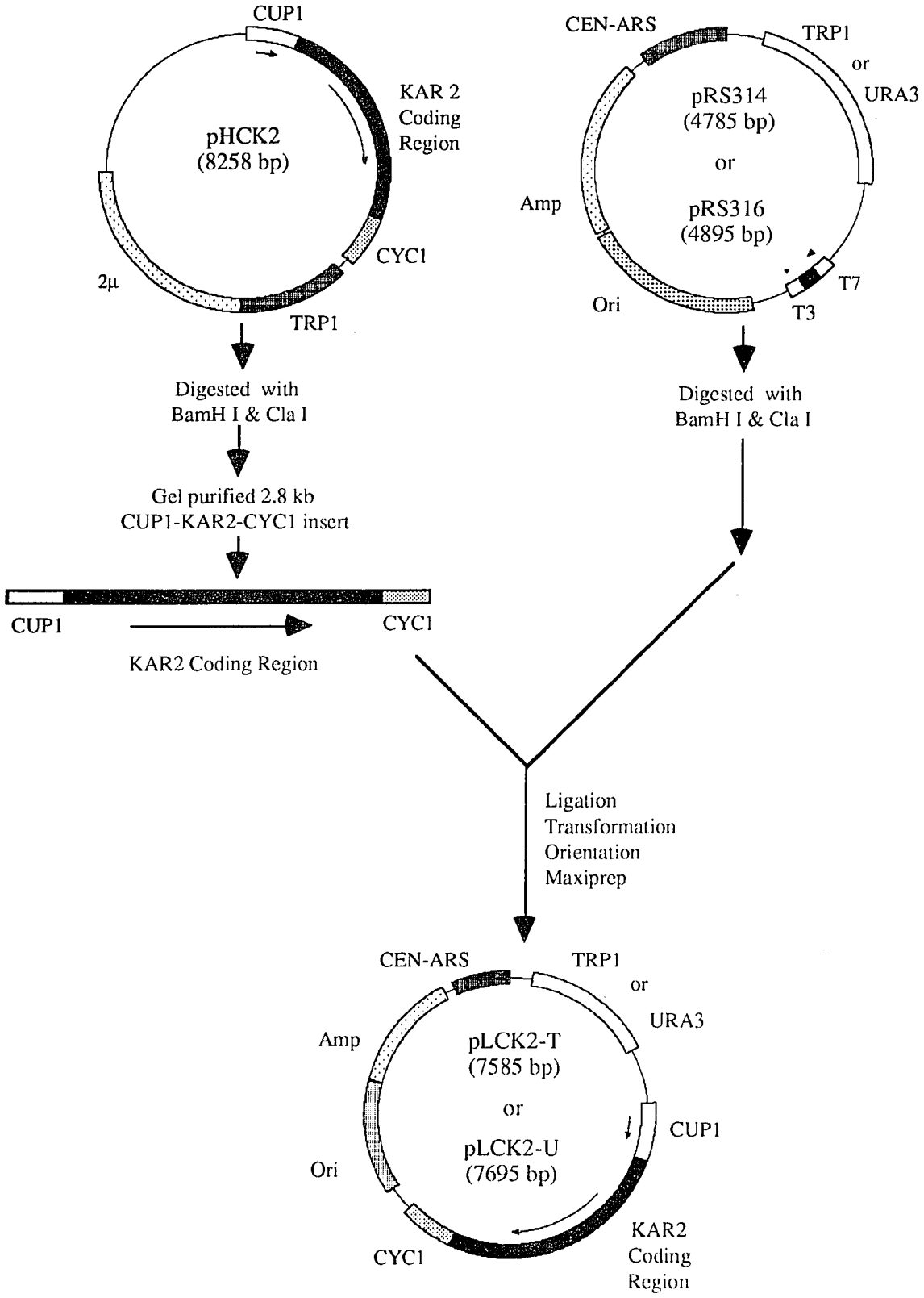

Figure 5. Construction of plasmid pGK2-HIS3.

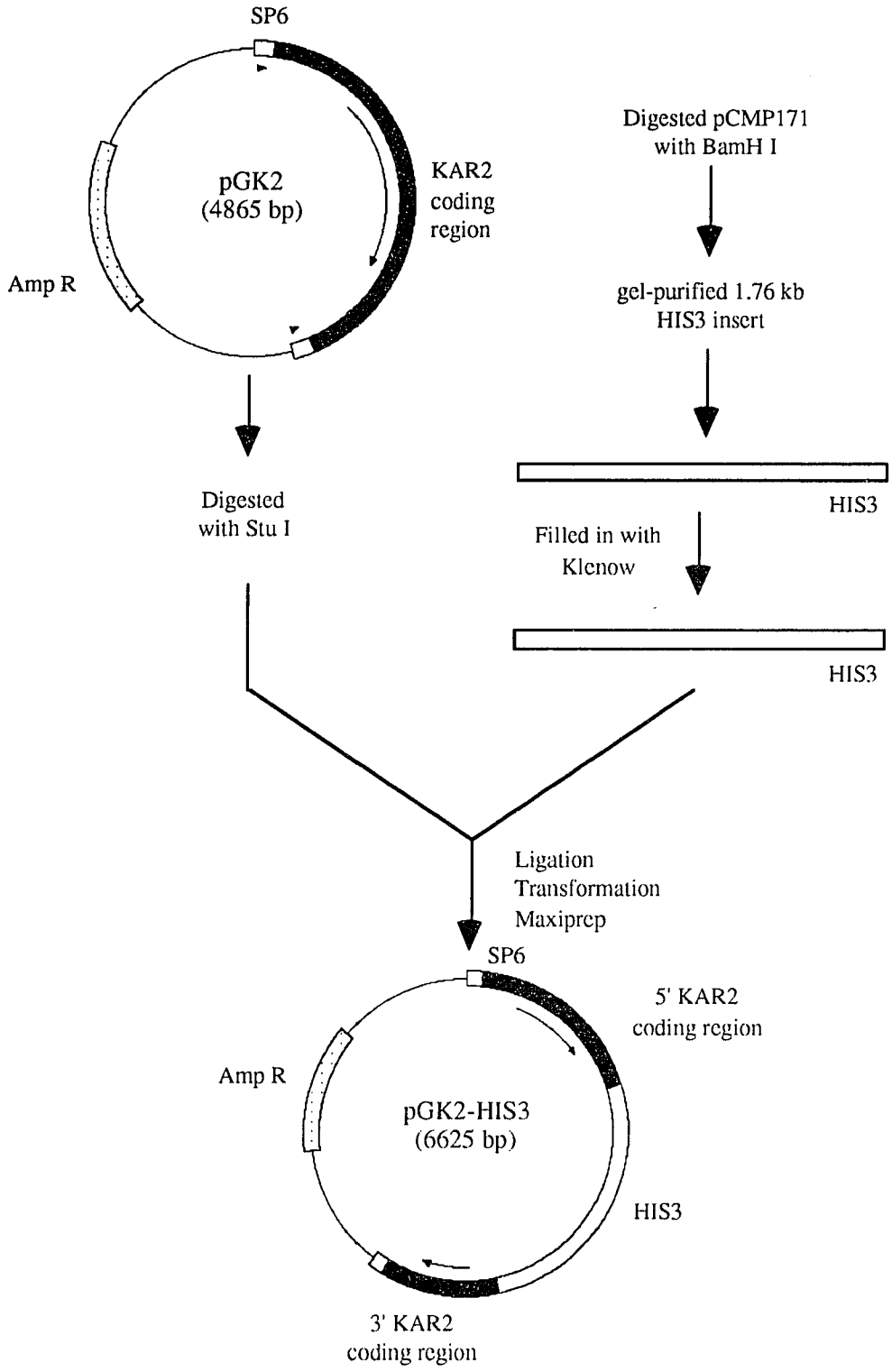

3. *Construction of low and high-copy wild-type and mutant MFα1 plasmids*

High and low-copy plasmids containing the MFα1 gene were constructed as follows. DNA from plasmid pHK2 was digested with EcoR I generating the 1.7 kb MFα1 containing insert, which was gel purified and subcloned into the unique EcoR I site of the polylinker of plasmids pRS314 and pRS316, resulting in the new plasmids pLCαF-T and pLCαF-U, respectively. The orientation of the MFα1 gene was chosen such that in vitro transcription of the MFα1 gene was under the control of the T7 promoter. The 1.7 kb MFα1 containing insert was also subcloned into the unique EcoR I site of the polylinker of the yeast episomal plasmid pYEP353, generating the new episomal plasmid pHCαF.

High and low-copy plasmids containing the mfα1-N123 gene were constructed as follows. DNA from plasmid M13-N123 was digested with EcoR I generating the 1.7 kb mfα1-N123 containing insert which was gel purified and subcloned into the unique EcoR I site of the polylinker of plasmids pRS314 and pRS316, resulting in the new plasmids pLCN123-T and pLCN123-U, respectively. The orientation of the mfα1-N123 gene was chosen such that in vitro transcription of the mfα1-N123 gene was under the control of the T7 promoter. The 1.7 kb mfα1-N123 insert was also subcloned into the unique EcoR I site of the polylinker of the yeast episomal plasmid pYEP353, generating the new episomal plasmid pHCN123. Maps of these plasmids are shown in Figure 6.

Figure 6. Low and high-copy ppαf and N123-ppαf expressing plasmids.

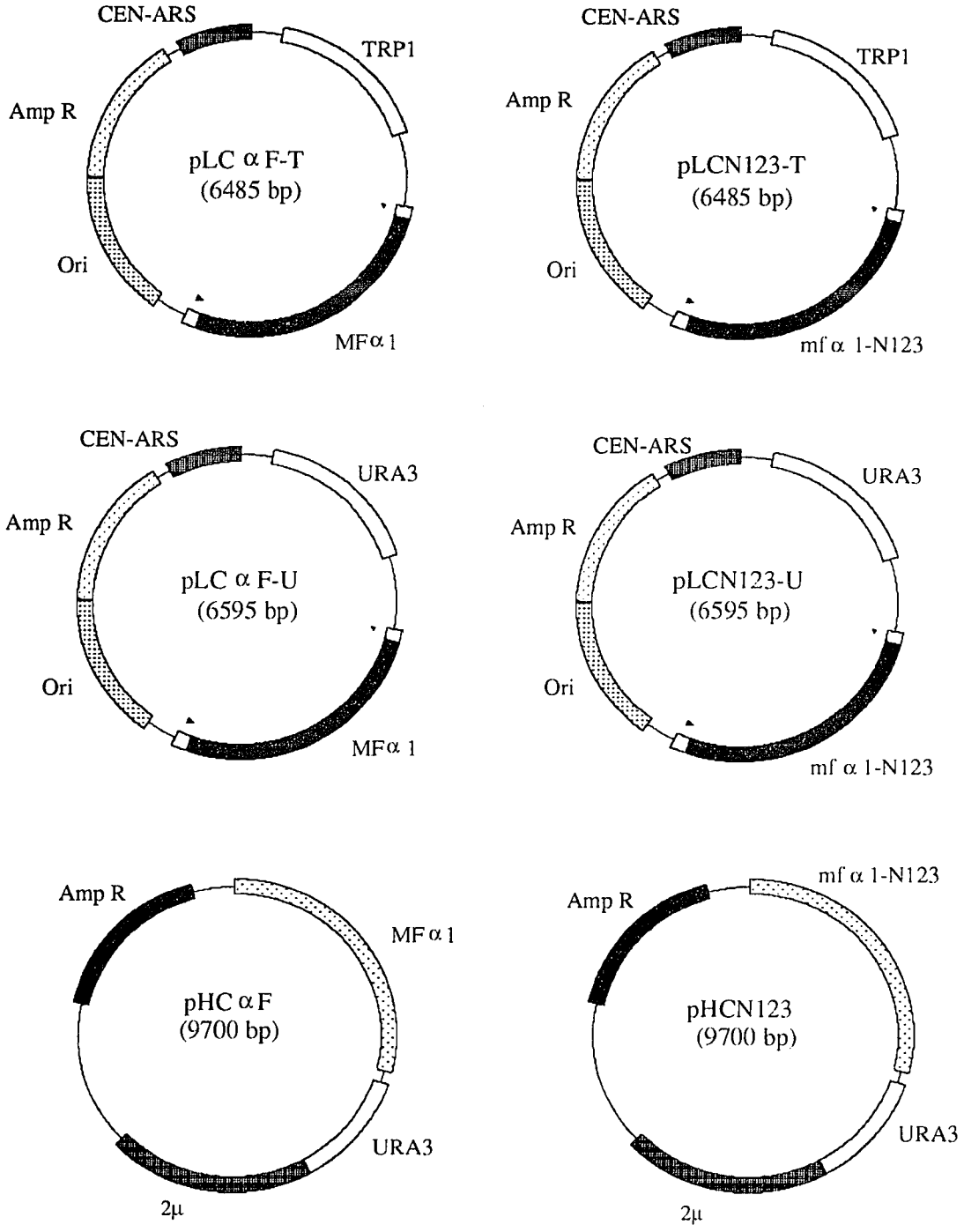

C. STRAIN CONSTRUCTION

1. *KAR2 disrupted strains*

a. Construction of the low-copy CUP1-KAR2 containing strains:

The low copy CUP1-KAR2 expressing strains were constructed by transforming the starting strains 2C and N123 with the centromeric plasmid pLCK2-T, generating the new strains 2CLCK2 and N123LCK2, respectively.

b. Disruption of the KAR2 Gene:

The KAR2 gene was disrupted using the one-step gene disruption method (Figure 7) as described [123]. The 3.8 kb insert resulting from the digestion of plasmid pGK2-HIS3 with Sal I contained the HIS3 gene flanked on either side by the KAR2 coding region. This insert was then used to transform strains 2CLCK2 and N123LCK2 to disrupt the chromosomal copy of the KAR2 gene and generate the new strains 2CΔ and N123Δ. His^+ yeast colonies were selected and screened for a successful disruption as described below.

c. Confirmation of the KAR2 disruption:

Disruption of the genomic KAR2 gene in strains 2CΔ and N123Δ was confirmed by three independent methods. First, Southern blot analysis was performed on genomic DNA isolated from a number of HIS^+ putative 2CΔ and N123Δ colonies. Genomic DNA from the starting strains 2C and N123, or the HIS^+ putatively disrupted strains 2CΔ and N123Δ, was digested with Xho I and probed with nick-translated KAR2 coding region DNA. The non-disrupted strains had a single reacting band of 2775 bp consistent with the Xho I fragment of genomic KAR2 DNA, while successfully disrupted strains had three reacting bands of 7643 bp (linearized plasmid pLCK2-T), 2821 bp (1494 bp of 5' KAR2 sequence + 1327 bp of HIS3 sequence), and 1719 bp (1281 bp of 3' KAR2 sequence + 430 bp of 3' HIS3 sequence). Second, colonies identified as disrupted by Southern analysis were analyzed by PCR using the KAR2 cloning

Figure 7. One-step disruption of the chromosomal KAR2 gene.

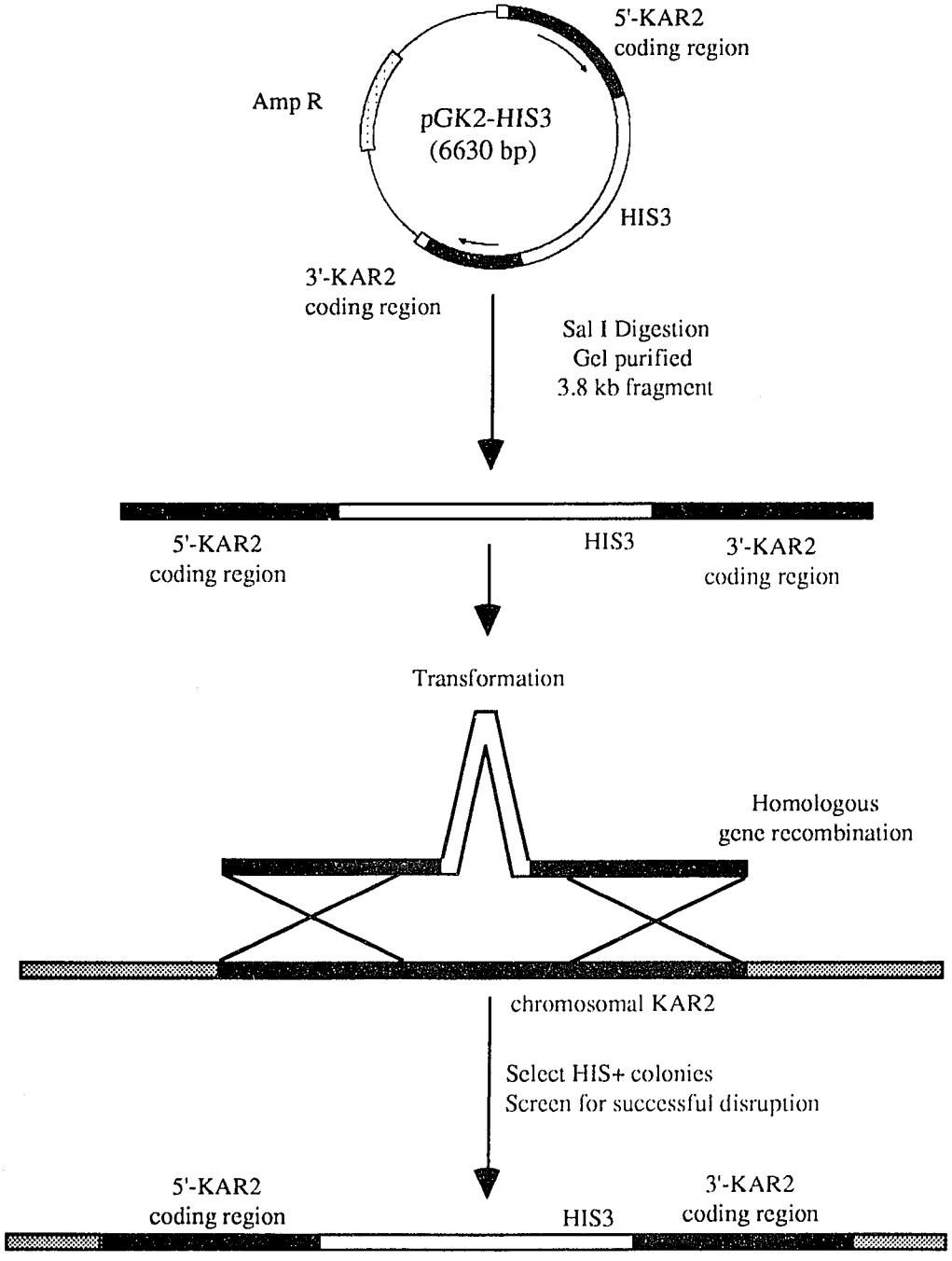

Disrupted chromosomal KAR2 gene

primers K2-10 and K2-11. In non-disrupted and control strains use of these two primers amplified a band 2775 bp in length corresponding to the intact KAR2 gene, while in the disrupted strains the amplified band was 4540 bp in length corresponding to the KAR2 gene with a 1765 bp HIS3 insert. As the third and final method of confirmation, strains that were shown to be disrupted by both Southern analysis and PCR amplification were subject to Northern analysis using probes specific to the 5' and 3' untranslated regions (UTR) of the KAR2 gene (Figure 8). The absence of BiP genomic mRNA after Northern analysis was considered to be an evidence for a successfully disrupted gene (see Results).

d. Construction of the high-copy Δ strains:

In addition to the lowcopy Δ strains, KAR2 disrupted strains overexpressing either ppαf (HC2CΔ) or N123-ppαf (HCN123Δ) were constructed by transforming the new strains 2CΔ or N123Δ with the high-copy episomal plasmids pHCαF and pHCN123, respectively.

2. *Other strains*

a. Construction of the high-copy CUP1-KAR2 containing strains:

The high copy CUP1-KAR2 expressing strains were constructed by transforming the starting strains 2C and N123 with the episomal plasmid pHCK2, generating the new strains 2CHCK2 and N123HCK2, respectively.

b. Construction of the high-copy ppαf and N123-ppαf strains:

High-copy ppαf and N123-ppαf strains were constructed by transforming strain $\alpha_1\alpha_2$ with the episomal plasmids pHCαf or pHCN123 respectively. Successful transformants were confirmed by Northern analysis, which demonstrated 10-fold higher levels of ppαf and N123-ppαf mRNA.

Figure 8. Construction of DNA probes specific for chromosomal and plasmid-derived BiP mRNA.

Chromosomal-derived BiP:

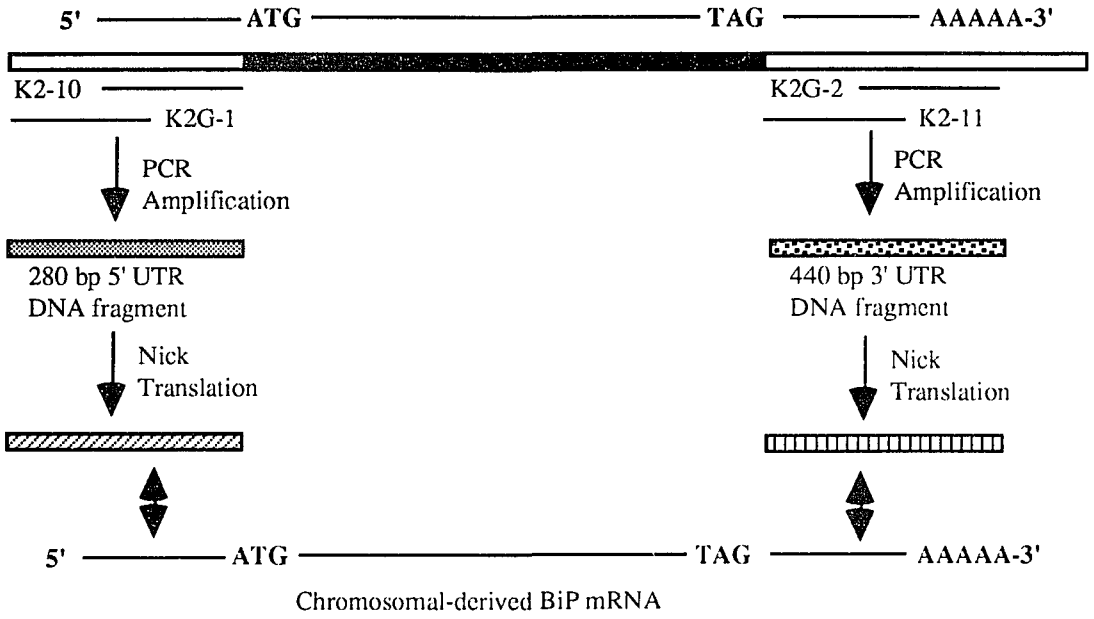

Plasmid-derived BiP mRNA:

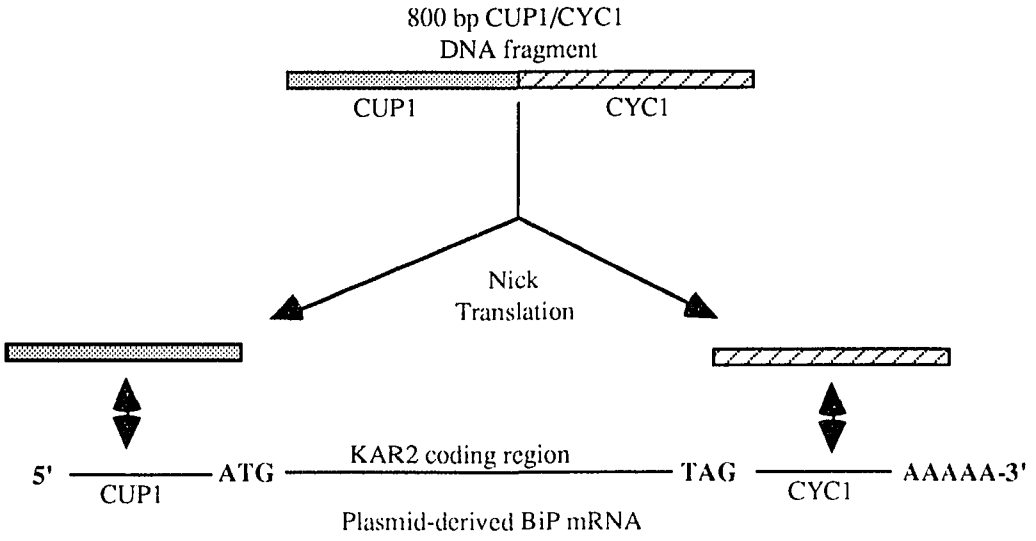

Table 5. Constructed Yeast Strains

Strain	Genotype
ppαf	
2CLCK2	MATα. **MFα1**, mfα2::LEU2C. ade2-1; can1-100; leu2-3,112; his3-11,15; trp1-1; ura3-1; **pLCK2-T**.
2CΔ	MATα. **MFα1**, mfα2::LEU2C, **kar2::HIS3**. ade2-1; can1-100; leu2-3,112; his3-11,15; trp1-1; ura3-1; **pLCK2-T**.
HC2CΔ	MATα. **MFα1**, mfα2::LEU2C, **kar2::HIS3**. ade2-1; can1-100; leu2-3,112; his3-11,15; trp1-1; ura3-1; **pLCK2-T; pHCαF**.
2CHCK2	MATα. **MFα1**, mfα2::LEU2C. ade2-1; can1-100; leu2-3,112; his3-11,15; trp1-1; ura3-1; **pHCK2**.
HC2C	MATα. **mfα1::LEU2C, mfα2::LEU2C.** ade2-1; can1-100; leu2-3,112; his3-11,15; trp1-1; ura3-1; **pHCαF.**
N123-ppαf	
N123LCK2	MATα. **mfα1-N123**, mfα2::LEU2C. ade2-1; can1-100; leu2-3,112; his3-11,15; trp1-1; ura3-1; **pLCK2-T**.
N123Δ	MATα. **mfα1-N123**, mfα2::LEU2C, **kar2::HIS3**. ade2-1; can1-100; leu2-3,112; his3-11,15; trp1-1; ura3-1; **pLCK2-T**.
HCN123Δ	MATα. **mfα1-N123**, mfα2::LEU2C, **kar2::HIS3**. ade2-1; can1-100; leu2-3,112; his3-11,15; trp1-1; ura3-1; **pLCK2-T; pHCN123**.
N123HCK2	MATα. **mfα1-N123**, mfα2::LEU2C. ade2-1; can1-100; leu2-3,112; his3-11,15; trp1-1; ura3-1; **pHCK2**.
HCN123	MATα. **mfα1::LEU2C, mfα2::LEU2C**. ade2-1; can1-100; leu2-3,112; his3-11,15; trp1-1; ura3-1; **pHCN123**.

D. YEAST RNA ISOLATION AND NORTHERN ANALYSIS

1. *Yeast RNA Isolation*

Yeast RNA was isolated as described with only minor modification [124]. Briefly, 5 to 10 ml cultures were grown under selective pressure to an OD_{600} of 1.0 to 1.5 (mid-log phase). The cells were harvested and resuspended in 400 µL of ice-cold AE buffer (50mM Na acetate pH 5.3, 10 mM EDTA) to which 40 µL of 10% SDS and 440 µL of hot phenol (equilibrated in AE Buffer) at 70° C were added. The suspension was vortexed, incubated at 70° C for 5 min, snap-frozen in liquid nitrogen, and then allowed to thaw during a 10 min centrifugation at 12,000g at room temperature. The upper aqueous phase extracted with 440 µL of phenol/chloroform, and RNA was precipitated with ethanol. RNA concentration and purity were determined by measuring the absorbance at 260 and 280 nm. The quality of the RNA was determined by ethidium bromide staining of total RNA run on a RNA formaldehyde gel (samples showing evidence of 18S and 28S rRNA degradation were discarded).

2. *Preparation of Northern blots*

RNA was separated in 1-1.3% agarose gels containing formaldehyde and transferred to nitrocellulose essentially as described [125].

3. *Probes*

a. DNA inserts for probe synthesis:

DNA fragments for probe synthesis by nick translation were prepared as follows: (1) The actin insert was prepared by double digestion of plasmid pGACT with EcoR I and Hind III, followed by gel purification of the resulting 700 bp fragment; (2) The ppαf insert was prepared by digestion of plasmid pHK2 with EcoR I, followed by gel purification of the resulting 1700 bp

fragment; (3) The insert specific for plasmid-derived BiP was prepared by double digestion of plasmid pYSK136 with BamH I and ClaI followed by gel purification of the resulting 800 bp fragment (Figure 8); (4) Inserts specific for chromosomal-derived BiP were prepared by PCR amplification of the 5' and 3' UTR of the KAR2 gene using the oligonucleotide primers (K2-10, K2G1) and (K2-11, K2G2) followed by gel purification of the resulting 280 (5' UTR) and 440 (3' UTR) bp fragments (Figure 8).

b. Labeling and purification:

Radiolabeled DNA probes for Northern blotting were prepared by nick translation (Promega Nick Translation Kit) of DNA fragments using dCTP as the radionucleotide. In a typical 50 µl reaction, 12.5 µl of dCTP (800 Ci/mmole) was used to label 1.0 µg of target DNA. Specific activities were typically 1-2 x 10^8 cpm/µg. Radiolabeled DNA was separated from free radionucleotide by spin chromatography.

4. *Hybridization*

Radiolabeled probes were hybridized to RNA immobilized on nitrocellulose membranes in heat-sealable bags as described [120]. Approximately 0.2 ml of hybridization solution (6X SSC, 5X Denhardt's reagent, 0.5% SDS, 100 µg/ml sheared salmon sperm DNA) was added per square centimeter of membrane. Membranes were preincubated for a minimum of two hours at 65° C before adding denatured probe. Nick translated probe was denatured by boiling for 5 min before adding directly to the bag at a concentration of 1 x 10^6 cpm/ml. Hybridization was carried out for at least 16 hours at 65° C. At the end of the hybridization period the membranes were washed sequentially with 1X SSC and 0.1% SDS (20 min at room temperature)

and three times in 0.2X SSC and 0.1% SDS (20 min at 65° C). The membranes were then allowed to dry and exposed to film.

The hybridization of probes was quantified in the following manner. Membrane slices containing the bands of interest were excised using the exposed film as a template. 5.0 ml of scintillation cocktail were added to each membrane slice and the samples were counted in a Beckman LS1801 counter. Membrane slices from regions without RNA were cut and counted in triplicate and subtracted as background from all data. In addition, all data points were normalized by their relative level of actin mRNA.

5. *Measurement of mRNA decay rates*

BiP mRNA decay rates were measured using a yeast conditional mutant strain (Y262) that rapidly ceases synthesis of mRNA when incubated at the nonpermissive temperature. mRNA decay rates were measured in cultures of 100 ml in which the temperature of the culture was abruptly switched from 24° C to 36° C by adding an equal volume of YPD medium at 48° C and transferring the culture to a water bath at 36° C for the remainder of the incubation. 10 ml aliquots of the culture were removed at the indicated time points to extract total RNA as described. The relative level of BiP mRNA was determined by Northern analysis followed by direct counting of excised bands as described above.

E. PULSE-CHASE ANALYSIS OF αf BIOGENESIS

1. *Preparation of radiolabeled cell lysates and media*

An overnight culture of the yeast strain of interest was grown up from a single colony in 100 ml of selective media in a 500-ml Erlenmeyer flask at 30° C. Mid-log phase cells were harvested by centrifugation, resuspended at an

OD_{600} of 1.0, and incubated for an additional 3 hours. The OD_{600} was measured and 50 OD_{600} units were harvested by centrifugation and resuspended in 4.0 ml of prewarmed selective media at a concentration of 12.5 OD_{600}/ml. Cells were then preincubated at 30° C for 15 min, during which time cells were exposed to TM (50 μg/ml).

To initiate the pulse, ^{35}S-methionine (1000Ci/mmole of ^{35}S-TRANS-Label) was added to the specified concentration, and cells were then incubated for 5 min. Aliquots were centrifuged, and cells were spun down and resuspended in selective medium containing unlabeled methionine at 10 mM and 1.0 mg/ml of BSA. Samples were brought to 1 mM PMSF and 10 mM NaN_3, rapidly chilled and centrifuged to pellet the cells. The supernatant was carefully removed and stored on ice. The cell pellets were washed once with ice-cold 10 mM NaN_3 and resuspended in ice-cold Yeast Extraction Buffer containing 1 mM PMSF. An equal volume of glass beads was added and the cell pellets were disrupted by vortexing for 20 min at 4° C. Total disruption of the yeast cell wall was always confirmed by examining the sample for intact yeast cells by phase microscopy (400X). The yeast cell lysate sample was then adjusted to 2.5% SDS, boiled for 5 min and centrifuged. The supernatant (cell lysate) was carefully removed and TCA precipitated cpm were determined.

2. *Immunoprecipitation*

a. Antibodies:

The anti-BiP antibody (gift of M. Rose) was prepared in New Zealand White rabbits using a fusion protein containing the carboxy terminal 216 residues of yeast BiP fused to the E. coli TrpE expressed from plasmid pATH2 [76]. The anti-αf antibody (gift of D. Shields) was prepared from New Zealand

White rabbits using the mature αf peptide coupled to keyhole limpet hemacyanin (KLH).

b. Immunoprecipitation of cell lysates and media samples:

The cell lysate samples were prepared for immunoprecipitation by the addition of 1.0 ml of 1X Antibody Buffer A (190 mM NaCl, 50 mM Tris-HCL pH 7.4, 6 mM EDTA, 2.5% (v/v) Triton X-100, 1 mM PMSF, 1 mg/ml BSA). 5 µl of anti-αf antibody were added and the samples were incubated for 12-16 hours at 4° C with rotation. 75 µl of a 33% (v/v) solution of Protein A Sepharose Cl-4B (Sigma) in Antibody Buffer B (150 mM NaCl, 10 mM Tris-HCL pH 8.3, 5 mM EDTA, 0.1% (v/v) Triton X-100, 1 mM PMSF, 1 mg/ml BSA) was then added and the samples were incubated for an additional 3 hours at 4° C. Each immunoprecipitated sample was then sequentially washed 4X with 1.0 ml of Ab Buffer B followed by 2 washes with PBS.

The media samples were prepared for immunoprecipitation by the addition of 0.35 ml of 4X Antibody Buffer A. 5 to 10 µl of anti-αf antibody were added, and the samples were processed as just described. The PAS pellets, in this case, were prepared for HPLC as described below.

3. *SDS-PAGE analysis*

The PAS pellets were resuspended in SDS-PAGE sample buffer, boiled for 5 min, centrifuged, and the resulting supernatant (cell lysate) was analyzed by SDS-PAGE on a Hoeffer SE 600 Cooled Vertical Slab Unit using 1.5 mm slab gels with a 5% stacking gel and a 18% separating gel. Following electrophoresis, labeled protein bands in gels were visualized by fluorography, using 2,5-Diphenyl-oxazole (PPO) in DMSO. Gels were then dried in a Hoeffer Easy Breeze Gel drier and exposed to film (Kodak XAR5) at -80° C. Protein bands of interest were quantitated by densitometry using the LKB 2222-020 Ultroscan XL Laser

densitometer on gel films of equal exposure time, and normalized using cell lysate TCA precipitable counts.

4. *High Performance Liquid Chromatography (HPLC)*

PAS pellets containing immunoprecipitated secreted αf were prepared for HPLC analysis by resuspending the washed PAS pellets in 50 µL of TEU buffer (8M Urea, 500mM Tris-HCl pH 8.8, 20mM EDTA, 100mM DTT) and incubating at 50° C for 30 min. An additional 50 µL of TEU buffer containing 0.66 M iodoacetic acid was then added and the samples were incubated in the dark at room temperature for 10 min. Each sample was then spun for 1 min in a microcentrifuge and the supernatent was removed and saved. The PAS pellet was then washed with 50 µL of TEU and combined with the first supernatant. 20 µL of 1.5% (w/v) TFA-80% CH_3CN was then added and the sample was filtered through a 0.22 µm Millipore Ultrafree-MC Filter (UFC3-0GV-25) by centrifugation at 2500g in a Millipore mini-centrifuge. The sample was then transferred to a 300 µl HPLC vial for automated sample injection. The samples were analyzed using a Hewlett Packard 1090 HPLC equipped with a VYDAC Reverse Phase C_{18} analytical column (4.6 mm ID x 1/4" x 25 cm L, 5 µm). ^{35}S-methionine labeled secreted αf was separated using 0.15% (w/v) TFA-H_2O-acetonitrile as the mobile phase. The elution gradient used to resolve the αf peptide was as follows: 0-5 min - 20% CH_3CN; 5-30 min - 20-60% CH_3CN, 30-35 min - 60-100% CH_3CN; 35-40 min - 100-20% CH_3CN, and from 40-45 min 20% CH_3CN (Figure 9D). The HPLC flow rate was 0.5 ml/min. Under these conditions two major αf-containing peaks of radioactivity were typically observed. The peak at 18.5 min represents methionine sulfone-containing αf, since treatment of the immunoprecipitated media sample with 5% H_2O_2 results in a single peak at 18.5 min (data not shown). The peak at 21 min represents the

unoxidized methionine form of the mature αf peptide. The peak at 7 min represents unincorporated ^{35}S-methionine. The ^{35}S-methionine-labeled αf in the eluate was detected by mixing with a high efficiency, non-gelling scintillation fluid (FLO-SCINT II) and applied to a Radiomatic FLO-ONE Beta detector for detection. The levels were quantified using manufacturer's software.

F. DETECTION OF BIP BY WESTERN BLOTTING

1. *Protein extraction*

Total yeast proteins were extracted essentially as described with only minor modification [126]. Briefly, 25 OD_{600} units of mid-log phase cells (OD_{600} = 1.0) were harvested, washed twice in ice-cold 10 mM Tris-HCl, 1 mM EDTA (pH 7.0), and resuspended in 250 µl of ice-cold Extraction buffer containing 1% Nonidet P-40, 0.5% deoxycholate, 0.1% Sodium dodecyl sulfate, 150 mM NaCl, 50 mM Tris-HCl (pH 8.0), 1 mM EDTA, leupeptin (1 µg/ml), Pepstatin (1µg/ml) and 1 mM phenylmethylsulfonyl fluoride (PMSF). An equal volume of 425-600 micron, acid-washed glass beads (Sigma) was added and the cells were disrupted by vortexing for 15 min at 4° C using a VWR Vortex-Genie 2 Mixer with the large sample head. Total disruption of the yeast cell wall was always confirmed by examining the protein extract for intact cells by phase microscopy. The protein extract was then clarified by centrifugation at 12,000g for 1 min at 4° C in a microcentrifuge. The supernatant was carefully removed and snap frozen in liquid N_2. Protein concentrations were determined using the DC Protein Assay (Bio-Rad), a colorimetric assay for protein concentration following detergent solubilization.

2. *Western analysis*

Proteins analyzed by SDS-PAGE on a Hoeffer mini-gel apparatus were transferred to nitrocellulose (Sigma) using a Hoeffer Semi-dry apparatus. Upon completion of protein transfer, the nitrocellulose membrane was blocked by incubating in Immunoblot buffer (500 mM NaCl, 25 mM Tris-HCl(pH 7.5) containing 10% (w/v) nonfat dried milk (Carnation) and 0.1% (v/v) Tween (Bio-Rad). Anti-BiP antibody at a 1/20,000 dilution was added, and the membrane was incubated for an additional 3 hours. The membrane was then extensively washed, and incubated with the secondary antibody, anti-rabbit Ig-Horse radish peroxidase (HRP) linked $F(ab')_2$ fragment from Donkey (Amersham) at a 1/5000 dilution for exactly 1 hour, followed by extensive washing. The antigen-antibody-antibody conjugated to HRP was detected using the Enhanced Chemiluminescence (ECL) system according to the manufacturer's protocols (Amersham).

G. IN VITRO TRANSCRIPTION AND TRANSLATION

1. *In vitro transcription and translation*

a. In vitro transcription:

RNA was synthesized in vitro from linearized DNA templates using SP6 or T7 RNA Polymerase (Promega or BRL) according to manufacturer's instructions. The DNA template was then removed by the addition of RNase-free DNase (Promega or Pharmacia). The reaction was then extracted with an equal volume of phenol:chloroform, followed by an extraction with chloroform alone. The RNA was then recovered essentially free of nucleotides by three successive ethanol precipitations. The final RNA pellet was resuspended in 50 µl of ddH_20. The concentration and purity was determined

by measuring the A_{260} and A_{280}. The RNA was stored at -80° C. Using this protocol, yields of 5-10 µg RNA/µg of DNA template were routinely obtained.

b. In vitro translation:

Protein was synthesized in vitro from RNA templates in the following manner. A typical 25 µl reaction contained: 0.2-1.0 µg RNA; 2.5 µl of 10x WGCB (20 mM Hepes-pH 7.2, 90 mM KAc, 16 mM $Mg(Ac)_2$, and 0.8 mM Spermine); 2.5 µl of 10x EGS-Met (12 mM ATP, 2.4 mM GTP, 96 mM creatinine phosphate, Amino acid mix (400 mM) without methionine, creatinine-phosphokinase (0.64 mg/ml); 2.5 µl of ^{35}S-Met (10 µCi/µl); 10 µl of Wheat Germ extract and 1 µl of 50 mM DTT. When specified, DPRM were included at 2.0 µl/25 µl reaction and 1.0 µl of 0.05% Nikkol was added to enhance translocation efficiency. The reaction components were all added on ice, and the typical reaction was incubated at 28° C for 60 min.

c. Preparation of Wheat Germ Extract:

Wheat Germ was prepared as described with several modifications [127]. Briefly, Wheat Germ (General Mills) was ground in a chilled mortar and pestle in WG Extraction Buffer (10 mM Tris-acetate pH 7.6, 90 mM KAc, 3 mM $Mg^{2+}(Ac)_2$, 1 mM DTT). The resulting suspension was centrifuged in a SS34 rotor at 14,000 rpm for 10 min. The supernatant was removed, adjusted by adding 200 µl of 1.0 M Tris-acetate pH 7.6 and 20 µl of 1.0 M $Mg^{2+}(Ac)_2$ for every 10.0 ml of supernatant, and recentrifuged under identical conditions. The resulting supernatant was applied to a Sephadex G-25 gel filtration column (1.5 x 25 cm; medium grade) equilibrated in WG Elution buffer (1 mM Tris-acetate pH 7.6, 50 mM KAc, 1 mM $Mg^{2+}(Ac)_2$, 0.028% β-mercaptoethanol), and the void volume was collected and centrifuged in a SS34 rotor at 14,000 rpm for 10 min before being snap frozen in liquid N_2.

2. *Rough microsomes*

a. Introduction:

Canine pancreatic rough microsomes (DPRM) were used in this project at several points to generate in vitro translated ppαf and BiP that had undergone ER processing. The DPRM preparation, however was part of an earlier project in which I developed a modification to their isolation protocol which significantly improved their purity and activity.

b. Isolation and characterization:

DPRM were initially isolated as described in the original protocol by Walter and Blobel [128]. All steps were carried out a 4° C in the cold room as quickly as possible. Briefly, the pancreas was removed, rinsed twice with ice-cold buffer A (250 mM Sucrose, 50 mM TEA (pH 7.5), 50 mM KAc, 6 mM $Mg^{2+}(Ac)_2$, 1 mM EDTA, 1 mM PMSF and 1 mM DTT), cleaned, minced with a razor blade, and homogenized in 4.0 ml buffer A per gram of pancreas in either a motor-driven Potter-Elvehjem homogenizer or Tekmar polytron. Assay of several different preparations revealed that the Potter-Elvehjem homogenizer, which disrupts by liquid shear, produced membranes with greater activity than the Tekmar polytron, which uses mechanical shear. The liquified pancreas was then loaded into 30.0 ml Corex tubes and centrifuged for 10 minutes at 1000 g_{av} in a SS34 rotor (Sorval) to pellet nuclei and cell debris. The floating fat layer was aspirated off and the resulting supernatant was then centrifuged at 10,000 g_{av} for 10 minutes in a SS34 rotor (Sorval) to pellet mitochondria and large sheets of non-vesiculated endoplasmic reticulum and plasma membrane. Again the floating fat layer was aspirated off and the resulting supernatant was layered over a 1.3M sucrose cushion in buffer A (load:cushion was 3:1) in 25.0 ml Sorval tubes and centrifuged at 4° C for 2.5 hours at 140,000 g_{av} (40,000 rpm) in a Ti 50.2 rotor (Sorval). The resulting

supernatant and membranous interface were removed by aspiration, and the pellet containing rough microsomes was resuspended by manual homogenization (4 strokes) in Buffer B (250 mM Sucrose, 50 mM TEA (pH 7.5), and 1 mM DTT) using a Dounce homogenizer (type B).

c. Purification by gel filtration:

To assure consistent performance with minimal translation inhibition and background, the DPRM were further processed by a column washing step to remove adsorbed ribosomes and proteins. DPRM prepared in this way were typically much less inhibitory to protein synthesis, but showed no loss of translocation activity when compared to the original unwashed DPRM. Briefly, the DPRM in buffer B were taken up in 100 volumes of wash buffer (50 mM TEA (pH 7.5), 6 mM $Mg^{2+}(Ac)_2$, 0.5 mM EDTA and 1 mM PMSF) and applied to a Sephacryl S-1000 column equilibrated in wash buffer. The size of DPRM is estimated to be > 100 $x10^6$ Da, while small polysomes and ribosomes have been estimated to be less than 20 $x10^6$ Da based on size fractionation on Sepharose columns. Gel Filtration on Sephacryl S-1000, with a measured exclusion limit of 100 $x10^6$ Da, should be able to exploit this five-fold difference in size and rapidly separate DPRM from free polysomes and ribosomes. The resulting microsomal fraction eluted at the Vo of the column, well separated from free-polysomes and ribosomes. The DPRM containing fractions were then pelleted by centrifugation at 4° C for 1 hour at 90,000 g_{av} (32,000 rpm) in a Ti 50.2 rotor (Sorval). The DPRM pellets were resuspended by manual homogenization (4 strokes) in buffer B using a Dounce homogenizer (type B). The yield of rough microsomes was then quantified by absorbance at A_{260} and A_{280} in 1% SDS. Application of this protocol typically yielded 50 A_{280} units of membranes per gram of canine pancreas. The efficiency of membrane translocation of the purified DPRM was determined by assaying the efficiency of signal peptide

cleavage and core glycosylation, using ppαf mRNA. Protection of the processed secretory proteins from exogenous trypsin was used to confirm the lumenal location of the processed pre-protein. Ppαf is processed by DPRM with at least 80% efficiency, and the processed product is resistant to trypsin digestion, confirming a luminal location.

III. RESULTS

CHAPTER I. BIP FUNCTION IN THE YEAST SECRETORY PATHWAY

A. *Role of Asn-linked glycosylation in the transport and processing of yeast prepro-α-factor*

To test the role of Asn-linked glycosylation in pro-α-factor (pαf) transport and processing without the use of tunicamycin (TM), we studied a yeast strain (designated N123), which expresses a triple glycosylation mutant of prepro-α-factor (N123-ppαf). The N123 strain, constructed by Dr. S. Caplan, contains an integrated mutant MFα1 gene in which all three Asn-linked glycosylation recognition sites have been changed from Asn-Thr-Thr to Asn-Thr-Ala by site-directed mutagenesis [129]. Since the N123 strain is isogenic to the wild-type strain (2C) at all loci except the MFα1 locus, any differences in αf biogenesis can be attributed to the expression of N123-ppαf.

To quantify the effect of a lack of glycosylation on ppαf, we utilized two parallel approaches. First, N123-ppαf processing and secretion were measured in strain N123 by pulse-chase analysis in the absence and presence of TM. Second, as an alternative but complementary approach, an identical analysis was performed on strain 2C in the absence and presence of TM. In both cases, early log-phase yeast were pulse-labeled with ^{35}S-methionine and chased for increasing times in the presence of excess unlabeled methionine. Cell lysates and media samples were prepared as described in the Experimental Procedures. The level of ^{35}S-methionine-labeled intracellular precursor was quantitated by immunoprecipitation with anti-αf antibodies followed by SDS polyacrylamide gel electrophoresis (SDS-PAGE). Radiolabeled protein markers

Figure 9. Analysis of wild-type and mutant ppαf transport and processing.

(A) In vitro translation (IVT) of wild-type and mutant ppαf mRNA. mRNA was synthesized by T7 RNA polymerase using plasmids pLCαF or pLCN123. The resulting mRNA was translated in a wheat germ IVT system containing ^{35}S-methionine, in the absence or presence of canine pancretic rough microsomes (RM) as described. For protection studies, the IVT reaction was incubated with Proteinase K (PK) on ice for 1 hour. **(B)** SDS-PAGE profile of vitro synthesized markers and immunoprecipitated pαf from a typical pulse-chase analysis using strain HC2C in the presence of TM. **(C)** SDS-PAGE profile of immunoprecipitated gpαf and N123-pαf from a typical pulse-chase analysis using strains HC2C & HCN123. In both **B** and **C** yeast cell lysates were prepared as described and subjected to immunoprecipitation with anti-αf antibody, followed by SDS-PAGE on 18% polyacrylimide gels. **(D)** HPLC elution gradient profile for analysing immunoprecipitated media samples for secreted αf. The gradient of 0.15% TFA-acetonitrile (organic phase) is indicated (dotted line). Elution of radiolabeled αf from a typical immunoprecipitated media sample is superimposed on the elution gradient (solid line). **(E)** HPLC elution profile time points from a typical pulse-chase analysis using strain HC2C. Media samples were prepared as described, and the secreted αf levels were determined by immunoprecipitation with anti-αf antibody followed by HPLC analysis.

Figure 9. Analysis of wild-type and mutant ppαf transport and processing.

A. In vitro

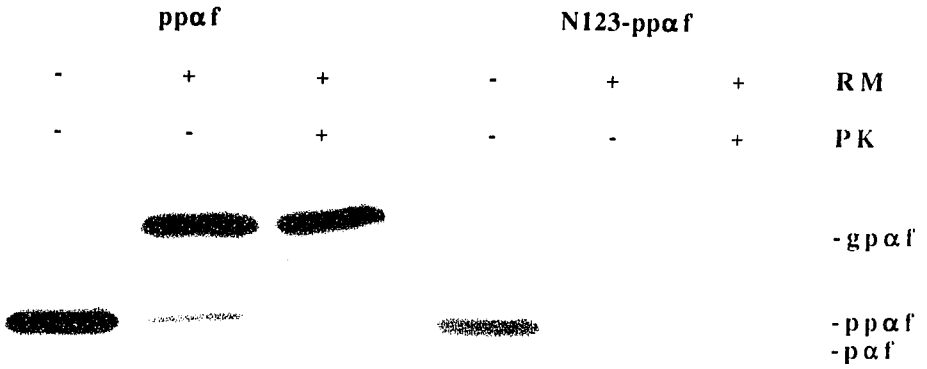

B. In vivo

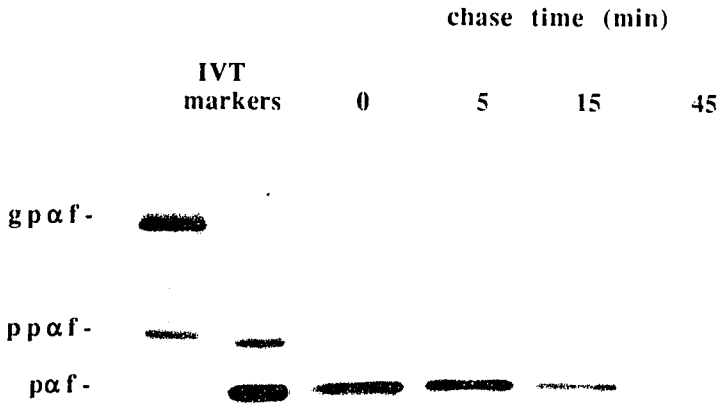

C. Pulse-chase analysis of wild-type and mutant pαf

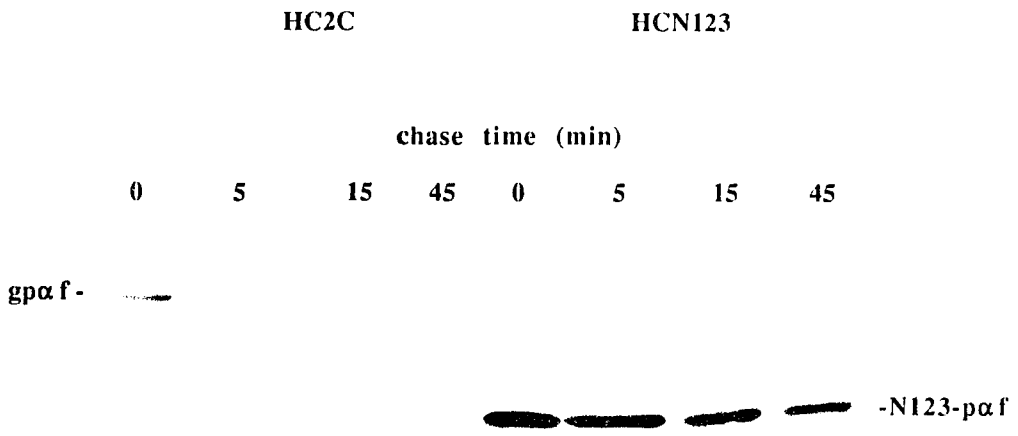

D. HPLC elution gradient

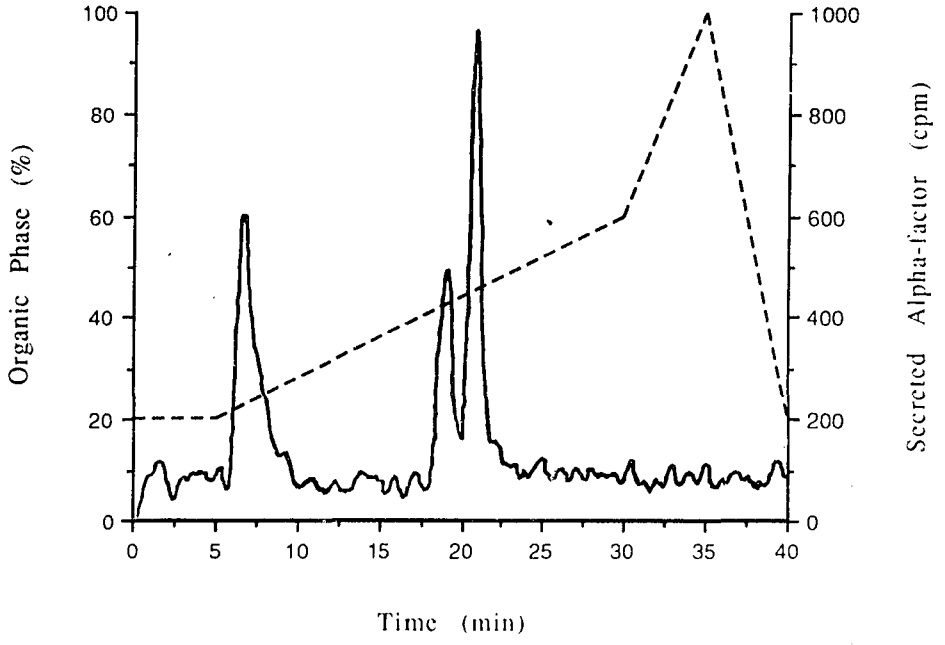

E. Typical HPLC analysis of secreted αf

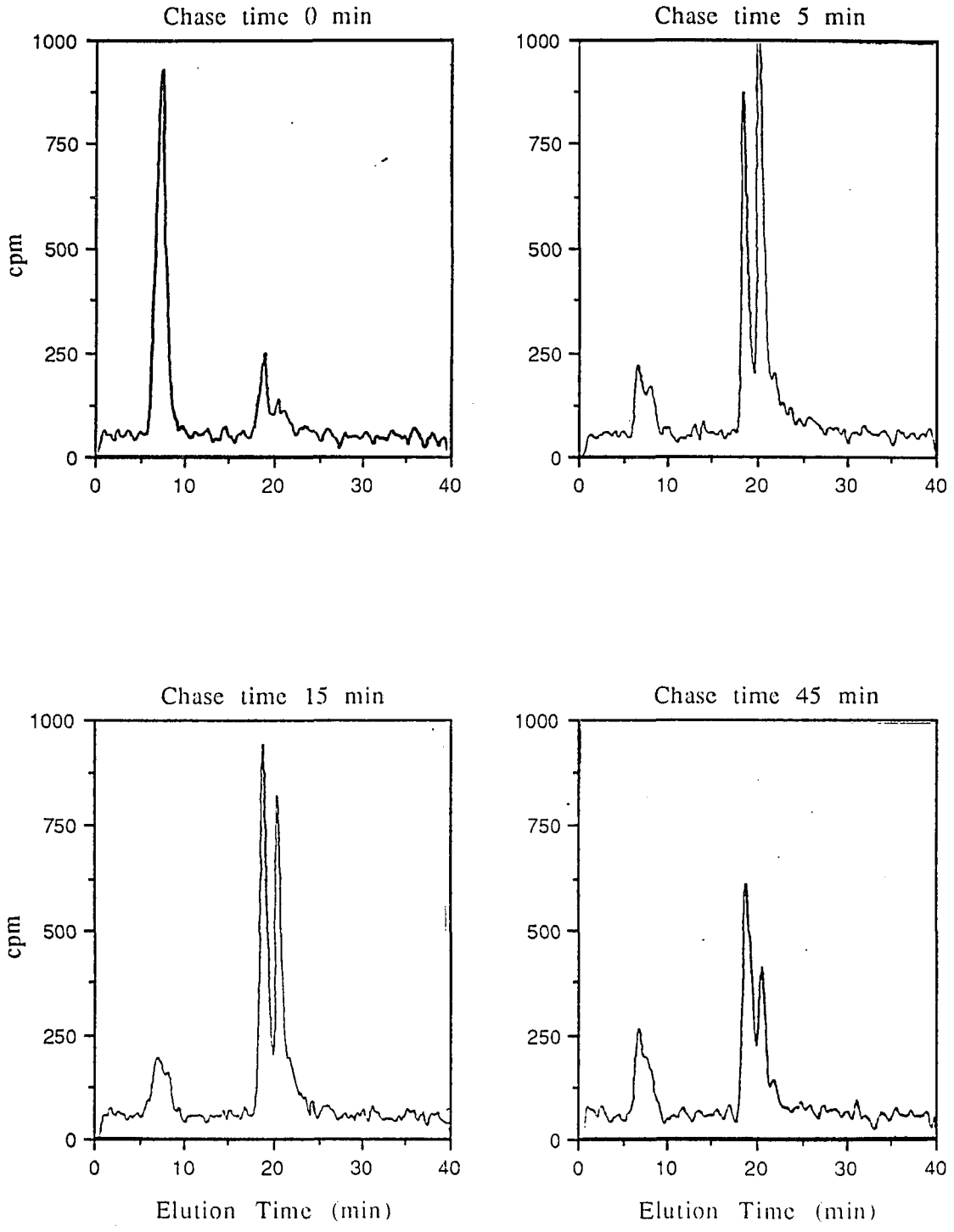

were generated from in vitro translation (IVT) of ppαf or N123-ppαf mRNA in the presence of canine pancreatic rough microsomes (RM). In vitro, ppαf is converted to gpαf by RM through signal peptide cleavage and Asn-linked glycosylation at all three acceptor sites, while N123-ppαf is converted into N123-pαf by signal peptide cleavage alone (Figure 9A). Use of these radiolabeled markers allowed identification of intracellular radiolabeled precursors (Figure 9B). A typical pulse-chase profile is shown in Figure 9C.

In the same experiments, the level of mature ^{35}S-methionine-labeled αf in the extracellular medium was quantified by immunoprecipitation with anti-αf antibody, followed by high-performance liquid chromatography (HPLC) on a C_{18} reverse phase column (Figure 9D). Under these conditions, two major αf-containing peaks of radioactivity are typically observed. The peak at 18.5 min represents methionine sulfone-containing αf, since treatment of the immunoprecipitated media sample with 5% H_2O_2 results in only a single peak at 18.5 min (data not shown). The peak at 21 min represents the unoxidized methionine form of the mature αf peptide. The peak at 7 min represents unincorporated ^{35}S-methionine. A typical series of elution profiles from a pulse-chase analysis is shown in Figure 9E.

Comparison of the wild-type and N123 strains revealed that, in the wild-type strain, pulse-labeled gpαf rapidly disappears from cells ($t_{1/2}$ < 5 min), with a corresponding rapid appearance of radiolabeled αf in the extracellular medium (Figure 10, top panel, circles). In contrast, in strain N123, N123-pαf disappears much more slowly ($t_{1/2}$ = 25 min), and the secretion of αf is delayed and never attains as high a level as that seen in the wild-type strain (Figure 10; top panel, squares). By the end of a 60 min chase period, the total amount of αf secreted by the mutant strain was only 10% of the amount secreted by the wild-type strain, yet 75% of N123-pαf had disappeared. Since equal amounts of

Figure 10. Comparison of transport and processing of wild-type and mutant pαf.

Equal amounts of log-phase wild-type (**2C**) and ppαf triple glycosylation mutant (**N123**) cells were pulse-labeled with ^{35}S-methionine (200 μCi/ml) for 5 min and chased for increasing times in the presence of excess unlabeled methionine. TM (50 μg/ml) was added where indicated 15 min prior to the start of the pulse. Yeast cell lysates were prepared as described, and the level of intracellular precursor was determined by immunoprecipitation with anti-αf antibody followed by 18% SDS-PAGE. The relative level of radioactivity in each band was determined by densitometry. Media samples were prepared as described, and secreted αf levels were determined by immunoprecipitation with anti-αf antibody followed by HPLC analysis. The amount of radioactivity in the eluted αf peaks were determined by continuous flow scintillation counting. The relative levels of intracellular precursor and secreted αf were normalized to the level of TCA-precipitable ^{35}S-labeled protein (cpm) in the cell lysates at time zero. **Top panel**, comparison of strains 2C (open circles), and N123 (open squares) in the absence of drug treatment. **Middle panel**, strain 2C in the absence (open circles), or presence (solid circles) of TM. **Bottom panel**, strain N123 in the absence (open squares), or presence (solid squares) of TM.

Figure 10. Comparison of transport and processing of wild-type and mutant pαf.

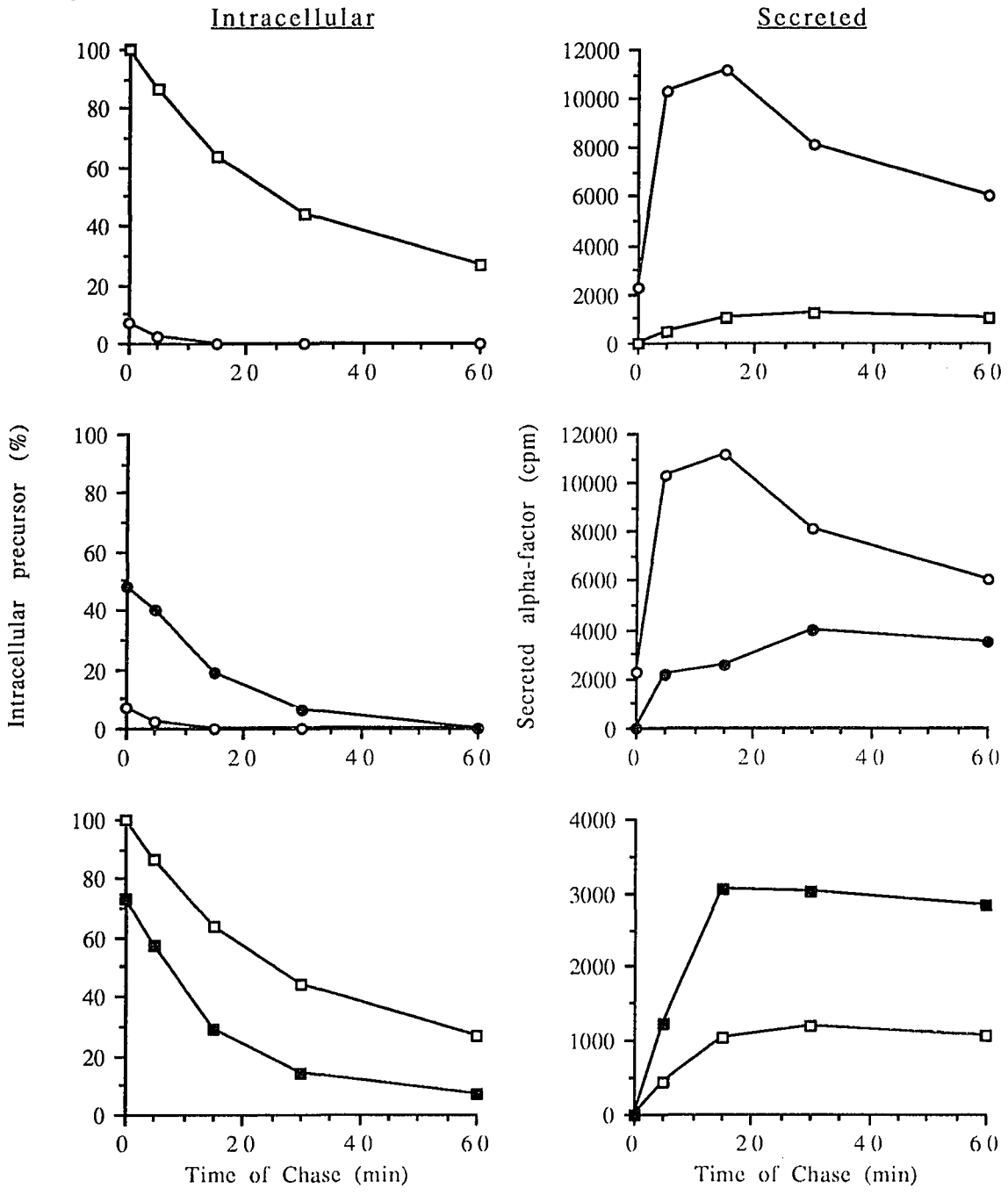

wild-type and mutant ppαf mRNA are present in the two strains as measured by Northern analysis (data not shown), we infer that equivalent amounts of ppαf and N123-ppαf were synthesized during the 5 min pulse. This leads to the conclusion that a significant proportion of the newly synthesized N123-pαf is degraded during the chase without generating mature αf.

Treatment of strain 2C with TM results in a slower disappearance of non-glycosylated pαf relative to gpαf ($t_{1/2}$ = 12 min), and a significant reduction in αf secretion (Figure 10, middle panel, solid circles). By the end of a 60 min chase period, the total amount of αf secreted by the TM-treated cells was 36% of the amount secreted by the control cells, yet all of the intracellular non-glycosylated pαf has disappeared. As in the case of N123-pαf, this observation suggests that a significant proportion (60%) of non-glycosylated pαf is degraded intracellularly.

A surprising result was obtained when strain N123 was subjected to pulse-chase analysis in the presence of TM (Figure 10, bottom panel, solid squares). Under these circumstances, N123-pαf disappears more rapidly than in the absence of TM ($t_{1/2}$ = 13 min vs. $t_{1/2}$ = 25 min). Most important, the level of αf secreted in the N123 strain in the presence of TM is 2.5-fold *greater* than in the absence of TM treatment. It appears that TM treatment mobilizes an additional proportion of intracellular N123-pαf to support the processing and secretion of mature αf.

This analysis demonstrated, first, that the disruption of the Asn-linked glycosylation sites of ppαf by site-directed mutagenesis or TM treatment leads to a severe reduction in αf secretion. Concomitant with the reduced secretion was a delay in ER to Golgi transport of the precursor, as manifested by the corresponding accumulation of intracellular non-glycosylated pαf. Since some mature αf is still secreted in the absence of Asn-linked glycosylation, we

conclude that glycosylation of pαf is important but not essential for the biological activity of the proregion in ER-to-Golgi transport and KEX2 mediated proteolytic processing.

More intriguing was the apparent rescue of αf secretion by TM treatment in strain N123. In this case, the mutant precursor is itself never glycosylated, thus the effect of TM on N123-pαf processing and secretion must be due to *trans*-acting factors. One possible candidate is the yeast ER lumenal heat shock protein BiP. The documented ability of TM to induce the expression of BiP in yeast is consistent with its proposed function in higher eukaryotic cells, where it is believed to recognize non-glycosylated (and presumably malfolded) polypeptides and possibly act to refold them or mediate their degradation. The observation that αf secretion can be enhanced by treating the N123-ppαf expressing cells with TM suggested that BiP might be involved in the transport and processing of N123-pαf.

B. *N123-ppαf is an inducer of BiP expression*

The defect in αf transport and processing exhibited by non-glycosylated pαf and N123-pαf might be due to their interaction with BiP in the lumen of the yeast ER. To gain support for this hypothesis, we asked whether simple expression of N123-ppαf changes the level of BiP expression within the cell. Though the precise signal transduction pathway involved has not been identified, in higher eukaryotic cells it is clear that accumulation of malfolded proteins in the ER can induce BiP transcription. Though other circumstances have been shown to induce BiP in yeast (TM treatment, expression of sec mutations, heat shock), to our knowledge no mutant yeast secretory protein has yet been shown to be an inducer of BiP.

I therefore compared the steady state level of BiP mRNA in strain 2C to that in strain N123 by Northern analysis. Since the mutant strain is isogenic to the wild-type strain at all loci except for the MFα1 locus [55], I reasoned that any differences in steady state BiP levels could be attributed to the expression of N123-pαf. To ensure that subtle differences in media or incubation conditions could not influence the results of these studies, both strains were analyzed in parallel (see experimental procedures) and the level of BiP mRNA was normalized to that of actin mRNA in each sample. Quantitation of BiP mRNA levels in the two strains grown and analyzed under identical conditions revealed a steady state BiP mRNA level approximately 2-3 fold greater in the mutant strain than in the wild-type (Figure 11).

To extend this observation, we tested whether increasing the expression level of N123-ppαf could induce BiP mRNA to an even greater extent. The steady state level of BiP was compared between strains HC2C and HCN123, which contain the MFα1 or mfα1-N123 gene, respectively, on episomal plasmids. The levels of ppαf mRNA are approximately 10-fold greater in these high-copy strains relative to those containing a single chromosomal copy of MFα1 (see Figure 12). The starting strain $\alpha_1\alpha_2$, in which both the MFα1 and MFα2 loci had been disrupted, was included as a control to see if overexpression of wild-type ppαf would in itself induce BiP.

We observed that high level expression of N123-ppαf resulted in a steady state level of BiP mRNA that is 5 to 6-fold greater than the level seen in the high-copy wild-type strain (Figure 12). Furthermore, when compared to the null $\alpha_1\alpha_2$ starting strain, overexpression of wild-type ppαf had no effect on BiP mRNA levels, arguing that the effect of N123-ppαf was not due to the increased flux of a secretory protein through the ER. Notably, all three strains responded equally to TM treatment, arguing that induction of BiP mRNA by

Figure 11. Expression of N123-ppαf increases the state-state level of BiP mRNA.

Total RNA was isolated from log-phase wild-type (2C) or mutant (N123) cells, separated on a 1.0% agarose gel containing 2% formaldehyde, transferred to nitrocellulose and simultaneously probed under conditions of high stringency with labeled fragments of DNA that recognized either actin or BiP mRNA. (**A**) Level of steady state BiP and actin mRNA in 5, 10, or 20 μg of total RNA. (**B**) The amount of radioactive label hybridized to BiP and actin mRNAs were quantitated by excising individual bands and liquid scintillation counting. The level of BiP mRNA (cpm) was normalized to the level of actin mRNA (cpm) at each data point. The data are presented as the fold induction over the steady state level found in the wild-type strain (indicated above the respective column).

Figure 11. Expression of N123-ppαf increases the state-state level of BiP mRNA.

A.

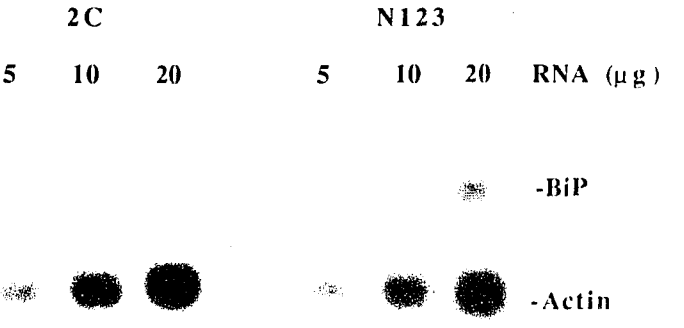

B.

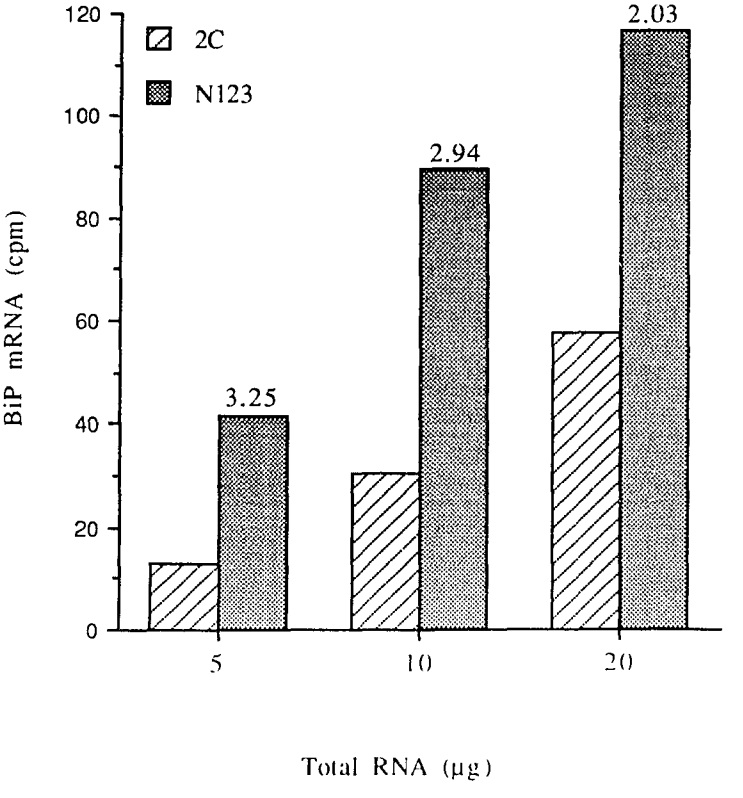

Figure 12. Dose-dependent induction of BiP mRNA by N123-ppαf.

Total RNA was isolated from strains $\alpha_1\alpha_2$ (Null), HC2C and HCN123 that had been incubated in the absence or presence of 5 μg/ml TM for two hours, and analyzed as in Figure 11. **(A)** Level of steady state BiP and actin mRNA in 10 μg of total yeast RNA. **(B)** The Northern blot data was quantitated as in Figure 11. The data are presented as the fold induction over the steady state level found in strain $\alpha_1\alpha_2$ in the absence of drug treatment.

Figure 12. Dose-dependent induction of BiP mRNA by N123-ppαf.

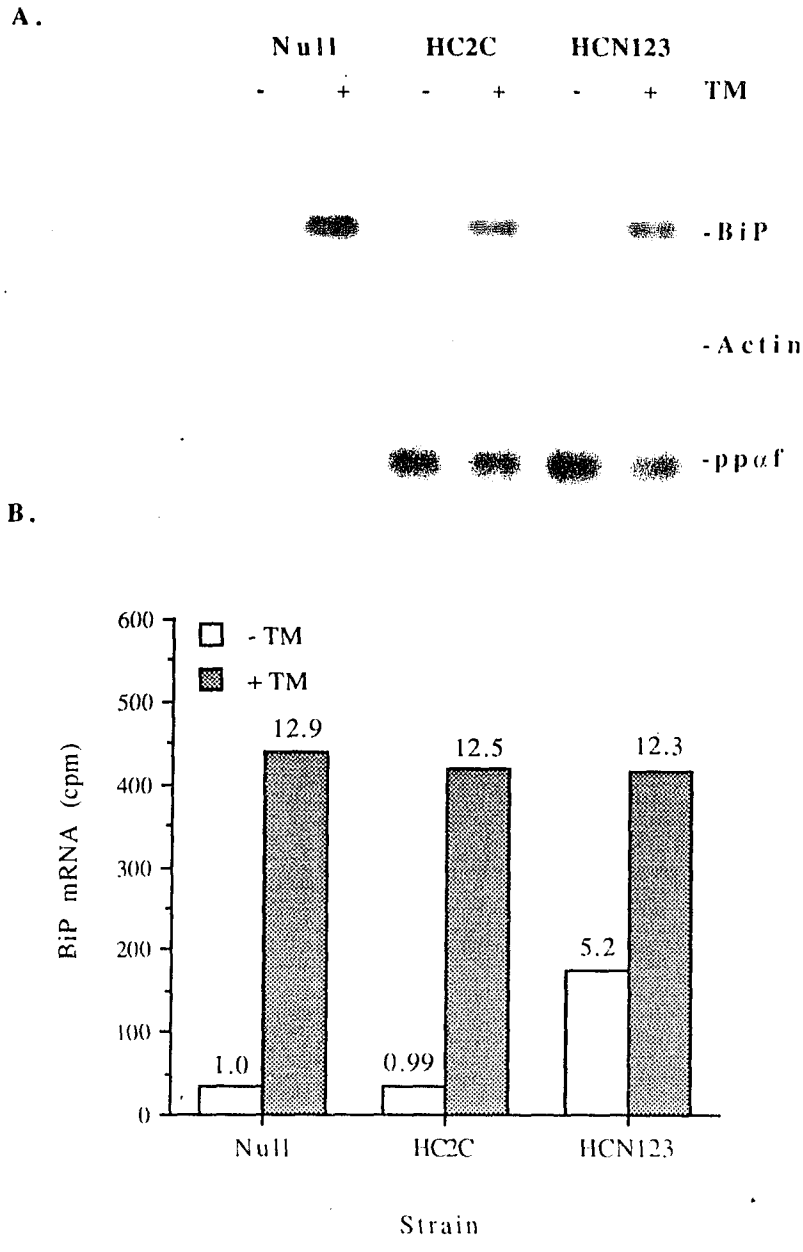

N123-pαf does not saturate the transcriptional capacity of the KAR2 gene. This argues against a synergistic effect between TM and N123-pαf on BiP induction, and suggests that the underlying mechanism of transcriptional induction of these two stimuli are similar and may be mediated through the same mechanism.

These results are the first demonstration in yeast that expression of a defective yeast secretory protein (N123-ppαf) induces the expression of BiP in a dose-dependent manner, and argues for a possible interaction between BiP and N123-pαf within the yeast ER lumen. Further, these data, along with the enhancement of αf secretion seen in strains expressing N123-ppαf in the presence of TM, provided the basis for two alternative hypotheses which investigated whether yeast BiP serves a positive or negative function in the biogenesis of N123-pαf. The "rescue" hypothesis presumes a positive role for BiP and argues that induction of BiP following exposure to TM results in a level of free BiP sufficient to bind N123-pαf, promote its folding and subsequent transport, which in turn leads to a higher level of αf secretion. On the other hand, TM treatment also induces the accumulation of large amounts of other non-glycosylated secretory and membrane proteins, which may also be substrates for BiP and thus compete with N123-pαf for BiP binding. The alternative "escape" hypothesis presumes a negative role for BiP and predicts that in the presence of TM the bulk level of non-glycosylated proteins overwhelms even the TM-induced level of free BiP, resulting in the competitive displacement of N123-pαf from BiP and a corresponding increase in the level of αf secretion. The escape hypothesis accommodates an additional postulate, that BiP mediates protein degradation within the secretory pathway, perhaps within the ER.

C. *Construction and verification of yeast strains expressing CUP1-KAR2*

In order to distinguish between the rescue and escape hypotheses, I constructed from strains 2C and N123 a number of new yeast strains in which BiP expression could be regulated independently of inducers such as TM treatment and the presence of malfolded proteins within the ER lumen. As a first step, we isolated the coding region of the KAR2 gene and constructed a series of plasmids that put the KAR2 coding region under the control of the yeast metallothionine promoter (CUP1). This was done so that the cellular level of BiP mRNA, and thus the level of BiP protein, could be regulated by the concentration of copper sulfate (Cu^{2+}) within the growth media. After transforming the haploid wild-type (2C) and triple glycosylation mutant (N123) strains with a centromeric plasmid containing the KAR2 coding region under the control of the CUP1 promoter, we disrupted the genomic copy of the KAR2 gene using a one-step gene disruption method. The results of these manipulations were isogenic strains expressing ppαf or N123-ppαf, whose level of BiP was unresponsive to TM and was now under the control of the copper-responsive CUP1 promoter.

The coding region of the KAR2 gene was isolated from yeast genomic DNA (strain 2C) by PCR using oligonucleotide primers complimentary to the 5' and 3' ends of the KAR2 coding region. The resulting 2.0 kb fragment was cloned into the in vitro transcription plasmid pGEM-1, generating the new plasmid pGK2. DNA sequencing confirmed that the insert corresponded to the published KAR2 gene (data not shown).

The 2.0 kb fragment was shown to contain a functional copy of the KAR2 coding region by two independent methods (Figure 13). First, plasmid pGK2 was linearized downstream of the 3' end of the KAR2 coding region and

transcribed in vitro using SP6 RNA polymerase. The resulting 2.1 kb mRNA directed the synthesis in the wheat germ system of a 71 kD protein that was recognized by a BiP-specific antibody in Western analysis. Furthermore, supplementing the wheat germ translation system with RM resulted in cotranslational translocation of the protein into the RM and cleavage of its signal peptide (Figure 13A). Overexpression of this insert in yeast from the episomal plasmid pHCK2 resulted in the appearance of a protein band that co-migrated with a major band of approximately 71 kD that was induced by TM in the wild-type strain (Figure 13B). Second, a yeast centromeric plasmid (pLCK2-T) containing the cloned KAR2 coding region under the control of the CUP1 promoter was capable of providing the essential function of yeast BiP in strains whose genomic KAR2 gene was disrupted (see below).

To disrupt the KAR2 gene in strains 2C and N123, a two-step approach was used. Since the KAR2 gene is essential for growth, and the strains of interest are haploid, it was necessary to first transform both of these strains with the yeast centromeric plasmid pLCK2-T, which contains the KAR2 coding region under the control of the CUP1 promoter. The resulting strains, 2CLCK2 and N123LCK2, were then disrupted using the one-step gene disruption method as described [123]. Briefly, a 1.76 kb fragment containing the yeast HIS3 gene was blunt-end ligated into the unique Stu I restriction site within the coding region of the KAR2 gene. The resulting 3.8 kb fragment containing the HIS3 gene flanked by the coding region of the KAR2 gene was used to transform yeast strains 2CLCK2 and N123LCK2, and HIS^+ transformants (designated 2CΔ and N123Δ) were screened for successful recombination by three independent methods. (1) Southern blot analysis: genomic DNA was isolated from a number of HIS^+ putative 2CΔ and N123Δ colonies, as well as from the starting strains 2C and N123, digested with Xho I, and probed with nick-translated KAR2 DNA. The

Figure 13. Expression of the cloned KAR2 coding region in vitro and in vivo.

(A) In vitro translation (IVT) of in vitro transcribed BiP mRNA. BiP mRNA was synthesized in vitro using SP6 RNA polymerase and plasmid pGK2 as template. The resulting 2100 bp mRNA was translated in a wheat germ IVT system containing ^{35}S-methionine, in the absence or presence of RM. Proteinase K treatment was as described in Figure 9. **(B)** Yeast protein extracts were prepared from early log-phase cells that had been incubated in the absence or presence of TM (10 μg/ml, 2 h) or Cu^{2+} (0.2mM, 3 h) as indicated. Yeast protein extracts (25 μg) were separated by 10% SDS-PAGE and visualized by staining with Coomassie Blue. The migration of IVT BiP after Proteinase K protection is indicated.

Figure 13. Expression of the cloned KAR2 coding region in vitro and in vivo.

A.

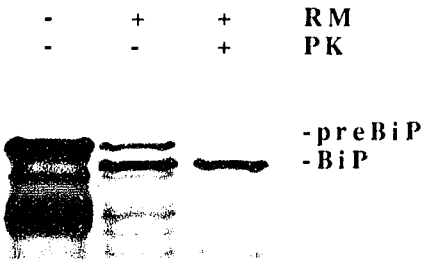

B.

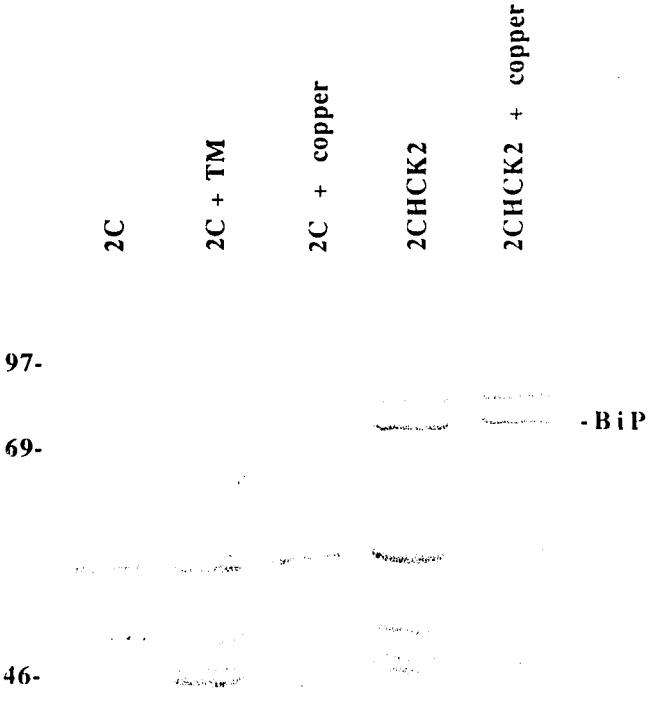

non-disrupted strains had a single hybridizing band of 2775 bp consistent with the Xho I fragment of genomic KAR2 DNA, while successfully disrupted strains had three reacting bands consistent with the presence of the HIS3 insert (data not shown). (2) PCR: Colonies identified by Southern analysis were analyzed by PCR using the oligonucleotide primers K2-10 and K2-11. In non-disrupted and control strains, use of these two primers amplified a band 2775 bp in length corresponding to the intact KAR2 gene, while in the disrupted strains the amplified band was 4540 bp in length corresponding to the KAR2 gene with a 1765 bp HIS3 insert. (3) Northern analysis: Total RNA was isolated from strains shown to be disrupted by both Southern analysis and PCR amplification, and subjected to Northern blot analysis using probes specific to the 5' and 3' untranslated regions (UTR) of the KAR2 gene (see below). The absence of BiP mRNA derived from the genomic copy of the KAR2 gene was considered to be confirmatory evidence for a successfully disrupted gene.

D. *Differential regulation of BiP expression in the native and recombinant strains*

Once the KAR2-disrupted strains expressing ppαf and N123-ppαf were created, we wished to confirm the different expected patterns of KAR2 regulation. Probes were developed that could discriminate between BiP mRNA transcribed from the chromosomal KAR2 gene and that produced from the CUP1-KAR2 containing plasmids, as well as measure total (chromosomal + plasmid-derived) BiP mRNA (see Experimental Procedures).

To compare BiP expression levels among the different strains, total RNA was isolated from: (1) the starting strains 2C and N123 (containing an intact chromosomal KAR2 gene); (2) the disrupted strains 2CΔ and N123Δ, (containing the CUP1-KAR2 construct on a low-copy centromeric plasmid),

and (3) the undisrupted strains 2CHCK2 and N123HCK2, (containing the CUP1-KAR2 construct on a high-copy episomal plasmid). The RNAs were hybridized in parallel with the three sets of probes described (Figure 14). The relative level of total BiP mRNA is consistent with the increase in levels predicted by the copy number of the CUP1-KAR2 containing plasmids (Figure 14A). It should be noted that the level of basal transcription from the CUP1 promoter is apparently several-fold higher than from the endogenous KAR2 promoter, explaining the increase in total BiP mRNA seen in strain 2CΔ over strain 2C. Furthermore, the specificity of the plasmid-derived probe is demonstrated, and again the intensity of the signal reflects the copy number of the CUP1-KAR2 containing plasmids (Figure 14B). Finally, in the disrupted strain, no chromosome-derived mRNA can be detected (Figure 14C). Taken together, these experiments demonstrate both the predicted specificity of the probes, as well as the identity of the recombinant strains. Parallel analysis of the corresponding N123 strains gave identical mRNA patterns (data not shown).

The starting (2C) and KAR2-disrupted (2CΔ) strains were then treated with either Cu^{2+}, TM, or both, prior to isolation of total RNA (Figure 15). These treatments had the predicted effects: The endogenous KAR2 promoter was unresponsive to Cu^{2+}, but was highly induced by treatment with TM. Conversely, the CUP1 promoter was induced by Cu^{2+} but unaffected by TM. In neither strain did the combination of Cu^{2+} and Tm have an additive effect.

To optimize CUP1-mediated expression of BiP, strain 2CΔ was treated with increasing concentrations of Cu^{2+} prior to RNA and protein isolation. We observed a dose-dependent increase in BiP mRNA and protein levels, with a maximal induction evident using 0.5 mM Cu^{2+} (Figure 16). In this case, a 3 hour incubation time with Cu^{2+} was chosen, based on preliminary time-course experiments, and this became the standard incubation time for induction of

Figure 14. BiP expression in native and recombinant yeast.

Total RNA (5 μg) was isolated from yeast strains 2C, 2CΔ, and 2CHCK2, transferred to nitrocellulose and hybridized with probes that recognize total BiP mRNA (**A**), plasmid-derived BiP mRNA (**B**) or chromosomal BiP mRNA (**C**). Labeled actin probe was included in all three blots as a control for loading and transfer to nitrocellulose. Longer exposure of the blot in (**C**) did not reveal genomic BiP mRNA in strain 2CΔ (data not shown).

Figure 14. BiP expression in native and recombinant yeast.

A. Total BiP

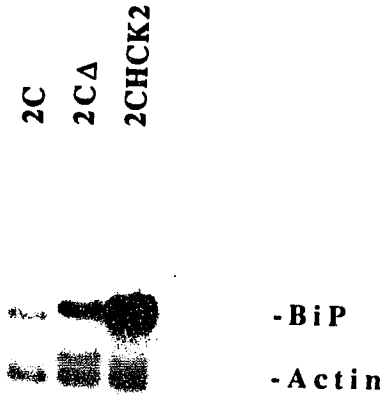

B. Plasmid-derived BiP

C. Chromosome-derived BiP

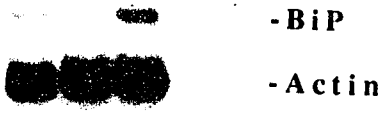

Figure 15. Differential regulation of BiP mRNA by Cu^{2+} and TM in native and recombinant yeast strains.

Total RNA was isolated from yeast strains 2C and 2CΔ after treatment with Cu^{2+} (0.2 mM, 3 h), TM (1 μg/ml, 1 h), or a combination of Cu^{2+} and TM, transferred to nitrocellulose and hybridized with probes that recognize either chromosomal (**A**) or plasmid-derived (**B**) BiP mRNA. (**A**) Level of BiP and actin mRNA after Cu^{2+} and TM treatment in strain 2C. (**B**) Level of BiP and actin mRNA after Cu^{2+} and TM treatment in strain 2CΔ. Labeled actin probe was included as a control for loading and transfer to nitrocellulose.

Figure 15. Differential regulation of BiP mRNA by Cu^{2+} and TM in native and recombinant yeast strains.

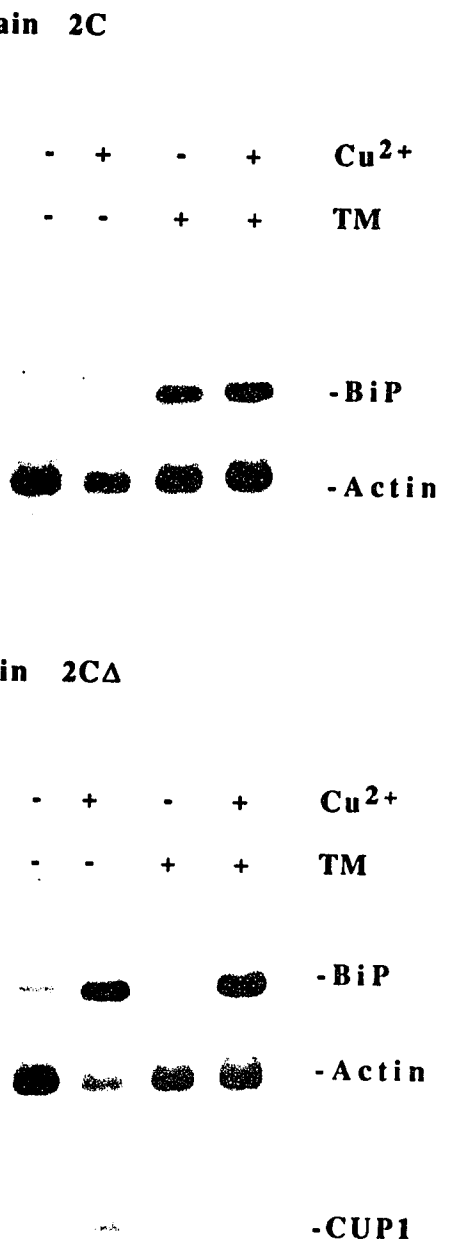

Figure 16. Cu^{2+}-mediated induction of BiP in the recombinant strain.

Early log-phase cells from strain 2CΔ were treated with Cu^{2+} at the indicated concentration for three hours before removing aliquots of cells for total RNA and protein isolation. **(A)** Northern analysis of total RNA. Total cellular RNA (5 μg) was isolated as described, separated on a 1.0% agarose gel containing 2% formaldehyde, transferred to nitrocellulose and probed with a labeled fragment of DNA that recognized BiP mRNA (**insert**). Labeled actin probe was included as a control for loading and transfer to nitrocellulose. The amount of radioactive label hybridized to BiP and actin mRNAs were quantified by excising individual bands and liquid scintillation counting. The level of BiP mRNA (cpm) was normalized to the level of actin mRNA (cpm) at each data point. The data are presented as the fold induction over the level found in strain 2C in the absence of drug treatment. **(B)** Western analysis of total protein. Cell lysates were prepared as described and equal amounts of total protein (2.5 μg) was separated by 8% SDS-PAGE, transferred to nitrocellulose and probed with anti-BiP antibody (**insert**). BiP protein was visualized using the Enhanced Chemiluminescence system according to manufactures instructions (Amersham). Relative BiP protein levels were determined by densitometry and presented as the fold induction over the BiP protein level found in strain 2C in the absence of drug treatment.

Figure 16. Cu^{2+}-mediated induction of BiP in the recombinant strain.

A. Plasmid-derived BiP mRNA

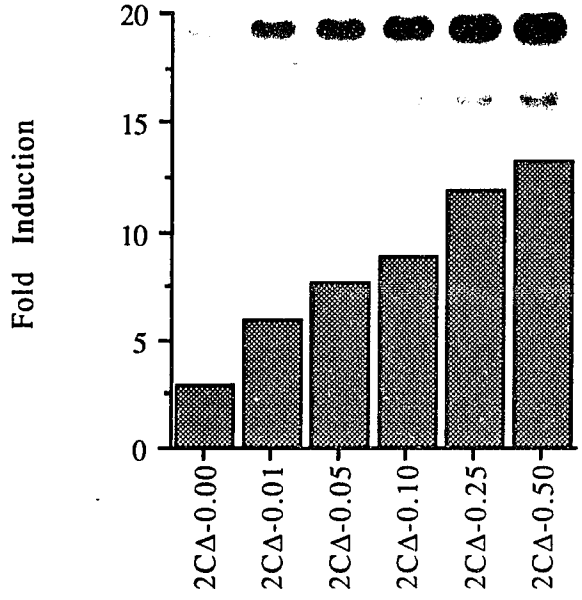

B. Plasmid-derived BiP Protein

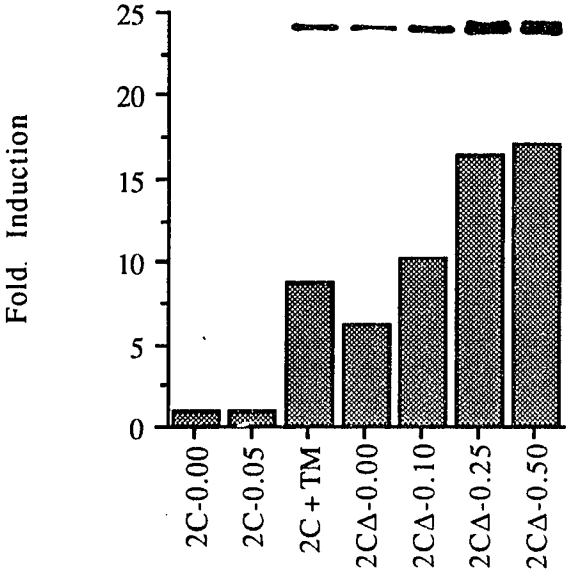

CUP1 in later experiments. To arrive at a standard Cu^{2+} concentration for induction, it was necessary to take into account the translational inhibition effects of increasing concentrations of Cu^{2+}. Under the growth conditions used, Cu^{2+} treatment at a concentration > 0.3 mM resulted in a 50% reduction in the incorporation of ^{35}S-methionine into total protein (data not shown). For this reason, a standard treatment of 0.2 mM Cu^{2+} was used in all subsequent experiments; this gave < 5% inhibition of translation but allowed a 10 to 15-fold induction in the level of mRNA and protein. Taken together, these experiments verified the identity of the different yeast strains, and established conditions for maximal induction of BiP by Cu^{2+}.

E. *Co-expression of BiP and N123 is deleterious to growth*

The experiments described above put us in a position to compare the effects of BiP overexpression on the transport and processing of gpαf and N123-pαf. To control for unpredictable effects on growth of both the wild type and mutant strains, the following experiment was performed. Strains containing either the chromosomal KAR2 gene, centromeric CUP1-KAR2 plasmid, or the episomal CUP1-KAR2 plasmid were treated with 0-0.5 mM Cu^{2+} for increasing times, and cell division was monitored by direct counting of cells in a hemacytometer (Figure 17). First, it is evident that, at these concentrations, Cu^{2+} has no effect on the growth of the original 2C and N123 strains. Second, increasing the expression of BiP from the CUP1 promoter control has no effect on cells expressing wild type pαf until the highest concentration of Cu^{2+}, and hence BiP, was reached. By contrast, in the N123-ppαf strains, the dose-dependent inhibition of growth was more apparent. For example, in strain N123Δ, a 50% reduction in cell number was observed at the

Figure 17. Overexpression of BiP from the CUP1 promoter results in a dose-dependent growth rate reduction in strains expressing N123-ppαf.

Equal amounts of early log-phase cells from the wild-type strains (2C, 2CΔ, and 2CHCK2; open symbols) and the mutant strains (N123, N123Δ and N123HCK2; solid symbols) were diluted to a final concentration of 5 x 10^5 cells/ml in 100 ml of selective medium containing Cu^{2+} at 0.0 (circles), 0.1 (diamonds), 0.3 (triangles) and 0.5 mM (squares). The cells were incubated at 30° C with continous shaking. At the indicated times, an aliquot of each culture was removed for determination of cell number as described.

Figure 17. Overexpression of BiP from the CUP1 promoter results in a dose-dependent growth rate reduction in strains expressing N123-ppαf.

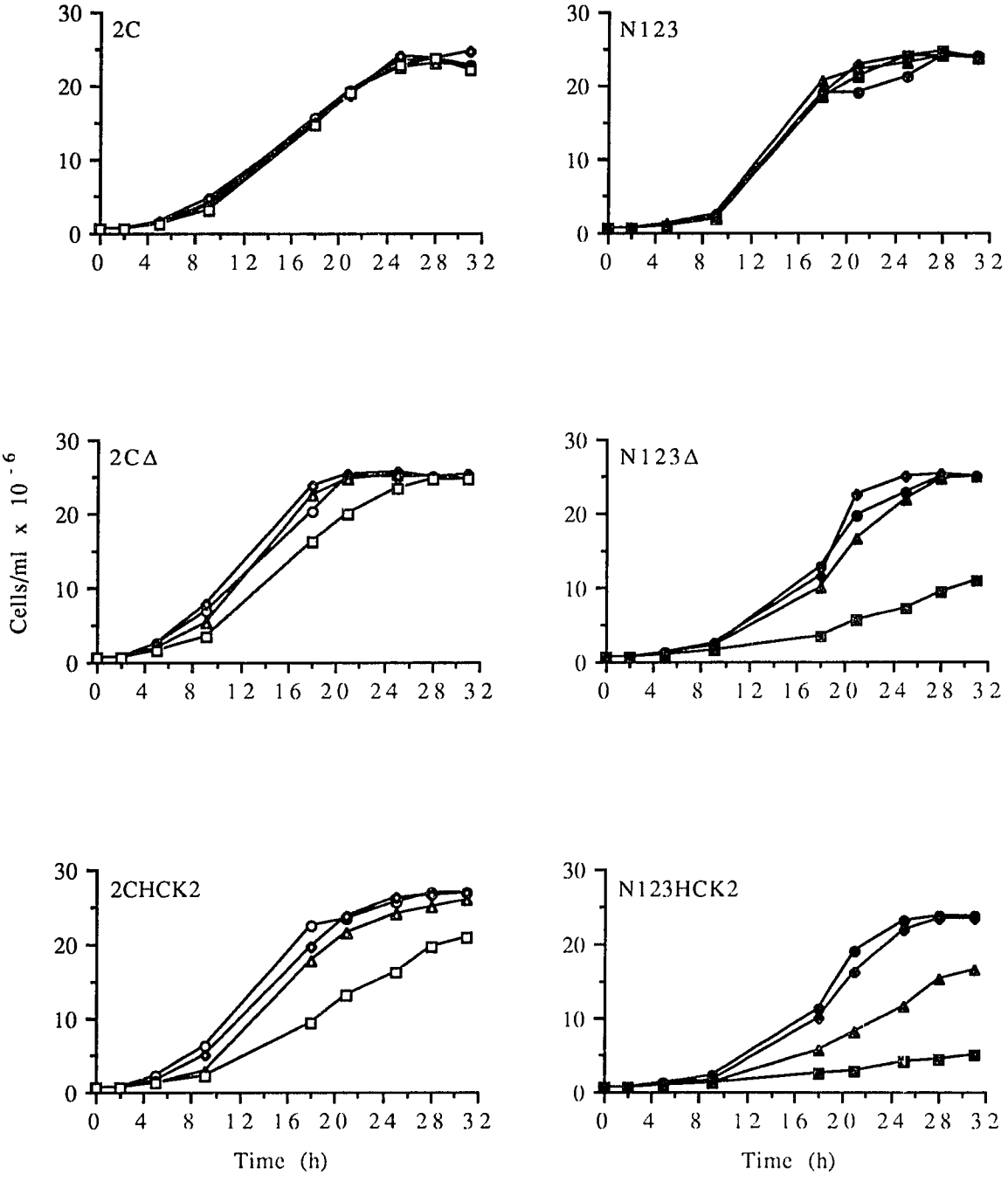

highest dose of Cu^{2+}, and the growth of strain N123HCK2 was almost completely inhibited under the same conditions.

The striking difference in response to Cu^{2+} between isogenic strains differing only at the MFα1 locus strongly suggests that co-accumulation of N123-pαf *and* BiP has a deleterious effect on cell growth, and argues that a physical interaction between these two polypeptides occurs in the lumen of the ER. This may reflect the phenomenon of "synthetic lethality" observed among genes whose products physically associate [130].

F. *Effect of BiP overexpression on N123-ppαf transport and processing*

Quantitative pulse-chase analysis was used to compare the levels of intracellular pαf and secreted αf in strains expressing ppαf and N123-ppαf from high-copy episomal plasmids (Figure 18). Use of these high-copy strains allowed us to maintain the level of the secreted αf signal, while lowering the level of ^{35}S-methionine used in the pulse, and reducing the sample size from 1.0 ml to 0.5 ml (which resulted in a significant reduction in the utilization of anti-αf antibody). Otherwise, the experimental protocols were essentially identical to those performed in the integrated strains (see Figure 10).

The patterns of pαf disappearance and αf secretion and the effect of the N123 mutation in the high-copy strains are very similar to those observed in the original 2C and N123 strains. First, the N123 secretory defect is as pronounced under high expression conditions as in the single copy strain (Figure 18, top panel). Second, ppαf responds to TM treatment with a similar reduction in pαf transport and αf secretion (Figure 18, middle panel). Finally, TM treatment of the high copy N123 strain results in a 2.5-fold enhancement of αf secretion (Figure 18, bottom panel).

Figure 18. Comparison of transport and processing in strains that overexpress wild-type and N123-ppαf.

Equal amounts of log-phase high-copy wild-type (HC2C) and N123-ppαf (HCN123) cells were pulse-labeled with ^{35}S-methionine (75 μCi/ml) for 5 min and chased for increasing times in the presence of excess unlabeled methionine. TM (50 μg/ml) was added as indicated 15 min prior to the start of the pulse and maintained throughout the chase period. Intracellular pαf and extracellular αf were isolated and quantified as described earlier in Figure 10. Comparison of strains HC2C (open circles), and HCN123 (open squares) in the absence of drug treatment (**top panel**); strain HC2C in the absence (open circles), or presence (solid circles) of TM (**middle panel**); and strain HCN123 in the absence (open squares), or presence (solid squares) of TM (**bottom panel**).

Figure 18. Comparison of transport and processing in strains that overexpress wild-type and N123-ppαf.

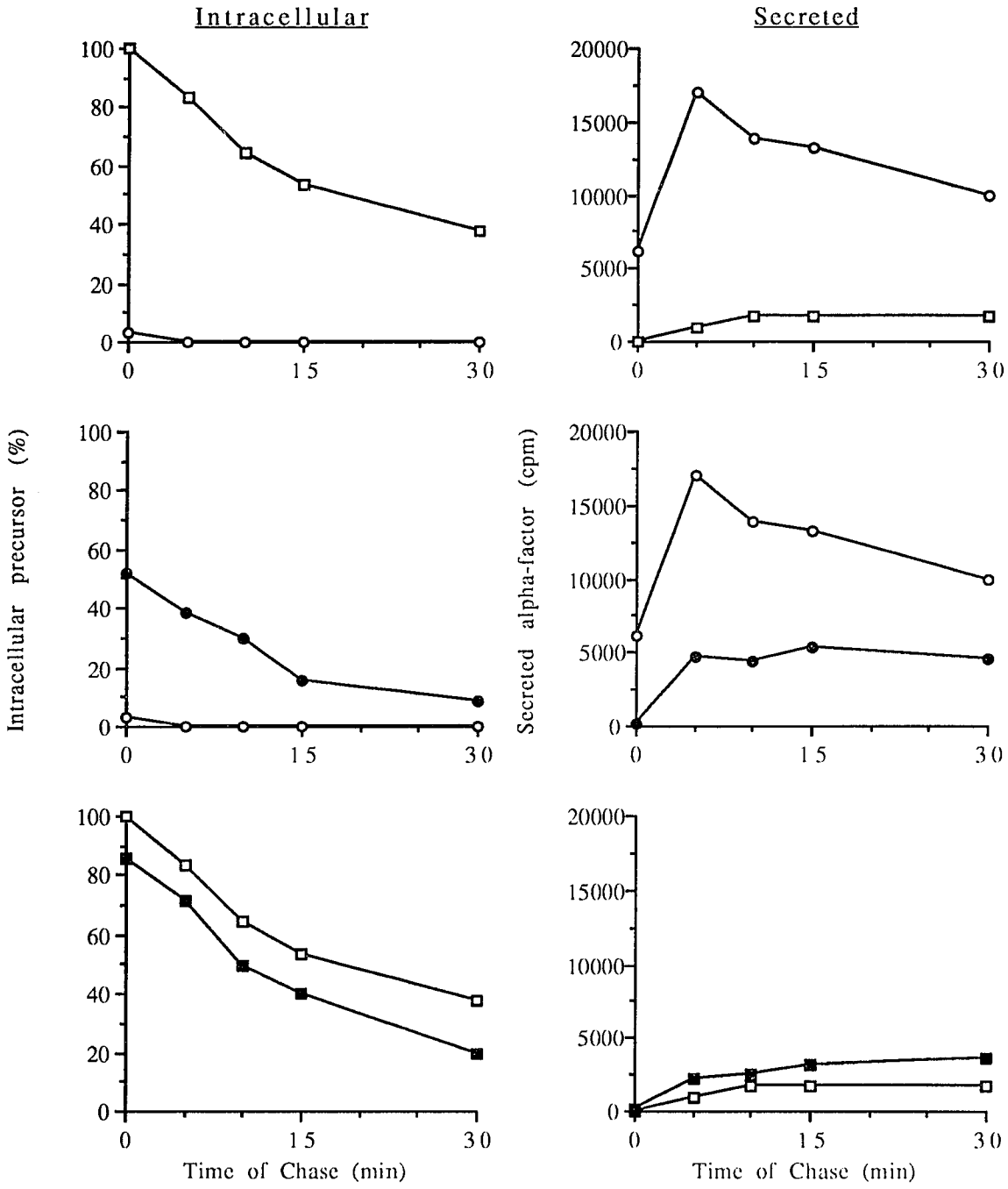

To distinguish between the "rescue" and "escape" hypotheses proposed earlier, quantitative pulse-chase analysis was performed using the high-copy Δ strains, which contain a disrupted KAR2 gene as well as high-copy ppαf and N123-ppαf expressing plasmids (Figures 19 and 20). Since the level of BiP expression in these strains is both under the control of Cu^{2+} and unresponsive to TM, the large amounts of non-glycosylated secretory and membrane proteins arising from TM treatment should act as substrates for BiP and thus decrease the level of free (i.e. uncomplexed) BiP. Under these conditions of a relative BiP deficiency, the "escape" hypothesis predicts that TM treatment should cause an *increase* in the level of secreted αf in the strain expressing N123-ppαf, while the "rescue" hypothesis predicts a corresponding *decrease* in αf secretion. In either case, by pretreating the cells with Cu^{2+} to elevate the level of BiP prior to TM treatment, we should be able to block TM's ability to modulate N123-pαf transport and processing, confirming our assumption that TM treatment influences N123-pαf transport and processing through its ability to change the level of free BiP within the ER.

In strain HC2CΔ, pulse-labeled gpαf disappears rapidly ($t_{1/2}$ < 5 min), with a corresponding rapid appearance of radiolabeled αf in the extracellular medium, a result similar to that seen in the both the low-copy and high-copy non-disrupted strains (Figure 19, top panel, solid lines). After Cu^{2+} pretreatment (which increases BiP levels approximately 10-fold) similar results are seen (Figure 19, top panel, dashed lines), however approximately 10% of the radiolabeled precursor remains as signal peptide-containing ppαf for the entire chase period (data not shown). A small corresponding decrease in αf secretion is also observed under these conditions. As in the non-disrupted KAR2 strains, exposure to TM slows the disappearance of non-glycosylated pαf relative to gpαf, and significantly reduces αf secretion

Figure 19. Comparison of transport and processing of ppαf in the high-copy wild-type Δ strains.

Equal amounts of log-phase cells from strain HC2CΔ were pulse-labeled with ^{35}S-methionine (125 μCi/ml) for 5 min and chased for increasing times in the presence of excess unlabeled methionine. TM (50 μg/ml) was added as indicated 15 min prior to the start of the pulse and maintained throughout the chase period. Intracellular pαf and extracellular αf were isolated and quantified as described earlier in Figure 10. The **top panel** compares transport and processing of gpαf in the absence (solid lines) or presence (dotted lines) of Cu^{2+} pretreatment. The **middle panel** compares transport and processing in the absence (open circles), or presence (solid circles) of TM. The **bottom panel** compares transport and processing of TM treated cells in the absence (solid lines), or presence (dotted lines) of Cu^{2+} pretreatment.

Figure 19. Comparison of transport and processing of ppαf in the high-copy wild-type Δ strains.

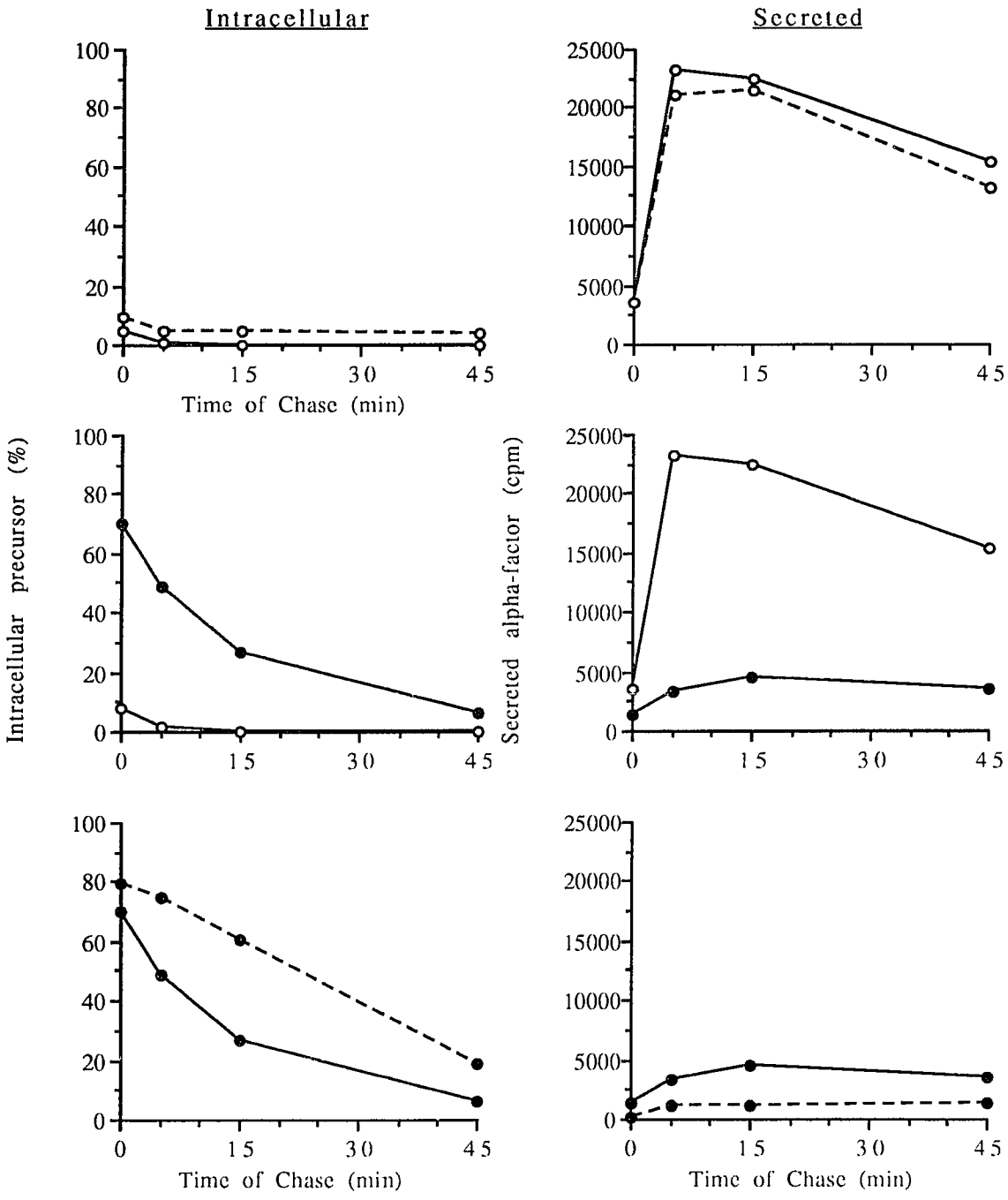

(Figure 19, middle panel, solid circles). Cu^{2+} pretreatment prior to TM exposure results in an increased accumulation of intracellular pαf, and a 3-fold reduction in αf secretion (Figure 19, bottom panel, dashed lines).

In strain HCN123Δ, pulse-labeled N123-pαf disappears slowly ($t_{1/2}$ = 35 min); the secretion of αf is delayed, and is only 8% of the level seen in strain HC2CΔ (Figure 20, top panel, solid lines). After Cu^{2+} pretreatment, transport and processing are mildly inhibited and the level of secreted αf is somewhat reduced relative to the untreated control (Figure 20, top panel, dashed lines). Most important, TM treatment increases the rate of N123-pαf disappearance ($t_{1/2}$ = 11 min), and a 2.5-fold enhancement of αf secretion is observed (Figure 20, middle panel, solid squares). Pretreatment of cells with Cu^{2+} prior to TM treatment, increases the level of intracellular N123-pαf and decreases αf secretion 2-fold (Figure 20, bottom panel, dashed lines).

The key finding in this series of experiments is that even under circumstances in which the level of BiP cannot be induced, TM still has the capacity to increase the utilization of N123-pαf as measured by an increase in αf secretion. Further, this effect can be reversed by overexpressing BiP from the CUP1 promoter prior to treating the cells with TM. These data are consistent with the "escape" hypothesis, which postulates that BiP functions to retain N123-pαf within the ER lumen, prevent ER-to-Golgi transport, and thus suppress subsequent processing and secretion of mature αf.

Figure 20. Comparison of transport and processing of N123-ppαf in the high-copy mutant Δ strains.

Equal amounts of log-phase cells from strain HCN123Δ were pulse-labeled with ^{35}S-methionine (125 μCi/ml) for 5 min and chased for increasing times in the presence of excess unlabeled methionine. TM (50 μg/ml) was added as indicated 15 min prior to the start of the pulse and maintained throughout the chase period. Intracellular N123-pαf and extracellular αf were quantified as described earlier in Figure 10. The **top panel** compares transport and processing of N123-pαf in the absence (solid lines) or presence (dotted lines) of Cu^{2+} pretreatment. The **middle panel** compares transport and processing of N123-pαf in the absence (open squares), or presence (solid squares) of TM treatment. The **bottom panel** compares transport and processing N123-pαf in TM treated cells in the absence (solid lines), or presence (dotted lines) of Cu^{2+} pretreatment.

Figure 20. Comparison of transport and processing of N123-ppαf in the high-copy mutant Δ strains.

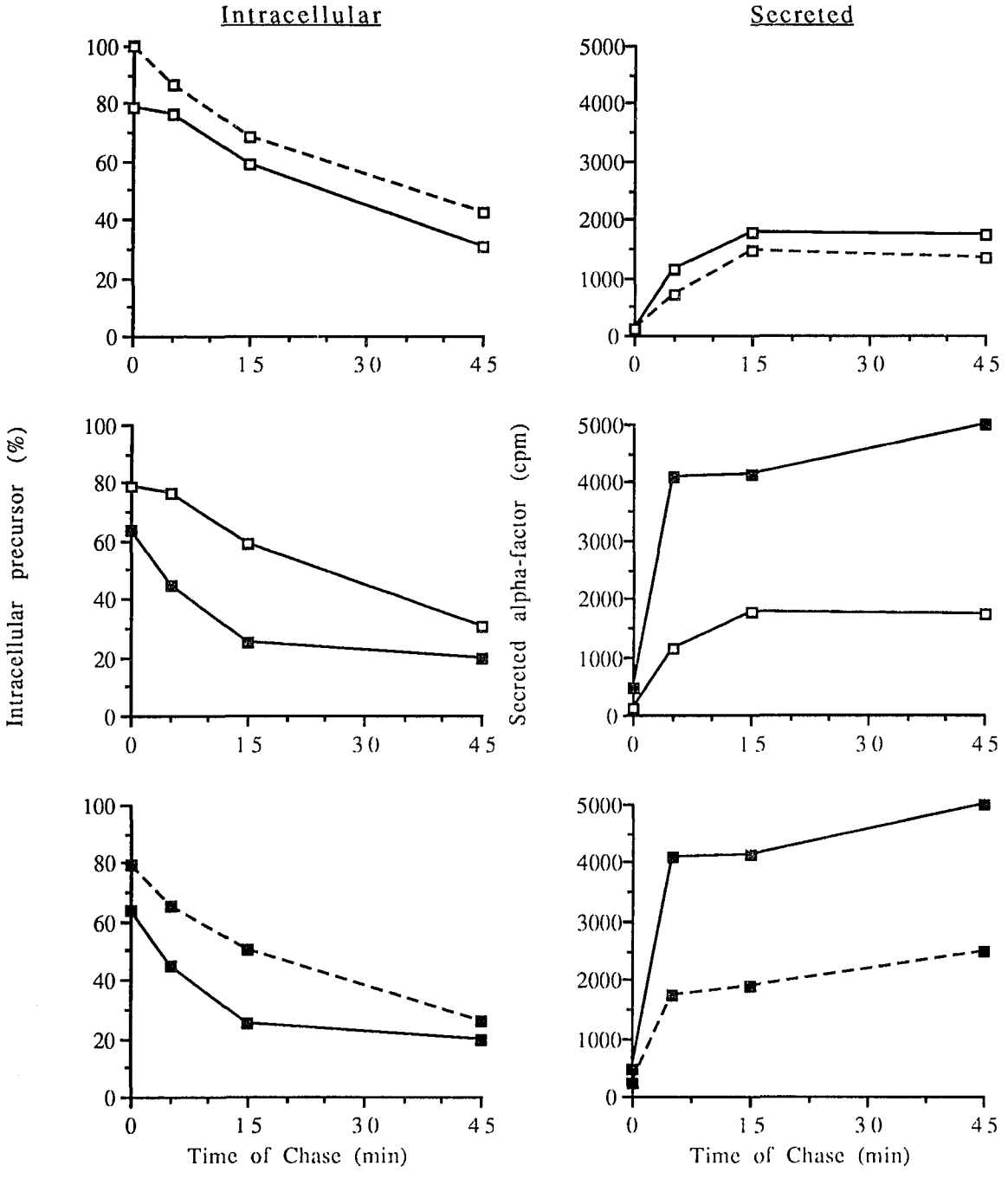

G. *Intracellular site of N123-pαf degradation*

Our results demonstrated that a substantial fraction of non-glycosylated pαf and N123-pαf is degraded intracellularly, most probably prior to the KEX2-mediated proteolytic cleavage within the Golgi apparatus. To further localize the degradative site within the yeast secretory pathway, the temperature-sensitive sec18 strain of *S. cerevisiae* was transformed with a centromeric plasmid (pLCN123-U) containing the mutant mfα1-N123 gene. Since ER-to-Golgi transport is tightly blocked in this strain at the nonpermissive temperature, use of this strain allowed us to examine the fate of both gpαf and N123-pαf in the same cells and determine whether degradation of N123-pαf occurs prior to the sec 18 secretory block. Early log phase cells growing at the permissive temperature of 25° C were shifted to the restrictive temperature of 37° C for 15 min, labeled with ^{35}S-methionine for 10 min, and chased for increasing times in the presence of unlabeled methionine. Cell lysates and media samples were prepared as described before. Equal amounts of cell lysate from each time point were immunoprecipitated with anti-αf antibody and analyzed by SDS-PAGE. In addition, the media samples were immunoprecipitated with anti-αf antibody to monitor the secretion of αf.

Approximately equal amounts of ppαf and N123-ppαf were synthesized during the 10 min pulse (Figure 21, zero time). The level of wild-type gpαf did not change during the chase period, a result previously observed in the sec 18 strain. Importantly, N123-pαf also persists, indicating that no degradation occurred under these conditions. Furthermore, none of the media samples contained secreted αf (data not shown), consistent with a tight block of ER-to-Golgi vesicular transport.

The most straightforward interpretation of these data is that the site of N123-pαf degradation is distal to the sec 18 block (i.e. post-ER). An alternative

Figure 21. Degradation of N123-pαf does not occur when ER-to-Golgi transport is blocked.

Early log-phase cells from strain sec18-N123 growing at the permissive temperature (25° C) were shifted to the restrictive temperature (37° C) for 15 min prior to pulse-labeling with ^{35}S-methionine (200 μCi/ml) for 10 min. Cells were than chased for increasing times in the presence of excess unlabeled methionine. Intracellular gpαf and N123-pαf were isolated and quantitated as described in Figure 10. **(A)** 18% SDS-PAGE analysis of intracellular gpαf and N123-pαf. **(B)** The data are presented as the percentage of the peak level of gpαf (circles), or N123-pαf (squares).

Figure 21. Degradation of N123-pαf does not occur when ER-to-Golgi transport is blocked.

A.

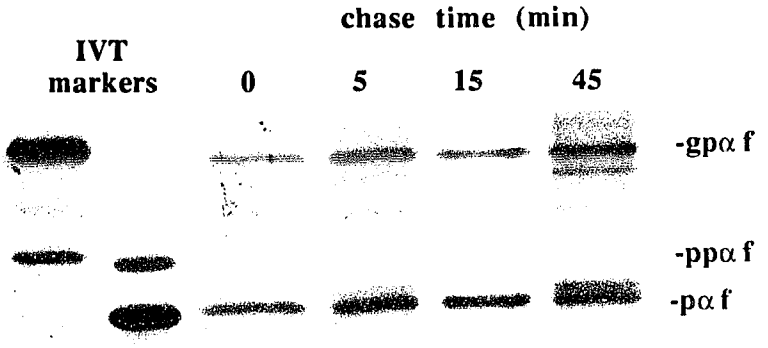

B.

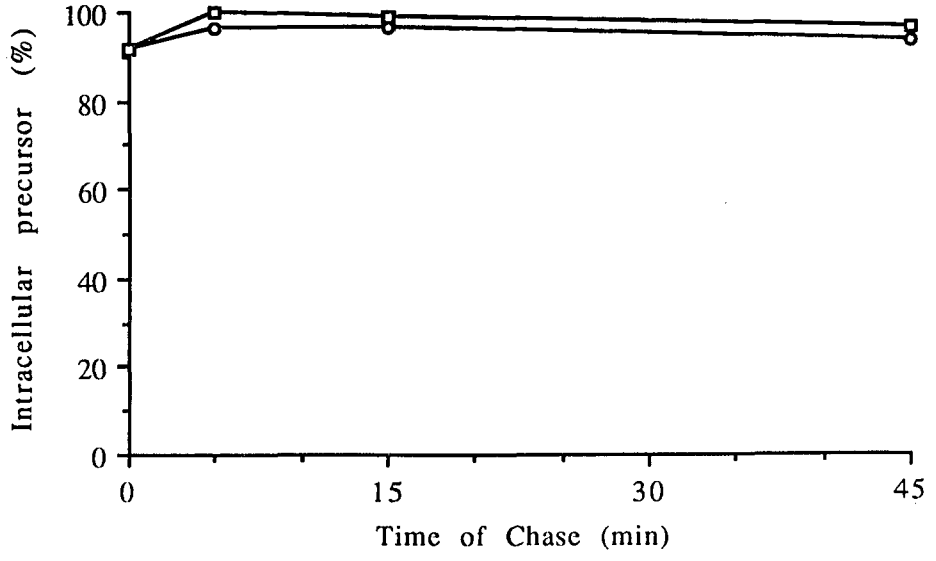

possibility is that degradation normally occurs in the ER, but the elevated temperature used in this experiment inhibits the proteolytic process.

CHAPTER II. INDUCTION OF YEAST BIP BY TM: INVESTIGATION OF MECHANISM AND FUNCTION OF THE RESPONSE

In the studies just described, BiP was assigned a specific, negative, role in the processing and transport of a mutant secretory pathway protein (N123-pαf). The data suggest that BiP binds non-glycosylated and presumably malfolded pαf polypeptides, preventing their "escape" and possibly mediating their entry into a degradative pathway.

In the studies detailed below, we examined the general role of BiP in the cellular stress response, using induction by TM as a model. Although the expression of BiP in yeast is induced by a variety of stressors, including TM treatment, in none of these circumstances has the precise effect of BiP induction been determined. We set out to ask two questions. First, does induction of BiP by TM represent a functional response to a secretory pathway specific stress; and, second, is the transcriptional induction sensitive to the intraluminal concentration of BiP in the ER?

For these studies we were able to utilize a subset of the previously constructed strains, i.e. those expressing wild-type ppαf and containing the chromosomal and/or plasmid-derived BiP gene. As a first step, we thoroughly characterized the response of the chromosomal BiP promoter to TM treatment. In the pulse-chase experiments described in chapter 1, a high dose of TM (50 μg/ml) was used for a short time to inhibit glycosylation rapidly (presumably by quickly depleting the level of the N-acetylglucosamine PP_i dolichol within the cell). In these studies, in contrast, we wished to induce BiP to an intermediate level. We therefore analyzed in detail the dose and time-dependence of BiP induction in response to TM in the control strain 2C (Figure 22).

Figure 22. Dose and time-dependent induction of BiP mRNA and protein by TM.

Early log-phase cells from the wild-type strain 2C were treated with TM at a concentration of 0.25 μg/ml (open circles), 1.0 μg/ml (open circles with dotted line) or 5.0 μg/ml (solid circles). At the indicated times, aliquots of cells were removed for the isolation of total RNA or protein as described. (A) Level of BiP mRNA after TM treatment. Total cellular RNA (5 μg) was isolated as described, separated on a 1.0% agarose gel containing 2% formaldehyde, transferred to nitrocellulose and probed under conditions of high stringency with labeled fragments of DNA that recognized BiP and actin mRNA. The amount of radioactive label hybridized to BiP and actin mRNAs was quantified and normalized as described in Figure 11. The data are presented as the fold induction over the BiP level found at time zero. (B) Level of BiP protein after TM treatment. Yeast cell lysates were prepared and analyzed as described previously in Figure 16. Relative BiP protein levels were determined by densitometry and presented as the fold induction over the BiP level found at time zero.

Figure 22. Dose and time-dependent induction of BiP mRNA and protein by TM.

A. BiP mRNA

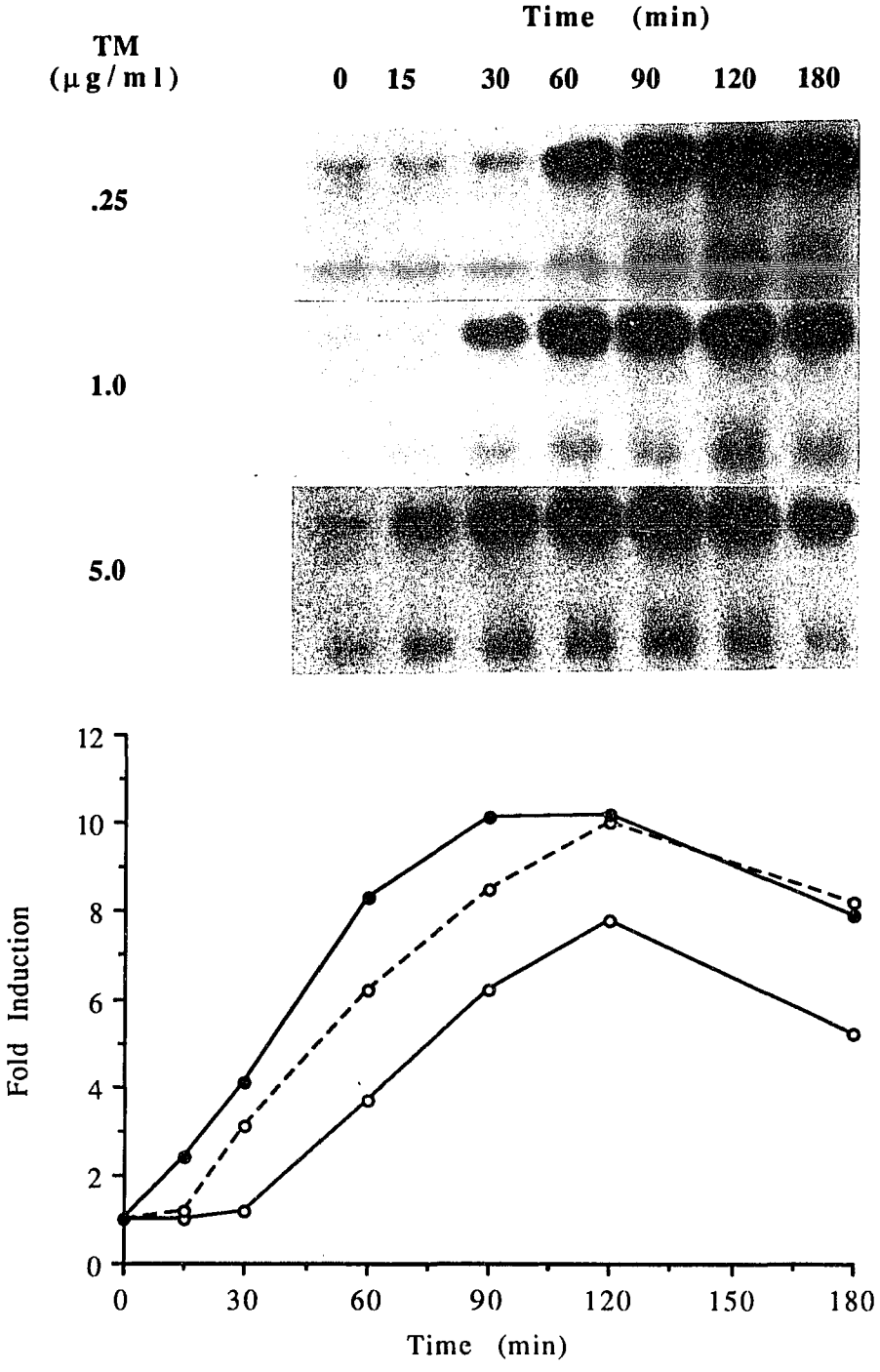

B. BiP Protein

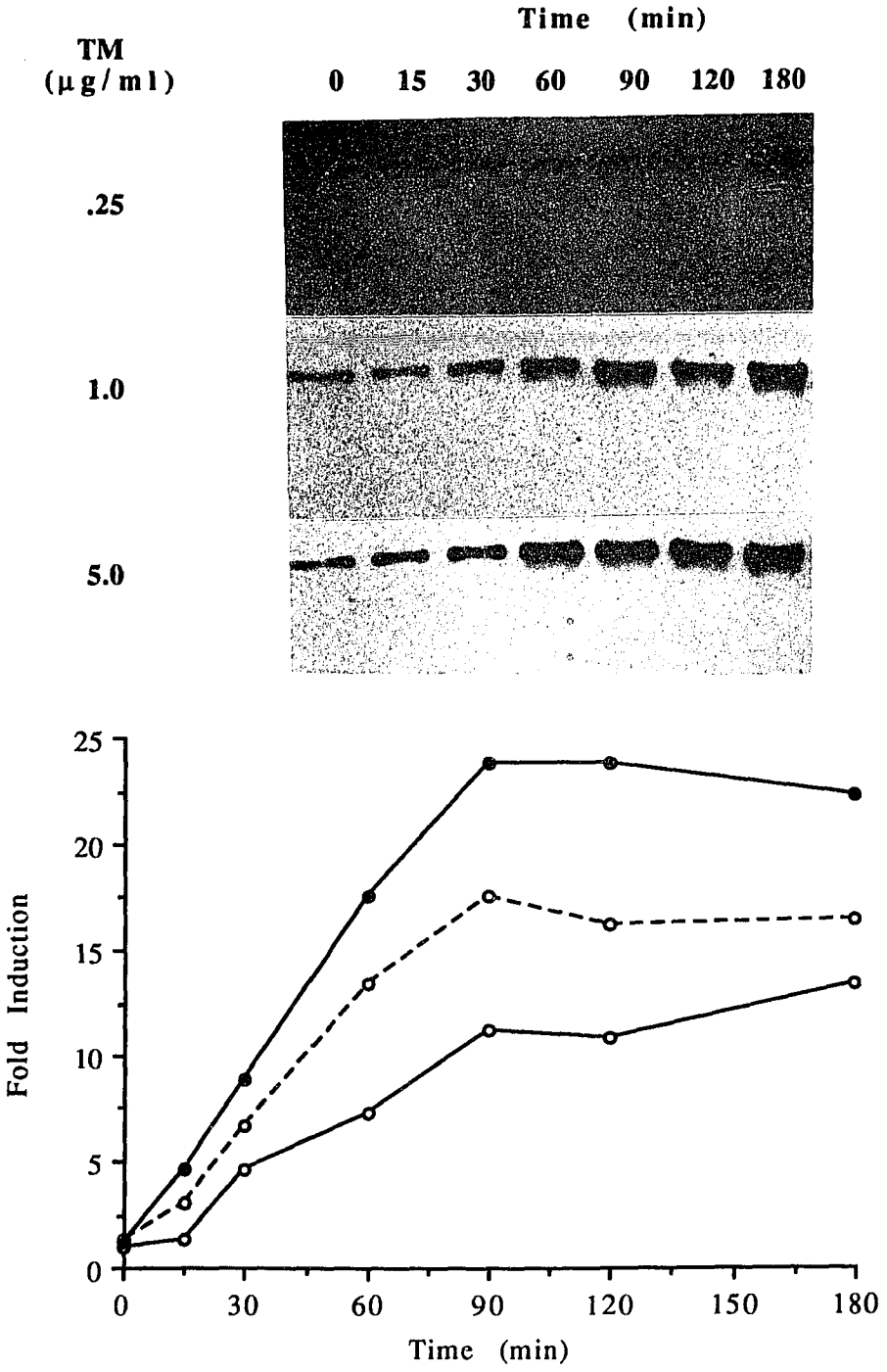

Cells were incubated at the indicated dose of TM for increasing times, after which cells were harvested and split into two aliquots. One aliquot was used to isolate total RNA, which was subjected to Northern analysis to determine BiP mRNA levels (Figure 22A). The second aliquot was used to generate cell lysates, which were analyzed by Western blotting using an anti-BiP antibody (Figure 22B). The results indicated that a dose of 1 μg/ml TM produced an intermediate level of induction of both BiP mRNA and protein that was linear over a period of 90 min, and that this response saturates at 5 μg/ml TM.

A. *Induction of yeast BiP enhances cell survival of TM treatment*

We tested whether the overexpression of BiP prior to TM treatment enhances the cell's ability to survive the cytotoxic effects of this drug. Since BiP is a hsp70 heat shock protein that has evolved to function within the lumen of the ER, we hypothesized that overexpression of BiP could protect the cell from TM. Such a finding would be analogous to the protective role conferred by cytosolic heat shock proteins in response to thermal stress [131, 132].

To directly test this hypothesis, I performed experiments comparing the effect of TM on cell viability in strains 2C and 2CΔ. Briefly, log-phase cells from these two strains were incubated for 3 hours in the absence or presence of Cu^{2+} to induce BiP protein levels about 10-15 fold over basal levels. It is important to note that, even in the absence of exogenous Cu^{2+}, strain 2CΔ has steady state BiP protein levels that are approximately 4-5 fold greater than the level seen in strain 2C. Cells from both strains were then challenged with three different doses of TM (0.2, 0.5, or 5.0 μg/ml). At the specified time points,

aliquots were removed to determine both cell number and viability. Cell number was determined by direct counting in a hemacytometer as described in the Experimental Procedures. Cell viability was determined at each time point by spreading cell onto selective plates and counting colonies after five days of growth.

Strains 2C and 2CΔ are similar in their sensitivity to TM's dose-dependent ability to inhibit cell division (Figure 23). The ability of TM to arrest cells in the G_1 phase of the cell cycle without inhibiting cell growth is well documented [133, 134]. As a consequence, yeast cell growth was monitored by direct counting in a hemocytometer rather than by measuring optical density, since the continued increase in optical density of cells treated with TM is due to the increase in cell size, not an increase in cell number. Examination of the TM-treated cultures indicated that cells from both strains were approximately twice the diameter of the control cells, a result consistent with that reported by other investigators [44, 134]. Comparison of the growth of strain 2CΔ in the absence and presence of Cu^{2+} suggests that overexpression of BiP does not have a deleterious affect on growth in the wild-type strain.
Examination of cell viability in response to increasing concentrations of TM demonstrates that the wildtype strain 2C is dramatically more sensitive to the lethal effects of TM than is strain 2CΔ (Figure 24). Comparison of cell viability between these two strains after five hours at the indicated dosage of TM, in the absence and presence of Cu^{2+} pretreatment, argues that cell viability is enhanced in direct proportion to the initial BiP level (Figure 24A). The observed proportionality between the level of BiP expression at the time of TM challenge and maintenance of cell viability during extended incubations in the presence of this drug suggests that, under our experimental conditions,

Figure 23. Dose-dependent inhibition of yeast cell division by TM.

Log-phase cells from yeast strains 2C and 2CΔ were diluted to a concentration of 1.2 x 10^6 cells/ml and incubated for 3 hours in the absence or presence of 0.2 mM Cu^{2+} as specified. At time zero, TM was added (solid symbols) to a final concentration of 0.2, 0.5, or 5.0 μg/ml as indicated. At the specified times, aliquots were removed to determine cell number as described.

Figure 23. Dose-dependent inhibition of yeast cell division by TM.

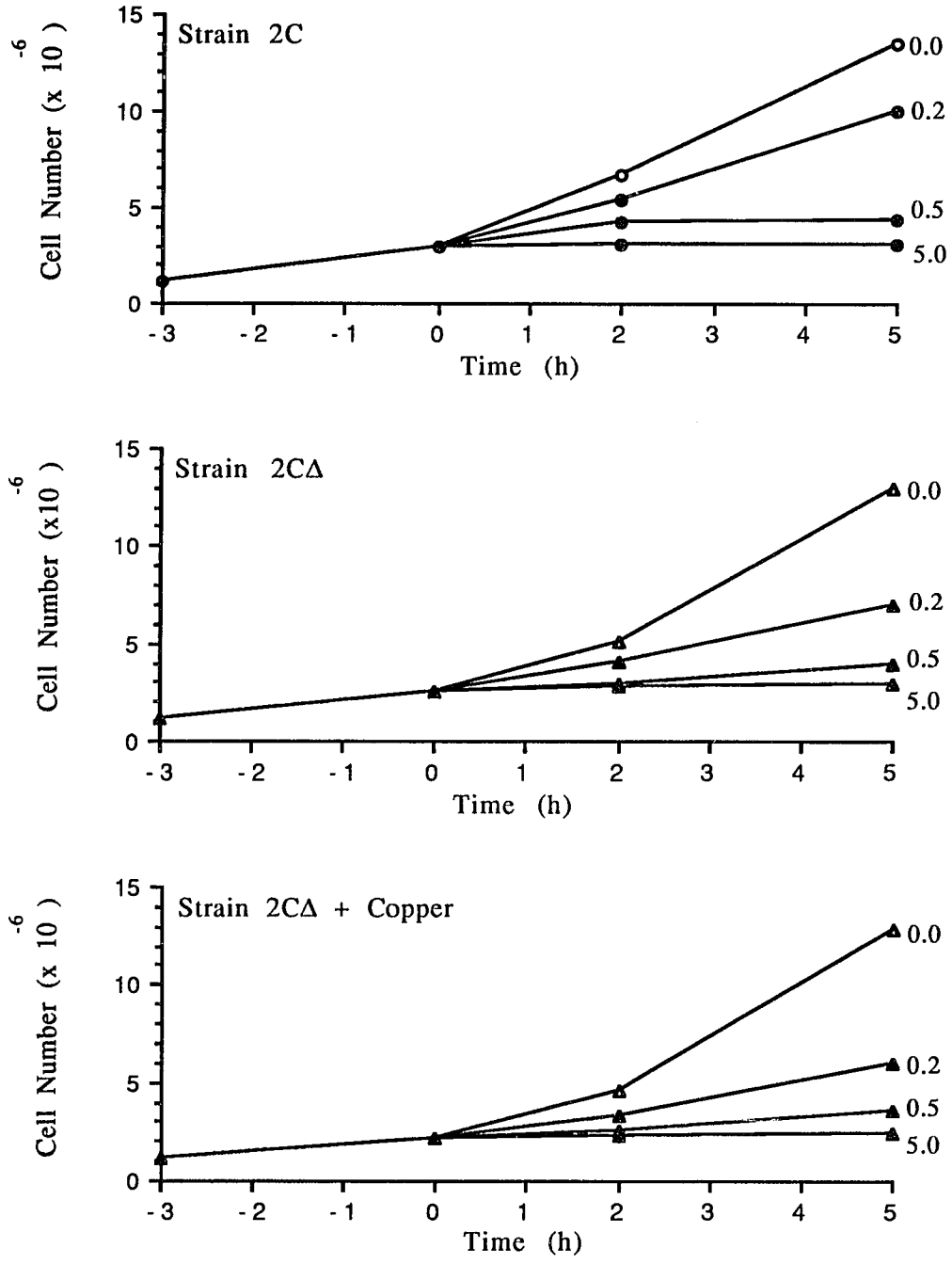

Figure 24. BiP overexpression maintains cell viability in response to TM challenge.

Log-phase cells from yeast strains 2C and 2CΔ were diluted to a concentration of 1.2 x 10^6 cells/ml and incubated for 3 hours in the absence (solid line) or presence (dotted line) of 0.2 mM Cu^{2+}. At time zero, TM was added (solid symbols) to a final concentration of 0.2, 0.5, or 5.0 μg/ml. At the indicated times, aliquots were removed to determine cell number and viability as described. (A) Dose response of cell viability in response to 0.2, 0.5, and 5.0 μg/ml TM challenge. (B) Time course of cell viability after a 5.0 μg/ml TM challenge. Cell viability was determined at each time point by spreading aliquots of the reactions on to selective plates and counting colonies after five days of growth.

Figure 24. BiP overexpression maintains cell viability in response to TM challenge.

A. Dose response.

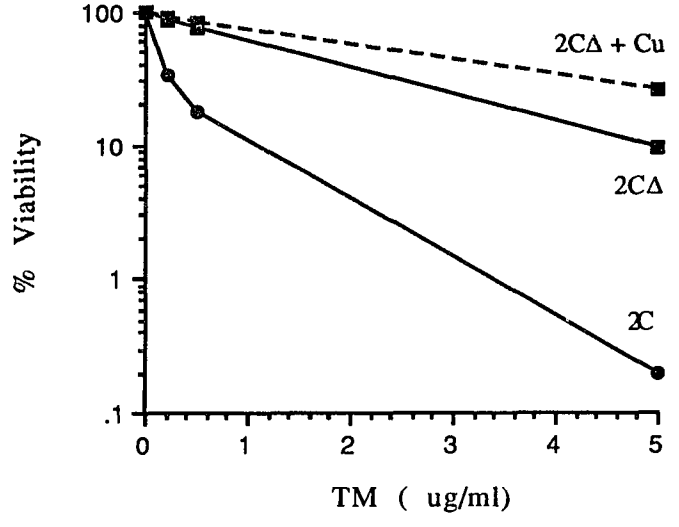

B. Time Course.

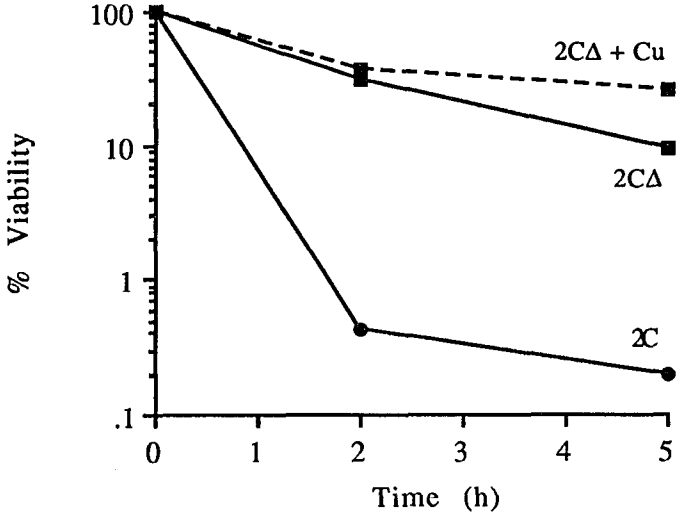

elevated levels of *pre-existing* BiP are more effective than BiP induced in response to stress.

The extreme sensitivity of strain 2C to 5 μg/ml of TM is also evident in the time course experiment, where only 0.2% of the treated cells remained viable at the end of a five hour incubation (Figure 24B). In comparison, strain 2CΔ is significantly more resistant, with 9.3% of the cells remaining viable after the same treatment. In the presence of Cu^{2+}, which increases the BiP levels 10-fold over those found in strain 2C, strain 2CΔ is even more resistant to TM treatment, with 25.7% of the cells remaining viable at the end of the incubation.

We conclude that overexpression of BiP increases the cell's long-term ability to survive a lethal ER stress as represented by TM treatment. However, overexpression of BiP has no effect on counteracting the acute divisional arrest that occurs during TM treatment. Most important, having a pre-stress elevation of BiP (as seen in the elevated basal transcription in the 2CΔ strain in the absence of Cu^{2+}) was observed to confer a greater degree of protection than the BiP induced during the stress.

B. *Overexpression of BiP from the CUP1 promoter inhibits the induction of genomic BiP by TM*

The sequence of events that results in the elevated synthesis of BiP in response to an ER stress such as TM treatment is not well understood. It has been proposed that the cell is able to sense the secretory load within the ER lumen and initiate a signaling pathway whose ultimate effect is increased transcription of the BiP gene. A fundamental question is: what is the primary signal in the ER that ultimately initiates the transcriptional response? Is it the aberrant or malfolded protein, a complex of BiP with such proteins, or

perhaps the level of free BiP? As a first step to distinguish between these possibilities, I examined the kinetics of BiP induction in response to TM treatment after overexpressing BiP from the exogenous CUP1 promoter (Figure 25).

To examine the potential feedback regulation of BiP transcription, the control strain (2C) and strains containing the low-copy (centromeric), and high-copy (episomal) CUP1-KAR2 plasmids were pretreated with Cu^{2+} to stimulate the production of "exogenous" BiP from the CUP1 promoter. As a consequence, the level of BiP mRNA prior to challenging the cells with TM was approximately 15-fold higher in the low-copy strain, and 40-fold higher in the high-copy strain (Figure 25A). All three strains were then challenged with 1 μg/ml TM for increasing times. At each time point, an aliquot of cells was removed and total RNA was extracted and subjected to Northern analysis, using a probe specific for chromosome-derived BiP mRNA (Figure 25B). The basal level of chromosome-derived BiP mRNA is identical in all three strains; this suggests that simple overexpression of BiP protein does not influence the basal transcription rate of the BiP gene. Furthermore, we consistently observed that increasing the initial level of BiP prior to a TM challenge produced a significant time lag in the induction of BiP mRNA. Finally, the absolute level of BiP mRNA at the end of the study was consistently only 50% of the control level.

The observation that BiP overexpression dampens the TM-mediated transcriptional induction of the KAR2 gene, provides some insight into the mechanism by which the cell senses the presence of malfolded proteins within the ER lumen. If the acute level of malfolded proteins resulting from TM treatment remains constant during BiP overexpression, then the level of BiP-malfolded protein complexes should also increase under these conditions.

Figure 25. Induction of chromosomal-derived BiP mRNA by TM can be inhibited by overexpression of plasmid-derived BiP mRNA.

Equal amounts of early log-phase cells from strains 2C (circles), 2CLCK2 (squares) and 2CHCK2 (triangles) were pretreated with 0.2 mM Cu^{2+} for three hours, prior to challenging cells with TM. Total RNA was isolated, transferred to nitrocellulose and subjected to Northern analysis. (A) Plamid-derived BiP mRNA levels after Cu^{2+} treatment, detected using a probe specific for plasmid-derived BiP mRNA. The amount of radioactive labeled plamid-derived BiP and actin mRNAs were quantitated and normalized as described in Figure 11. The data are presented as the fold induction over the level found in wild-type cells in the absence of treatment. (B) Induction of chromosomal-derived BiP mRNA levels in response to TM (1 μg/ml) challenge after Cu^{2+} induction of plasmid-derived BiP. The amount of radioactive labeled chromosome-derived BiP and actin mRNAs were quantitated and normalized as described in Figure 11. The data are presented as the fold-induction over the level of chromosomal-derived BiP prior to the TM challenge.

Figure 25. Induction of chromosomal-derived BiP mRNA by TM can be inhibited by overexpression of plasmid-derived BiP mRNA.

A. Induction of plasmid-derived BiP mRNA

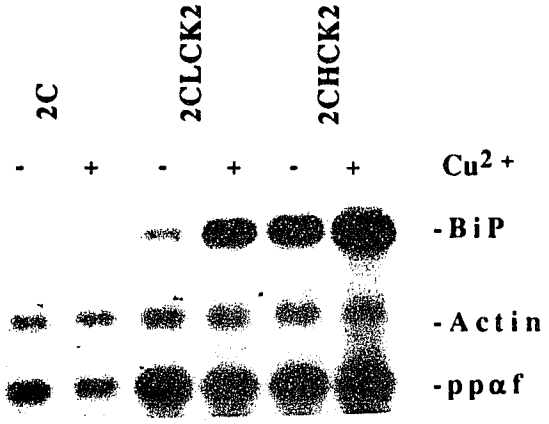

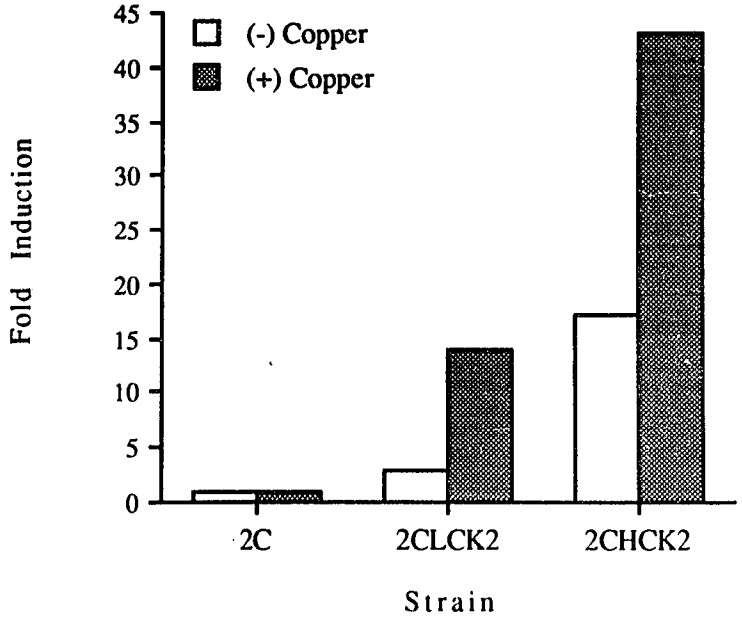

B. Induction of chromosomal-derived BiP mRNA

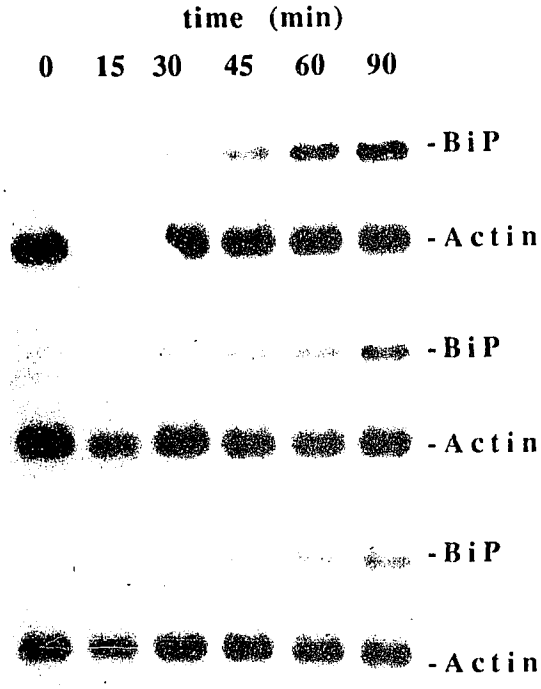

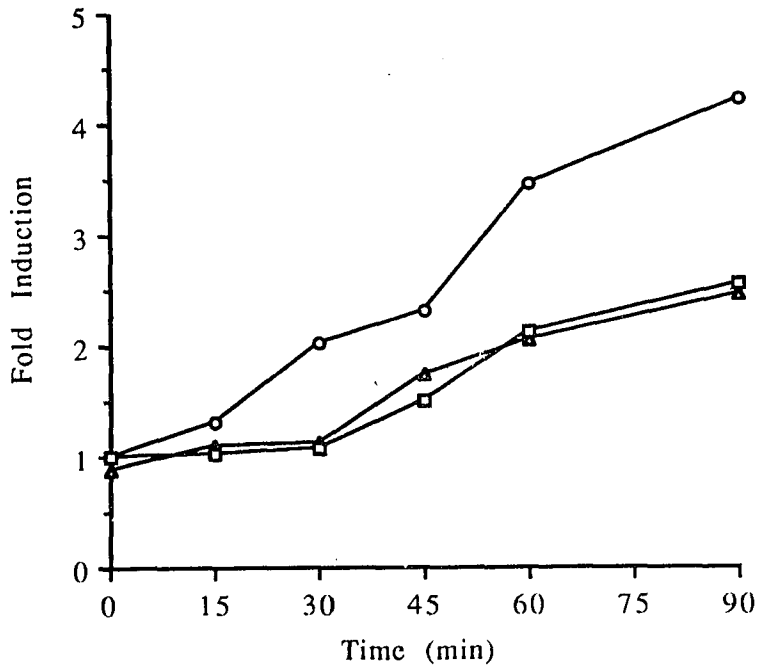

In this case, our data suggest that the level of these complexes is not the parameter sensed by the cell. Instead, the results support a model in which the level of free BiP is sensed by the cell and the level of transcription of the KAR2 gene is regulated accordingly. Though this experiment does not identify the molecular entity that acts as the signal, it supports the idea that BiP itself is involved in its own regulation (see discussion).

C. *TM-mediated induction of BiP occurs at the level of transcription*

In the course of these studies, we occasionally observed a mild increase of plasmid-derived BiP mRNA in TM-treated samples, suggesting that these transcripts were stabilized by TM treatment. To investigate this observation, I measured the half-life of BiP mRNA directly in the absence and presence of TM. To accomplish this most simply, I utilized the RY262 strain of *S. cerevisiae*, which contains a mutant RNA polymerase II that is rapidly inactivated at nonpermissive temperatures. Briefly, cells were grown at the permissive temperature in the absence or presence of 1 μg/ml TM for two hours, abruptly shifted to the nonpermissive temperature and incubated for increasing times, after which total RNA was isolated and subjected to Northern analysis. Comparison of the absolute level of BiP mRNA as a function of time following the shift to the nonpermissive temperature allowed the stability of BiP mRNA to be directly observed (Figure 26). The results unequivocally demonstrate that TM does not stabilize BiP mRNA, and may in fact mildly destabilize it. Therefore, the increase in steady-state BiP mRNA levels following TM treatment is most certainly a consequence of an increased rate of transcription.

Figure 26. BiP mRNA decay in the absence and presence of TM.

Early log-phase cells from the temperature-sensitive RNA polymerase II mutant strain Y262 were grown at the permissive temperature (25° C) for 2 hours in the absence (open circles) or presence (closed circles) of 1 μg/ml TM before shifting to the nonpermissive temperature (36° C) to stop transcription. Total cellular RNA (5 μg) was isolated from each point as described, separated on a 1.0% agarose gel containing 2% formaldehyde, transferred to nitrocellulose and hybridized under strigent conditions with probes that recognize actin, ppαf, and BiP mRNA (A). The amount of radioactive label hybridized to BiP, actin and ppαf mRNAs was determined as previously described in Figure 11. (B) The data are presented as the percentage of the starting BiP mRNA level, prior to the shift to the restrictive temperature.

Figure 26. BiP mRNA decay in the absence and presence of TM.

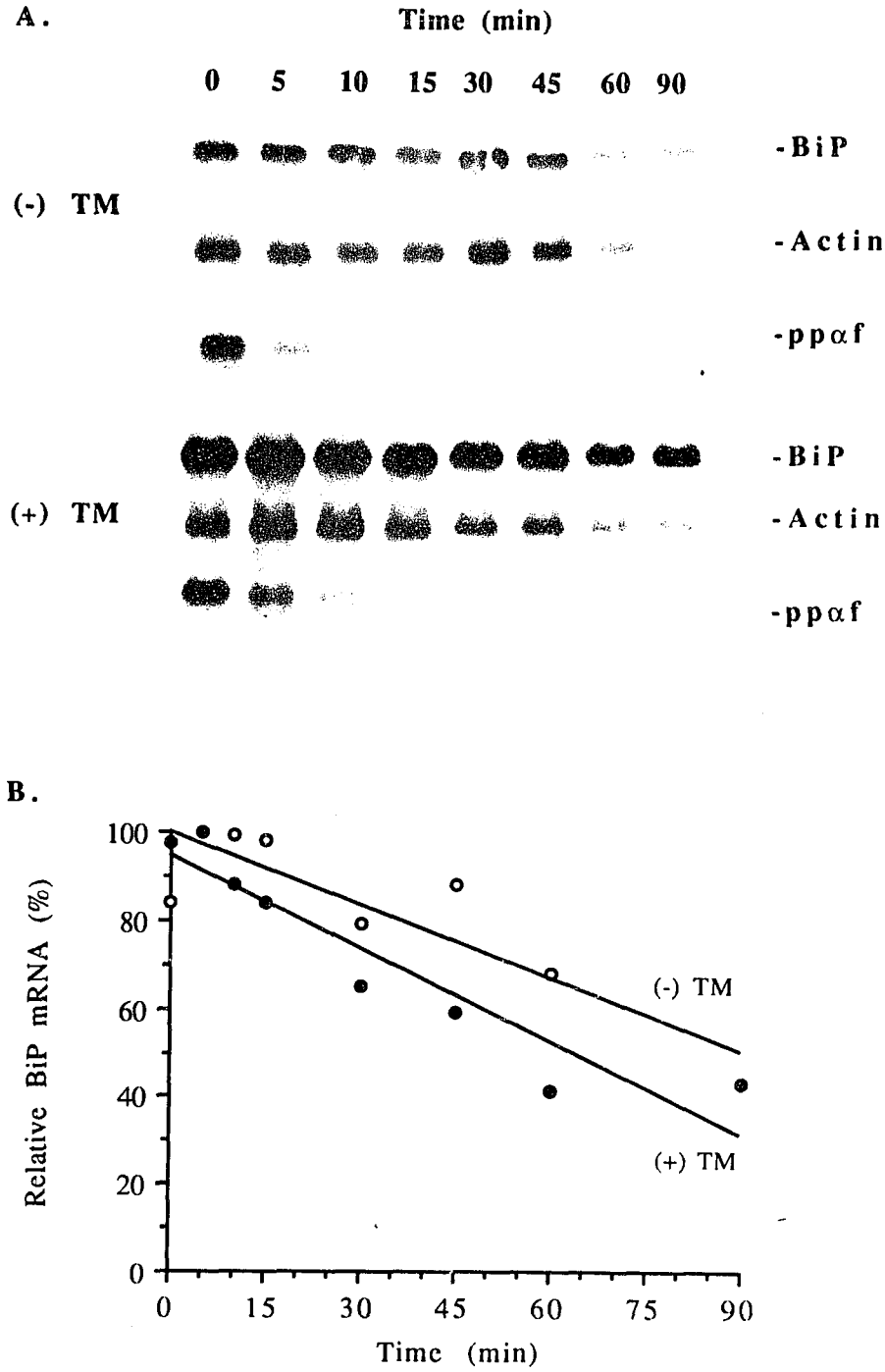

IV. DISCUSSION

General role of glycosylation in the biogenesis of ppαf

The use of a triple glycosylation mutant of ppαf combined with pulse-chase labeling and HPLC analysis of secreted radiolabeled αf allowed us to examine in a rigorous and quantitative manner the role of Asn-linked glycosylation in the transport and processing of a well-characterized model yeast secretory protein. Our analysis demonstrated, that disruption of Asn-linked glycosylation leads to a severe reduction in αf secretion and a concomitant delay in ER-to-Golgi transport of the precursor (see Figure 10). Importantly, these results were confirmed in the wild-type strain using tunicamycin (TM) treatment as an alternative strategy to inhibit Asn-linked glycosylation. The data suggest that the observed reduction in αf secretion is a consequence of a loss of Asn-linked glycosylation, and not a secondary effect of TM treatment or of the mutations used to disrupt the glycosylation consensus sequences.

Our results strengthen the conclusions of earlier studies that examined the impact of Asn-linked glycosylation on αf secretion by mating and halo assays [55, 135]. In those studies, the role of Asn-linked glycosylation on ppαf transport and secretion was observed to be dose-dependent, i.e. a ppαf mutant in which all three Asn-linked glycosylation sites are disrupted (strain N123) exhibited a greater reduction in αf secretion, than ppαf glycosylation mutants with any combination of two Asn-linked glycosylation sites disrupted (strains N1N2, N1N3, and N2N3). These, in turn, exhibit a greater reduction than mutants with any one single site disrupted (strains N1, N2, and N3) [55]. In addition, no one site predominates in its effect on αf secretion, supporting a general role for oligosaccharides in ppαf transport and processing.

One possible explanation for these results is that co-translocational Asn-linked glycosylation prevents an initial non-specific aggregation of ppαf as it is being translocated through the ER membrane. At a subsequent stage, the presence of core-glycosylation on gpαf may prevent non-specific protein-protein interactions within the lumen of the ER that could lead to protein aggregation and failed transport.

Support for this model comes from several studies. In vitro studies using purified yeast invertase revealed that glycosylation stabilizes the protein and prevents aggregation during refolding after guanidine HCl denaturation. In addition, the presence of glycosylation allows invertase to fold properly under conditions of high protein concentration, where aggregation is kinetically favored over folding. In vivo studies have also demonstrated a role for Asn-linked glycosylation in folding, since underglycosylated or improperly glycosylated proteins are often misfolded, even in the presence of functional BiP [136-139].

We hypothesize that during biosynthesis, rapid co-translational translocation and core-glycosylation help to avoid nonspecific aggregation of newly synthesized glycoproteins. Since the hydrophilic carbohydrate units increase the solubility of partially unfolded proteins, the tendency to form aggregates decreases with the amount of glycosylation [140, 141]. Because core-glycosylation occurs within the ER, the solubilization of the nascent polypeptide chain may provide a mechanism to avoid misfolding and aggregation at the high protein levels typically found within the ER [142, 143].

Luminal role for BiP in the maturation of N123-pαf

Many proteins require the aid of molecular chaperones to attain their final tertiary structures, and consequently, chaperones have been found in all

subcellular compartments where protein folding occurs. It is becoming increasingly clear that the mechanism by which these proteins exert their effect is through their ability to aid protein folding and assembly by binding nascent polypeptide chains and preventing the formation of "improper", but thermodynamically stable, alternative structures or aggregates incompatible with protein function. It was predicted, and subsequently verified, that chaperones recognize and bind specific structural motifs that are present in nascent (or mutant) polypeptides, but are absent or inaccessible in their mature (or wild-type) counterparts.

The most intriguing result from our initial studies was the apparent rescue of αf secretion seen in the N123 strains after TM treatment (Figure 10). To account for this observation we proposed two alternative hypotheses: The "rescue" hypothesis, which postulates that induction of BiP following exposure to TM leads to a relative *surplus* of BiP within the ER which is free to bind N123-pαf and non-glycosylated pαf and promote their folding and subsequent transport out of the ER, effectively rescuing them from aggregation. In contrast, the "escape" hypothesis postulates that in the presence of TM the relative level of BiP is *deficient*, since treatment with TM also results in a large number of non-glycosylated secretory and membrane proteins which may compete for BiP binding, leading to the escape of non-glycosylated pαf and N123-pαf. Most importantly, these results suggest for the first time a luminal role for yeast BiP, similar to that identified in mammalian cells, and distinct from the identified role of yeast BiP in ER translocation [31, 84, 85, 144].

To distinguish between these hypotheses we performed quantitative pulse-chase analysis using the high-copy Δ strains, which contained a disrupted KAR2 gene, as well as high-copy ppαf or N123-ppαf expressing plasmids. Since the level of BiP expression in these strains is under the

control of Cu^{2+} and unresponsive to TM, we were able to independently regulate the level of BiP. Under conditions where BiP levels were constant, exposure to TM enhanced αf secretion in both strains while depleting the level of intracellular precursor (see Figures 19 and 20), a result inconsistent with the rescue hypothesis. Rather, pretreatment with Cu^{2+} (which elevated BiP levels) resulted in a decrease in αf secretion and an increase in the levels of intracellular pαf and N123-pαf (see Figures 19 and 20), a result consistent with the escape hypothesis and indicative of negative role for BiP in transport and processing. Examination of the effect of BiP overexpression in the absence of a surplus of potential substrates (Cu^{2+} treatment in the absence of TM) suggests that the basal level of BiP resulting from the CUP1 promoter is adequate to prevent escape of N123-pαf in the absence of TM, since overexpression of BiP has little impact on the level of secreted αf or intracellular N123-pαf (see Figure 20). In addition, overexpression of BiP had minimal impact on the transport and processing of the wild-type ppαf (Figure 19). Our results are consistent with the "escape" hypothesis, and support a negative role for BiP in the processing and secretion of non-glycosylated wild-type pαf and mutant N123-pαf.

The question then arises, why does overexpression of BiP not completely inhibit αf secretion in strain HCN123Δ? One possibility is that the biogenetic defect resulting from the lack of glycosylation is incomplete, and a small percentage of the precursor is competent for transport and processing. There may be an equilibrium between malfolded, transport-incompetent precursors that are bound to BiP, and properly folded, transport-competent precursors that are not substrates. In the case of the glycosylated precursor (gpαf), this equilibrium should favor the transport-competent form, while in the case of the mutant N123-pαf or non-glycosylated pαf, the equilibrium may favor the

transport-incompetent form. One might predict that, irrespective of the BiP concentration, a small amount of newly synthesized N123-pαf will never bind to BiP.

Role for BiP in yeast translocation

A role for BiP in yeast translocation was first observed after demonstrating that a temperature sensitive mutant of yeast BiP accumulated signal peptide-containing secretory precursors on the cytoplasmic side of the ER membrane [31], and was subsequently confirmed by demonstrating a similar phenotype in wild-type cells depleted of BiP [31, 84]. Based on genetic and cross-linking studies, yeast BiP has been proposed to function at two distinct stages of ER translocation [85]. First, BiP appears to play a role in the initial interaction between the secretory protein and Sec61p, perhaps promoting or acting to stabilizing this interaction. Second, after the secretory protein is in contact with Sec61p, BiP is necessary to advance the translocation reaction from an initial complex with Sec61p to a more mature complex consisting of the secretory proteins, Sec61p and Sec63p, which is capable of translocating the secretory protein into the lumen of the ER.

Our data do not completely exclude a role for BiP in an earlier stage of N123-ppαf biogenesis. Under conditions of massive BiP overexpression, a small amount of signal peptide-containing ppαf and N123-ppαf was observed, suggesting that an *early* interaction between BiP and ppαf or N123-ppαf was stabilized (data not shown). Interestingly, treatment of the cells with TM abolished any evidence of the preprohormones, arguing that this phenomenon is also sensitive to the relative amounts of BiP and secretory protein substrates. In any case only a small percentage of nascent ppαf and N123-ppαf was subject to this effect.

Possible interaction of N123-pαf and BiP

The effects of manipulating BiP levels on the biogenesis of N123-pαf lead to the hypothesis that these proteins interact directly in the lumen of the ER. Direct demonstration of this interaction is lacking. The hypothesis is supported however, by two observations: (1) induction of BiP expression by N123-ppαf, and (2) the growth-inhibitory effects of co-expression of BiP and N123-ppαf.

Expression of N123-pαf from an integrated chromosomal copy of the gene induces BiP levels within the cell by approximately 2-3 fold (see Figure 11), and overexpression from a high copy episomal plasmid results in an even greater level of BiP induction (see Figure 12). Importantly, overexpression of the wild-type ppαf had no effect on steady state BiP levels, confirming the specificity of the response. To our knowledge, this is the first demonstration that a mutant yeast secretory protein (N123-ppαf) with a well-characterized defect in intracellular transport induces the expression of BiP in a dose-dependent manner.

The striking difference in growth rates between the mutant and wild-type strains in response to overexpression of BiP suggests that the physical interaction between BiP and N123-pαf is deleterious to the cell (see Figure 17). Perhaps the presence of large amounts of BiP in a complex with N123-pαf signals a reduction in cell growth similar to the arrest in the G_1 phase of the cell cycle that occurs in the presence of TM [133, 134]. However, unlike the giant cells seen after TM treatment, the growth-retarded N123 mutant cells seen in the presence of BiP overexpression are normal in size (data not shown).

Site of degradation of N123-pαf in the secretory pathway

Quantitation of the capacity of a given amount of wild-type or mutant precursor to generate a given amount of secreted αf leads to the conclusion that a significant fraction of non-glycosylated pαf and N123-pαf is degraded within the yeast secretory pathway, and that commitment to a degradative pathway most probably occurs prior to the KEX2-mediated proteolytic within the late Golgi. By using a sec18 strain transformed with a centromeric plasmid containing the mutant mfα1 gene we were able to block transport of N123-pαf out of the ER and demonstrate a lack of degradation. The most straightforward interpretation of these data is that the site of N123-pαf is distal to the sec18 block (i.e. post-ER), though there are other possible explanations (see Results). Since KEX2 proteolytic cleavage has been demonstrated to occur in a late Golgi compartment proximal to, or identical with, the site of vacuolar protein sorting[145], it is possible that the majority of N123-pαf is degraded in the Golgi, or more likely within the vacuole.

BiP protects yeast from secretory pathway stress

The fact that cells respond to different types of secretory pathway stress by inducing the synthesis of BiP suggests that BiP, in analogy to the cytosolic heat shock proteins, plays a role in protecting cells from the deleterious effects of ER stress. Surprisingly, prior to this study, this assumption had never (to our knowledge) been tested directly.

We therefore designed an experiment in which the intracellular level of BiP was adjusted using a heterologous stimulus (i.e. Cu^{2+}) prior to challenging cells with TM. We predicted that overexpression of BiP prior to TM challenge would counteract the cytotoxic effects of TM. The data confirmed a protective role for BiP and we observed that the level of cell survival was

proportional to the level of BiP pre-induction. Most importantly the enhancement in viability was seen in a strain whose chromosomal copy of the BiP gene had been disrupted (2CΔ) and hence, could no longer transcriptionally respond to TM treatment. The observation that the 5-fold increase in steady state BiP protein levels resulting from basal transcription from the CUP1 promoter in the 2CΔ strain is more protective than the subsequent induction of transcription seen after TM treatment in the wild-type strain (Figure 16) suggests that it is the BiP level at the initiation of the challenge that is important for survival.

Support for the observation that BiP protects the cell from ER stress comes from a negative study in mammalian cells [146]. In this study, the role of BiP expression on cell viability was examined by integrating approximately 800 copies of a 36 bp region conserved in the promoter of all glucose regulated proteins (GRP), including BiP, into the genome of Chinese hamster ovary cells (CHO). The strategy was to use the integrated "decoy" promoter to competitively inhibit the activation of the GRPs by competing for *trans*-acting factors. Under these conditions, transformed cells exhibited reduced viability and a 50% reduction in growth rate after exposure to calcium ionophore (a well-characterized inducer of GRPs).

Transcriptional induction of BiP by TM: What is the signal?

Having established that the transcription and induction of BiP by TM is a physiologically significant response, we wished to investigate the ER lumenal conditions that might regulate this phenomenon. The transduction of a signal from the ER lumen to the nucleus is a beautiful example of intracellular homeostasis. To date, there are few examples of this type of retrograde communication between intracellular organelles and the nucleus

[147]. One striking example in yeast can be seen in the influence of the mitochondrial state on transcription of the peroxisomal isoform of citrate synthase (CIT2 gene), where alteration of mitochondrial function (ρ^0) elevates transcription 6-30 fold over that seen in respiratory isogenic competent (ρ^+) cells [147, 148]. Importantly, the influence of the functional state of the mitochondria on expression of the CIT2 gene has been attributed to transactivation through a novel UAS element that is responsive to alterations in mitochondrial function [148]. In our system the question then arises, what is the signal in the ER that initiates the transcriptional activation of BiP?

To address this question, we tested whether pre-induction of BiP prior to TM challenge would influence TM-mediated transcription, and found that such treatment dampens the transcriptional response. This is consistent with studies in mammalian cells, in which overexpression of BiP from a recombinant plasmid significantly reduces the induction of the chromosomal BiP gene after exposure to TM or calcium ionophore [103]. Importantly, GRP94 induction was also suppressed by BiP overexpression, arguing that elevated levels of BiP serve to shut down the transcriptional activation of the GRP genes. Since the genes for BiP and GRP94 are coordinately regulated at the transcriptional level by common *trans*-acting factors acting through common regulatory domains [149], it is possible that the putative signal transmitted from the ER converges on these factors.

In our studies, simple overexpression of BiP was not completely effective in blocking the TM-mediated increase in chromosomal BiP transcription. There are several possible explanations for the intermediate level of feedback inhibition. First, electron microscopic examination of yeast cells that massively overexpress BiP revealed sac-like expansions of the nuclear envelope, as well as large tennis-racquet shaped vesicles throughout

the cytoplasm (data not shown). Immuno-electron microscopy demonstrated that these membranous structures contain a high concentration of BiP. This suggests that some of the excess BiP is sequestered, and thus rendered ineffective in binding substrate or interacting with the putative signaling apparatus. Notably, treatment of these cells with TM abolished these structures, suggesting that they only accumulate when BiP is overexpressed inappropriately. Some precedent exists for this observation, In *Drosophilia* cells, constitutive overexpression of hsp70 leads to a reduction in growth rate, which is followed by recovery and a redistribution of intracellular hsp70 from a diffuse pattern into discrete intracellular granules [150]. The protein granules appeared to be irreversibly inactivated, could not be dispersed with a second heat shock, and cells containing these granules do not show thermotolerance.

A second reason that the level of BiP transcription is not completely suppressed may be the poorly characterized effect of post-translational modifications on BiP function. While yeast BiP has not been demonstrated to be post-translationally modified, in mammalian cells BiP is exists in two pools; post-translationally modified free BiP, and unmodified bound BiP [151]. It may be that under conditions of overexpression, yeast BiP is inappropriately modified and thus incapable of signaling.

In an attempt to further characterize the nature of the signal, we examined the level of chromosomal BiP mRNA in a high-copy N123 strain containing the CUP1-KAR2 gene on a centromeric plasmid (pLCK2). In this case, the increased level of plasmid-derived BiP was able to abolish the induction of the chromosome-derived BiP mRNA by expression of N123-ppαf (data not shown). Besides supporting our feedback hypothesis, this result

suggests that the signaling pathway of N123 and TM treatment may share mechanistically similar features.

Future experiments

What are the consequences of BiP-N123-pαf interaction?

By devising procedures to lyse yeast cells in a more gentle fashion than is commonly used it should be possible to isolate complexes of BiP and N123-pαf. This would allow for the investigation of related issues, e.g. does substrate associated BiP turn over more rapidly than free BiP? It may be possible to cross-link N123-pαf to BiP, or to the yeast translocon. In addition, the use of ts mutants of BiP may pinpoint the role of wild-type BiP in retention and degradation of N123-pαf. Finally the use of vps mutants (defective in vacuolar targeting) may allow us to identify the intracellular site of degradation of N123-pαf

What are the components of the ER-to-nucleus signal transduction pathway?

A method to select for mutants defective in the transcriptional induction of BiP in response to ER signals would allow proteins all along the retrograde communication pathway from the ER lumen to the nucleus to be cloned and identified. While specific transcription factors involved in the activation of BiP transcription have been identified in yeast cell lysates, they have yet to be cloned [104, 108]. Most importantly, the following scheme would allow us to identify novel proteins involved in transmitting the signal across the ER membrane, and consequently allow the initial characterization of a novel signal transduction pathway.

The basis of the selection for mutants which fail to transcriptionally induce BiP in response to ER signals is based on the published observation that deletion of the carboxy terminal HDEL tetrapeptide in a KAR2 construct containing the wild-type promoter results in a corresponding transcriptional induction of this construct to maintain the level of BiP within the ER [105]. The important characteristic of this strain is that the loss of the HDEL-deleted BiP via secretion results in a strain whose retrograde communication pathway is constitutively activated to maintain BiP levels. The next step would be to transform this strain with a wild-type copy of the KAR2 gene on a centromeric plasmid containing the URA3 gene as a selectable marker. The presence of wild-type BiP should turn off the constitutive activation of the retrograde communication pathway (a result that could be documented by Northern analysis). Cells would then be mutagenized by standard techniques and screened for temperature sensitive mutants that fail to grow on 5-FOA plates, which selects against URA3 containing plasmids. Mutant cells that cannot increase the level of transcription from the remaining KAR2 gene containing the HDEL deletion should be unable to lose their copy of the wild-type KAR2 gene on the URA3 plasmid and hence, would fail to grow on 5-FOA plates. It is anticipated that mutations exhibiting this phenotype could occur in any of the components of the signaling pathway.

IV. BIBLIOGRAPHY

1. Bucking-Throm, E., *et al., Reversible arrest of haploid yeast cells at the initiation of DNA synthesis by a diffusable sex factor.* Experimental Cell Research, 1973. **76**: p. 99-110.

2. Duntze, W., V. MacKay, and T.R. Manney, *Saccharomyces cerevisiae: A diffusible sex factor.* Science, 1970. **168**: p. 1472-1473.

3. Hereford, L.M. and L.H. Hartwell, *Sequential gene function in the initiation of Saccharomyces cerevisiae DNA synthesis.* J. Mol. Biol., 1974. **84**: p. 445-461.

4. Lipke, P.N., A. Taylor, and C.E. Ballou, *Morphogenic effects of α-factor on Saccharomyces cerevisiae a cells.* J. of Bacteriol., 1976. **127**: p. 610-618.

5. Fehrenbacher, G., K. Perry, and J. Thorner, *Cell-cell recognition in Saccharomyces cerevisiae: Regulation of mating specific adhesion.* J. of Bacteriol., 1978. **134**: p. 893-901.

6. Baffi, R.A., *et al., Different function-structure relationships for α-factor induced morphogenesis and agglutination in Saccharomyces cerevisiae.* J. of Bacteriol., 1984. **158**: p. 1152-1156.

7. Stetler, G. and J. Thorner, *Molecular cloning of hormone responsive genes from yeast Saccharomyces cerevisiae.* Proc. Natl. Acad. Sci. USA, 1984. **81**: p. 1144-1148.

8. Singh, A., *et al., Saccharomyces cerevisiae contains two discrete genes coding for the α-factor pheremone.* Nuc. Acid Res., 1983. **11**: p. 4049-4063.

9. Kurjan, J. and I. Herskowitz, *Structure of a yeast pheremone gene (MFα): a putative α-factor precursor contains four tandem repeats of a mature α-factor.* Cell, 1982. **30**(933-943).

10. Kurjan, J., *α−Factor structural gene mutations in Saccharomyces cerevisiae: Effects on α−factor production and mating.* Mol. Cell Biol., 1985. **5**(4): p. 787-796.

11. Julius, D., *et al., Isolation of the putative structural gene for the lysine-arginine-cleaving endopeptidase required for processing of yeast prepro-alpha-factor.* Cell, 1984. **37**: p. 1075-1089.

12. Julius, D., R. Schekman, and J. Thorner, *Glycosylation and processing of prepro-α-factor through the yeast secretory pathway.* Cell, 1984. **36**: p. 309-318.

13. Julius, D., *et al., Yeast α-factor is processed from a larger precursor polypeptide: The essential role of a membrane-bound dipeptidyl aminopeptidase.* Cell, 1983. **32**: p. 839-852.

14. Dmochowska, A., *et al., Yeast KEX1 gene encodes a putative protease with a carboxypeptidase B-like function involved in killer toxin and α-factor precursor processing.* Cell, 1987. **50**: p. 573-584.

15. Fuller, R.S., R.E. Sterne, and J. Thorner, *Enzymes required for yeast prohormone processing.* Cell, 1988. **50**: p. 345-362.

16. Emter, O., *et al., Yeast pheremone α-factor is synthesized as a high molecular weight precursor.* Biochem. Biophys. Res. Commun, 1983. **116**: p. 822-829.

17. Waters, M.G. and E.A.E. Blobel, *Prepro-α-factor has a cleavable signal sequence.* J. Biol. Chem., 1988. **263**: p. 6209-6214.

18. Esmon, B., P. Novick, and R. Schekman, *Compartmentalized assembly of oligosaccharides on exported yeast in yeast.* Cell, 1981. **25**: p. 451-460.

19. Ballou, C.E., *The Yeast Cell Wall and Cell Surface,* in *The Molecular Biology of the Yeast Saccharomyces,* J.N. Strathern, E.W. Jones, andJ.R. Broach, Editor. 1982, Cold Spring Harbor Press: New York.

20. Achstetter, T. and D.H. Wolf, *Hormone processing and membrane-bound proteinases in yeast.* EMBO J., 1985. **4**: p. 173-177.

21. Eakle, K.A., M. Berstein, and S. Emr, *Characterization of a component of the yeast secretion machinary: identification of the SEC18 gene product.* Mol. Cell Biol., 1988. **8**(10): p. 4098-4109.

22. Block, M., *et al., Purification of an N-ethylmaleimide-sensitive protein catalyzing vesicular transport.* Proc. Natl. Acad. Sci. USA, 1988. **85**: p. 7852-7856.

23. Deshaies, R.J. and R. Schekman, *A yeast mutant defective at an early stage of import of secretory protein precursors into the endoplasmic reticulum.* J. Cell Biol., 1987. **105**: p. 633-645.

24. Rothblatt, J.A., *et al., Multiple genes are required for proper insertion of secretory proteins into the endoplasmic reticulum.* J. Cell Biol., 1989. **109**: p. 2641-2652.

25. Deshaies, R.J. and R. Schekman, *SEC 62 encodes a putative membrane protein required for protein translocation into the yeast endoplasmic reticulum.* J. Cell Biol., 1989. **109**: p. 2653-2664.

26. Deshaies, R., *et al., Assembly of yeast Sec proteins involved in translocation into the endoplasmic reticulum into a multi-subunit complex.* Nature, 1991. **349**: p. 806-808.

27. Feldheim, D., J. Rothblatt, and R. Schekman, *Topology and functional domains of Sec63p, an endoplasmic reticulum membrane required for s ecretory protein translocation.* Mol. Cell Biol., 1992. **12**(7): p. 3288-3296.

28. Stirling, C.J., *et al., Protein translocation mutants defective in the insertion of integral membrane proteins into the endoplasmic reticulum.* Mol. Cell Biol., 1992. **3**: p. 129-142.

29. Hansen, W., P.D. Garcia, and P. Walter, *In vitro protein translocation across the yeast endoplasmic reticulum: ATP-dependent post-translational translocation of the prepro-α-factor.* Cell, 1986. **45**: p. 397-406.

30. Rothblatt, J.A. and D.A. Meyer, *Secretion in yeast: translocation and glycosylation of prepro-α-factor in vitro can occur via an ATP-dependent post-translational mechanism.* EMBO J., 1986. **5**(5): p. 1031-1036.

31. Vogel, J.P., L.M. Misra, and M.D. Rose, *Loss of Bip/Grp 78 function blocks translocation of secretory proteins in yeast.* J. Cell Biol., 1990. **110**: p. 1885-1895.

32. Hann, B.C. and P. Walter, *The signal recognition particle in S. cerevisiae.* Cell, 1991. **67**: p. 131-144.

33. Kornfeld, R. and S. Kornfeld, *Assembly of asparagine-linked oligosaccharides.* Ann. Rev. Biochem., 1985. **54**: p. 631-664.

34. Kukuruzinska, M.A., M.L.E. Bergh, and B.J. Jackson, *Protein glycosylation in yeast.* Ann. Rev. of Biochem., 1987. **56**: p. 915-944.

35. Hasilik, A. and W. Tanner, *Carbohydrate moiety of Carboxypeptidase Y and perturbation of its biosynthesis.* Euro. J. Biochem., 1978. **91**: p. 567-575.

36. Lehle, L., R.E. Cohen, and C.E. Ballou, *Carbohydrate structure of yeast Invertase.* J. Biol. Chem., 1991. **254**: p. 12209-12218.

37. Trimble, R.B. and P.H. Atkinson, 1986. Science, **261**: p. 9815-9824.

38. Eyler, E.H., *The biological role of glycoproteins.* J. of Theoretical Biology, 1965. **10**: p. 89-113.

39. Olden, K., J.B. Parent, and S.L. White, *Carbohydrate moieties of glycoproteins a re-evaluation of their function.* Biochem. Biophys. Acta, 1982. **650**: p. 209-232.

40. Tkacz, J.S. and J.O. Lampen, *Tunicamycin inhibition of polyisoprenyl N-acetylglucosaminyl pyrophospahate formation in calf liver microsomes.* Biochem. Biophys. Res. Commun., 1975. **65**: p. 248-257.

41. Takatsuki, A., K. Kohno, and G. Tamura, *Inhibition of biosynthesis of polyisoprenol sugars in chich embryo microsomes by tunicamycin.* Agric. Biol. Chem., 1975. **39**: p. 2089-2091.

42. Tangen, O., J. Jonsson, and S. Orrenius, *Isolation of rat liver microsomes by gel filtration.* Analytic Biochemistry, 1973. **54**: p. 597-603.

43. Takatsuki, A., *et al., Structural elucidation of tunicamycin II. The structure of tunicamycin.* Agric. Biol. Chem., 1977. **41**: p. 2307-2309.

44. Barnes, G., *et al., Asparagine-linked glycosylation in Saccharomyces cerevisiae: Genetic analysis of an earlier step.* Mol. Cell Biol., 1984. **4**(11): p. 2381-2388.

45. Rine, J., *et al., Targeted selection of recombinant clones through gene dosage effects.* Proc. Natl. Acad. Sci. USA, 1983. **80**: p. 6750-6754.

46. Ferro-Novick, S., P. Novick, and R. Schekman, *Yeast secretory mutants that block the formation of active cell surface enzymes.* J. Cell. Biol., 1984. **98**: p. 35-43.

47. Clark, D.W., J.S. Tkacz, and J.O. Lampen, *Asparagine-linked carbohydrate does not determine the the cellular location of yeast vacuolar nonspecific alkaline phosphatase.* J. of Bacteriol, 1982. **152**: p. 865-873.

48. Swaiger, H., *et al., Carbohydrate-free carboxypeptidase Y is transferred into the lysosome-like yeast vacuole.* Biochem. Biophys. Res. Commun, 1982. **104**: p. 950-956.

49. Hoe, M.H. and R. Hunt, *Loss of one asparagine-linked oligosaccharide from human transferrin receptors results in specific cleavage and association with the endoplasmic reticulum.* J. Biol. Chem., 1992. **267**(7): p. 4916-4923.

50. Williams, A.M. and C.A. Enns, *A Mutated transferrin receptor lacking asparigine-linked glycosylation sites shows reduced functionality and an association with binding immunoglobulin protein.* J. Biol. Chem., 1991. **266**(26): p. 17648-17654.

51. Yamaguchi, K., *et al., Effects of site-directed removal of N-Glycosylation sites in Human Erythropoietin on its production and biological properties.* J. Biol. Chem., 1991. **266**(30): p. 20434-20439.

52. Dorner, A.J., D.G. Bole, and R.J. Kaufman, *The relationship of N-linked glycosylation and heavy chain-binding protein association with the secretion of glycoproteins.* J. Cell. Biol., 1987. **105**(6): p. 2665-2674.

53. Elbien, A.D., *Inhibitors of the biosynthesis and processing of N-linked oligosaccharide chains.* Ann. Rev. Biochem., 1987. **56**: p. 497-534.

54. Machamer, C.E., R.Z. Florkiewicz, and J.K. Rose, *A single N-linked oligosaccharide at either of the two normal sites is sufficient for transport of Vesicular Stomatitis Virus G Protein.* Mol. Cell Biol., 1985. **5**: p. 3074-3083.

55. Caplan, S., *et al., Glycosylation and structure of the yeast MFα1 α-factor precursor is important for efficient transport through the secretory pathway.* J. of Bacteriol., 1991. **173**: p. 627-635.

56. Lodish, H.F., *Transport of secretory and membrane glycoproteins from the rough endoplasmic reticulum to the Golgi.* J. Biol. Chem., 1988. **263**: p. 2107-2110.

57. Kozutsumi, Y., *et al., The presence of malfolded proteins in the endoplasmic reticulum signals the induction off glucose regulated proteins.* Nature, 1988. **332**: p. 462-464.

58. Kern, G., *et al., Stability, quaternary structure, and folding of internal, external, and core-glycosylated invertase from yeast.* Protein Science, 1992. **1**: p. 120-131.

59. Munro, S. and H.R.B. Pelham, *An Hsp70-like Protein in the ER: Identity with the 78 kd Glucose-Regulated protein and Immunoglobulin Heavy Chain Binding protein.* Cell, 1986. **46**(July 18): p. 291-300.

60. Lee, A.S., *Mammalian stress response: induction of the glucose-regulated protein family.* Curr. Opin. Cell Biol., 1992. **4**: p. 267-273.

61. Gething, M. and J. Sambrook, *Protein folding in the Cell.* Nature, 1992. **355**: p. 33-45.

62. Shiu, R.P.C., J. Pouyssegur, and I. Pastan, *Glucose depletion accounts for the induction of two transformation sensitive membrane proteins in rous sarcoma virus transformed chick embryo fibroblasts.* Proc. Natl. Acad. Sci. USA, 1977. **74**: p. 3840-3844.

63. Haas, I.G. and M. Wabl, *Immunoglobulin heavy chain binding protein.* Nature, 1983. **306**(November 24): p. 387-389.

64. Pouyssegur, J., R.P.C. Shiu, and I. Pastan, *Induction of two transformation sensitive membrane polypeptides in normal fibroblasts by a block in glycosylation or glucose deprivation.* Cell, 1977. **11**: p. 941-947.

65. Drummond, I.A.S., *et al., Depletion of intracellular calcium stores by calcium ionophore A23187 induces the gene for glucose-regulated proteins in hanster fibroblasts.* J. Biol. Chem., 1987. **262**: p. 12801-12805.

66. Lee, A.S., *Coordinated regulation of a set of genes by glucose and calcium ionophores in mammalian cells.* TIBS, 1987. (12): p. 20-23.

67. Peluso, R.W., R.A. Lamb, and P.W. Choppin, *Infection with paramyxoviruses stimulates synthesis of cellular polypeptides that are also stimulated in cells transformed by Rous sarcoma virus or deprived of glucose.* Proc. Natl. Acad. Sci., 1978. **75**: p. 6120-6124.

68. Stoeckle, M.Y., *et al., 78-Kilodalton glucose-regulated protein is induced in Rous sarcoma virus-transformed cells independently of glucose deprivation.* Mol. Cell. Biol., 1988. **8**: p. 2675-2680.

69. Wiest, D.L., *et al., Membrane biogenesis during B cell differentiation: most endoplasmic reticulum proteins are expressed coordinately.* J. Cell. Biol., 1990. **110**: p. 1501-1511.

70. Dorner, A.J., L.C. Wasley, and R.J. Kaufman, *Increased synthesis of secreted proteins induces expression of glucose-regulated proteins in Butyrate-treated chinese hamster ovary cells.* J. Biol. Chem., 1989. **264**(34): p. 20602 - 20607.

71. Pelham, H.R., *Speculations on the functions of the major heatshock and glucose-regulated proteins.* Cell, 1986. **46**: p. 959-961.

72. Gething, M., K. McCammon, and J. Sambrook, *Expression of wild-type and mutant forms of influenza hemagglutinin: the role of folding in intracellular transport.* Cell, 1986. **46**: p. 939-950.

73. Villa, A., *et al., Intracellular calcium stores in chicken purkinje neurons: Differential distribution of the low affinity high capacity calcium binding protein, Calsequestrin, of calcium ATPase and of the ER luminal protein, BiP.* J. Cell. Biol., 1991. **113**: p. 779-791.

74. Watowich, S.S., R.I. Morimoto, and R.A. Lamb, *Flux of the Paramyxovirus hemagglutinin neuraminidase glycoprotein through the endolasmic reticulum activates transcription of the GRP78 BiP gene.* J. of Virol., 1991. **65**: p. 3590-3597.

75. Hendershot, L.M., *Immunoglobulin heavy chain and binding protein complexes are dissociated in vivo by light chain addition.* J. Cell. Biol., 1990. **111**: p. 829-837.

76. Rose, M.D., L.M. Misra, and J.P. Vogel, *KAR2, a Karyogamy Gene, Is the Yeast Homolog of the Mammalian BIP/GRP78 Gene.* Cell, 1989. **57**: p. 1211-1221.

77. Normington, K., *et al., S. cerevisiae encodes an essential protein homologous in sequence and function to mammalian BIP.* Cell, 1989. **57**: p. 1223-1236.

78. Polaina, J. and J. Conde, *Genes involved in the control of nuclear fusion during the sexual cycle of Saccharomyces cerevisiae.* Molecular General Genetics, 1982. **186**: p. 252-258.

79. Pelham, H.R.B., K.G. Hardwick, and M.J. Lewis, *Sorting of soluble ER proteins in yeast.* EMBO J., 1988. **7**: p. 1757-1762.

80. Munroe, S. and H. Pelham, *A C-terminal signal prevents secretion of luminal ER proteins.* Cell, 1987. **48**: p. 899-907.

81. Pelham, H.R.B., *The retention signal for soluble proteins of the endoplasmic reticulum.* TIBS, 1990. **15**: p. 483-486.

82. Novick, P., C. Field, and R. Schekman, *Identification of 23 complementation groups required for post-translational events in the yeast secretory pathway.* Cell, 1980. **21**: p. 205-215.

83. Preuss, D., *et al., Structure of the yeast endoplasmic reticulum: Localization of ER proteins using immunofluorescence and immunoelectron microscopy.* Yeast, 1991. **7**: p. 891-911.

84. Nguyen, T.H., D.T.S. Law, and D.B. Williams, *Binding protein BiP is required for translocation of secretory proteins into the endoplasmic reticulum in Saccharomyces cerevisiae.* Proc. Natl. Acad. Sci. USA, 1991. **88**: p. 1565-1569.

85. Sanders, S.L., *et al., Sec61 and BiP directly facilitate polypeptide translocation into the ER.* Cell, 1992. **69**: p. 353-365.

86. Bulleid, N.J. and R.B. Freedman, *Defective co-translational formation of disulphide bonds in protein disulphide-isomerase deficient microsomes.* Nature, 1988. **335**: p. 649-651.

87. Brodsky, J.L., *et al., Reconstitution of protein translocation from solubilized yeast membranes reveals topologically distinct roles for BiP and cytosolic Hsc70.* J. Cell Biol., 1993. **120**: p. 95-102.

88. Kim, Y.K. and A.S. Lee, *Transcriptional activation of the Glucose-Regulated Protein genes and their heterologous fusion genes by ß-Mercaptoethanol.* Mol. Cell Biol, 1987. 7(8): p. 2974-2976.

89. Resendez, E., *et al., Calcium ionophore A23187 induces expression of Glucose-Regulated Genes and their heterologous fusion genes.* Mol.Cell Biol., 1985. 5(6): p. 1212-1219.

90. Resendez, E., *et al., Calcium ionophore A23187 as a regulator of gene expression in mammalian cells.* J.Cell Biol., 1986. **103**: p. 2145-2152.

91. Nakaki, T., R.J. Deans, and A.S. Lee, *Enhanced transcription of the 78,000-Dalton Glucose-Regulated Protein (GRP78) Gene and association of GRP78 with Immmunoglobulin Light Chains in a nonsecreting B-cell Myeloma Line (NS-1).* Mol. Cell Biol., 1989. **9**(5): p. 2233-2238.

92. Wooden, S.K., *et al., Transactivation of the grp78 promoter by malfolded proteins, glycosylation block, and calcium ionophore is mediated through a proximal region containing a CCAAT motif which interacts with CTF/NF-I.* Mol. Cell Biol., 1991. **11**(11): p. 5612-5623.

93. Lenny, N. and M. Green, *Regulation of endoplasmic reticulum stress proteins in COS cells transfected with Immunoglobulin mu Heavy Chain cDNA.* J. Biol. Chem., 1991. **266**(30): p. 20532-20537.

94. Grossman, A.D., J.W. Erickson, and C.A. Gross, *The htpR gene product of E. coli is a sigma factor for heat-shock promoters.* Cell, 1984. **38**: p. 383-390.

95. Grossman, A.D., *et al.*, σ^{32} *synthesis can regulate the synthesis of heat shock proteins in E. coli.* Genes and Development, 1987. **1**: p. 179-184.

96. Gamer, J., H. Bujard, and B. Bukau, *Physical interaction between heatshock proteins DnaK, DnaJ, and GrpE and the bacterial heat shock t ranscription factor* σ^{32}. Cell, 1992. **69**: p. 833-842.

97. Craig, E.A. and C.A. Gross, *Is Hsp70 the cellular thermometer?* TIBS, 1991. **16**: p. 135-140.

98. Morimoto, R., K. Sarge, and K. Abravaya, *Transcriptional regulation of heat shock genes.* J. Biol. Chem., 1992. **267**(31): p. 21987-21990.

99. Craig, E.A. and K. Jakobsen, *Mutations of the heat inducible 70 kilodalton genes of yeast confer temperature sensitive growth.* Cell, 1984. **38**: p. 841-849.

100. Boorstein, W.R. and E.A. Craig, *Transcriptional regulation of SSA3, an HSP70 gene from Saccharomyces cerevisiae.* Mol. Cell Biol., 1990. **10**(6): p. 3262-3267.

101. Stone, D.E. and E.A. Craig, *Self-Regulation of 70-Kilodalton Heat Shock Proteins in Saccharomyces cerevisiae.* Mol. Cell Biol., 1990. **10**(4): p. 1622-1632.

102. Abravaya, K., *et al., The human heat shock protein hsp70 interacts with HSF, the transcription factor that regulates heat shock gene expression.* Genes and Development, 1992. **6**: p. 1153-1164.

103. Dorner, A.J., L.C. Wasley, and R.J. Kaufman, *Overexpression of GRP78 mitigates stress induction of glucose regulated proteins and blocks secretion of selective proteins in Chinese hamster ovary cells.* EMBO J., 1992. **11**(4): p. 1563-1571.

104. Kohno, K., *et al., The promoter region of the yeast Kar2 (BiP) gene contains a regulatory domain that responds to the presence of unfolded proteins in the endoplasmic reticulum.* Mol. Cell Biol., 1993. **13**(2): p. 877-889.

105. Hardwick, K.G., *et al., ERD1, a yeast gene required for the retention of luminal endoplasmic reticulum proteins, affects glycoprotein processing in the Golgi apparatus.* EMBO J., 1990. **9**: p. 623-630.

106. Carlsson, L. and E. Lazarides, *ADP-ribosylation of the Mr 83,000 stress-inducible and glucose regulated protein in avian and mammalian cells: Modulation by heat shock and glucose starvation.* Proc. Natl. Acad. Sci. USA, 1983. **80**: p. 4664-4668.

107. Hendershot, L.M., J. Ting, and A.S. Lee, *Identity of the immunoglobulin Heavy-Chain-Binding protein with the 78,000-dalton Glucose-Regulated Protein and the role of posttranslational modifications in its binding function.* Mol. Cell Biol., 1988. **8**(10): p. 4250-4256.

108. Mori, K., *et al., A 22bp cis-acting element is necessary and sufficient for the induction of the yeast KAR2 (BiP) gene by unfolded proteins.* EMBO J., 1992. **11**: p. 2583-2593.

109. Silver, S. and T. Misra, Ann. Rev. Microbiol. 1988. **42**: p. 717-743.

110. Silver, S., *et al., Bacterial resistance ATPases: primary pumps for exporting toxic cations and anions.* TIBS, 1989. **14**: p. 76-80.

111. Hammer, D.H., *Metallothionein.* Ann. Rev. Biochem., 1986. **55**: p. 913-951.

112. Sherman, F., *Getting Started with Yeast.* Methods of Enzymology, ed. C. Guthrie and G. Fink. Vol. 194. 1991, 3-21.

113. Butt, T.R. and D.J. Ecker, *Yeast metallothionein and applications in biotechnology.* Microbiological Reviews, 1987. **51**: p. 351-364.

114. Karin, M., *et al., Structure and transcription of an amplified genetic locus: the CUP1 locus of yeast.* Proc. Natl. Acad. Sci., 1984. **81**: p. 337-341.

115. Ecker, D.J., *et al., Yeast metallothionein function in metal detoxification.* J. Biol. Chem., 1986. **261**: p. 16895-16900.

116. Gorman, J., *et al., Regulation of the yeast metallothionein gene.* Gene, 1986. **48**: p. 13-22.

117. Sherman, F., G. Fink, and J.B. Hicks, *Laboratory Course Manual for Methods in Yeast Genetics.* 1986, Appendix A.

118. Ito, H., *et al., Transformation of intact yeast cells treated with alkali cations.* J. of Bacteriol., 1983. **53**: p. 153-168.

119. Rose, M.D., F. Winston, and P. Hieter, *Laboratory Course Manual for Yeast Genetics.* 1989, Cold Spring Harbor: Cold Spring Harbor Laboratory. p. 169.

120. Sambrook, J., E.F. Fritsch, and T. Maniatis, *Molecular Cloning: A Laboratory Manual.* 2 ed. Vol. 1-3. 1989, Cold Spring Harbor: Cold Spring Harbor Press.

121. Mandel, M. and A. Higa, *Calcium dependent Bacteriophage DNA infection.* J. Mol. Biol., 1970. **53**: p. 159.

122. Miller, H., *Growth and Maintenance of Bacteria,* in *Guide to Molecular Cloning,* S.L. Berger and A.R. Kimmel, Editor. 1987, Academic Press: New York. p. 145-172.

123. Rothstein, R., *Guide to Yeast Genetics and Molecular Biology.* Methods in Enzymology, ed. J.N. Abelson and M.I. Simon. Vol. 194. 1991, New York: Academic Press.

124. Schmitt, M.E., T.A. Brown, and B.L. Trumpower, *A rapid and simple method for preparation of RNA from Saccharomyces cerevisiae.* Nuc. Acid Res., 1990. **18**(10): p. 3091-3092.

125. Fourney, R.J., *et al., Northern Blotting: Efficient RNA Staining and Transfer.* Focus, 1988. **10**(1): p. 5-7.

126. Gerst, J.E., *et al., CAP is a bifunctional component of the Saccharomyces cerevisiae adenylyl cyclase complex.* Mol. Cell Biol., 1991. **11**(3): p. 1248-1257.

127. Erickson, A.H. and G. Blobel, *Cell-Free translation of messenger RNA in a wheat germ system,* in *Methods of Enzymology.* 1983, Academic Press: New York. p. 38-50.

128. Walter, P. and G. Blobel, *Preparation of microsomal membranes for cotranslational protein translocation.* Methods of Enzymology, Vol. 96. 1983, Academic Press. 84-93.

129. Caplan, S., *The role of structural features of the MFα precursor in α-factor production and mating in Saccharomyces cerevisiae.* 1988, Columbia University:

130. Adams, A., D. Botstein, and D.G. Drubin, *A yeast actin-binding protein is encoded by SAC6, a gene found by suppression of an actin mutation.* Science, 1989. **243**: p. 231-233.

131. Riabowol, K.T., L.A. Mizzen, and W.J. Welch, *Heatshock is lethal to fibroblasts microinjected with antibodies to hsp70.* Science, 1988. **242**: p. 433-436.

132. Johnston, R.N. and B.L. Kucey, *Competative inhibition of hsp70 gene expression causes thermosensitivity.* Science, 1988. **242**: p. 1551-1554.

133. Arnold, E. and W. Tanner, *An obligatory role of protein glycosylation in the life cycle of yeast cells.* FEBS Lett., 1982. **148**: p. 49-53.

134. Yoshiki, K., *et al., Formation of fungal multinuclear giant cells by tunicamycin.* J. Gen. Appl. Microbiol., 1976. **22**: p. 247-258.

135. Caplan, S. and J. Kurjan, *Role of α-factor and the MFα1 α-factor precursor in mating in yeast.* Genetics, 1991. **127**: p. 299-307.

136. Machamer, C. and J. Rose, *Influence of glycosylation sites on the expression of the vesicular stomatitis virus G protein at the plasma membrane.* J. Biol. Chem., 1988. **263**: p. 5948-5945.

137. Ng, D., S. Hiebert, and R. Lamb, *Different roles of individual N-linked oligosaccharide chains in folding, assembly, and transport of the simian virus 5 hemagglutinin-neuroaminidase.* Mol. Cell Biol., 1990. **10**: p. 1989-2001.

138. Gibson, R., S. Schlesinger, and S. Kornfeld, *The nonglycosylated protein of vesicular stomatitis virus is temperature-sensitive and undergoes intracellular aggregation at elevated temperatures.* J. Biol. Chem., 1979. **254**: p. 3600-3607.

139. Gallagher, P., *et al., Addition of carbohydrate side chains at novel sites on influenza virus hemagglutin can modulate the folding, transport and activity of the molecule.* J. Cell Biol., 1988. **107**: p. 2059-2073.

140. Schulke, N. and F. Schmid, *Effect of glycosylation on the mechanism of renaturation of invertase from yeast.* J. Biol. Chem., 1988. **263**: p. 8832-8836.

141. Schulke, N. and F. Schmid, *The stability of invertase is not significantly influenced by glycosylation.* J. Biol. Chem., 1988. **263**: p. 8827-8831.

142. Fischer, G. and F. Schmid, *The mechanism of protein folding. Implications of in vitro refolding models for de novo protein folding and translocation in the cell.* Biochemistry, 1990. **29**: p. 2205-2212.

143. Jaenicke, R., *Protein folding: Local structures, domains, subunits, and assemblies.* Biochemistry, 1991. **30**: p. 3147-3161.

144. Musch, A., M. Wiedmann, and T.A. Rapoport, *Yeast sec proteins interact with polpeptides traversing the endoplasmic reticulum membrane.* Cell, 1992. **69**: p. 343-352.

145. Graham, T. and S. Emr, *Compartmental organization of Golgi-specific protein modification ans vacuolar sorting events defined in a yeast sec18 (NSF) mutant.* J. Cell. Biol., 1991. **114**: p. 207-218.

146. Li, X. and A.S. Lee, *Competitive inhibition of a set of endoplasmic reticulum protein genes (GRP78, GRP94, and ERp72) retards cell growth and lowers viability after ionophore treatment.* Mol. Cell Biol., 1991. **11**(7): p. 3446-3453.

147. Liao, X., *et al., Intramitochondrial functions regulate nonmitochondrial citrate synthase.* Mol. Cell Biol., 1991. **11**: p. 38-46.

148. Liao, X. and R. Butow, *RTG1 and RTG2: Two yeast genes required for a novel path of communication from mitochondria to the nucleus.* Cell, 1993. **72**: p. 61-71.

149. Chang, S.C., A. Erwin, and A.S. Lee, *Glucose-regulated protein (GRP94 and GRP78) genes share common regulatory domains and are coordinately regulated by common trans-acting factors.* Mol. Cell Biol., 1989. **9**: p. 2153-2162.

150. Feder, J., *et al., The consequences of expressing hsp70 in Drosophila cells at normal temperatures.* Genes and Development, 1992. **6**: p. 1402-1413.

151. Freiden, P.J., J.R. Gaut, and L. Hendershot, *Interconversion of three differentially modified and assembled forms of BIP.* EMBO J., 1992. **11**(1): p. 63-70.